uOttawa

L'Université canadienne
Canada's university

FACULTÉ DES ÉTUDES SUPÉRIEURES ET POSTOCTORALES

uOttawa

L'Université canadienne
Canada's university

FACULTY OF GRADUATE AND POSDOCTORAL STUDIES

Azra Sari

AUTEUR DE LA THÈSE / AUTHOR OF THESIS

M.A.Sc. (Mechanical Engineering)

GRADE / DEGREE

Department of Mechanical Engineering

FACULTÉ, ÉCOLE, DÉPARTEMENT / FACULTY, SCHOOL, DEPARTMENT

Evaporation of Biomass Pyrolysis Oil as Single Droplets

TITRE DE LA THÈSE / TITLE OF THESIS

Dr. W. Hallett

DIRECTEUR (DIRECTRICE) DE LA THÈSE / THESIS SUPERVISOR

CO-DIRECTEUR (CO-DIRECTRICE) DE LA THÈSE / THESIS CO-SUPERVISOR

EXAMINATEURS (EXAMINATRICES) DE LA THÈSE / THESIS EXAMINERS

Dr. R. Milane

Dr. M. Johnson

Gary W. Slater

Le Doyen de la Faculté des études supérieures et postdoctorales / Dean of the Faculty of Graduate and Postdoctoral Studies

EVAPORATION OF BIOMASS PYROLYSIS OIL AS SINGLE DROPLETS

by

Azra Sari

A thesis submitted to the Faculty of Graduate and Postdoctoral Studies
in partial fulfillment of the requirements for the degree of
MASTER OF APPLIED SCIENCE
in Mechanical Engineering

Department of Mechanical Engineering
Faculty of Engineering
University of Ottawa
August 2006

Your file Votre référence
ISBN: 978-0-494-25832-3
Our file Notre référence
ISBN: 978-0-494-25832-3

ACKNOWLEDGEMENT

I would like to thank my thesis supervisor, Dr. William Hallett, for his guidance, encouragement, and financial support during the project.

Special thanks to the technical staff of the Mechanical Engineering Department of the University of Ottawa for their support, suggestions, and assistance during the preparation of test setup.

Thanks are extended to the Natural Sciences and Engineering Research Council for their financial support and Ensyn Technologies, Ottawa for providing fuel samples.

Finally, I would like to thank my parents for their endurance support and patience.

ABSTRACT

Biomass pyrolysis oil is an organic liquid produced by the pyrolysis of biomass materials. The fuel is known as a clean, cost-effective, renewable resource and a potential replacement for petroleum fuels in boiler, gas turbine, and diesel engine applications. The fuel oils are usually introduced into the burner as sprays of droplets; therefore, the evaporation behaviour of individual fuel droplet has an important role in understanding of the combustion characteristics of the droplets in spray combustion and in the burner performance. Single droplet evaporation/combustion experiments have been performed by several researchers in the past years with different kind of fuels by using two main techniques: Suspended droplet/moving furnace technique and freely falling droplet technique. In this research, the suspended droplet technique has been preferred because of its advantages that the droplet is stationary and easily observed.

The mathematical model presented in this thesis is based on a model developed by Hallett and Clark (2006) to describe the evaporation of a pyrolysis oil droplet and its pyrolysis to gas and char. A well-mixed liquid phase is assumed in the previous model, which is reasonable owing to the vigorous bubbling during much of the evaporation process. However, this assumption is questionable during the pre-bubbling period. In order to gain some insight into this period, and into the onset and the location of bubbling, a diffusion-limited model, developed by Law and Law (1981) and extended by Hallett (2000) to a continuous mixture form, is used with some modifications to extend the earlier model. The results are compared to the experimental results, and conclusions for evaporation modelling are drawn.

NOMENCLATURE

A	surface area, m^2
B	transfer number for diffusion in Eq. (3.2-9)
c	molar density, $kmol/m^3$
C_P	specific heat, kJ/kmol K
C_{PL}	liquid phase specific heat, kJ/kmol K
D	diffusivity, m^2 /s
$\overline{D}$	averaged diffusivity, m^2 /s
E	activation energy, kJ/mol
f(I)	distribution function
G	mass flux, kg/m^2 s
G_{ij}	binary interaction parameter
I	distribution variable (= species molecular mass), kg/kmol
j	number of fuel distribution functions
K	pre-exponential term
L	lignin fraction unconverted
Le	Lewis number (=thermal diffusivity/mass diffusivity)
$\hat{m}_F$	$=GR/\rho D$
M	mol mass, kg/kmol
N	molar flux, $kmol/m^2$ s

P	total pressure, kPa
P_v	vapour pressure, kPa
P_{ATM}	atmospheric pressure, kPa
r	radial position, m
R	droplet radius, m
$\overline{R}$	universal gas constant, = 8.3144 kJ/kmol K
s_{fg}	entropy of vaporization, kJ/kmol K
Sh_o	Sherwood number at low mass transfer rates
T	temperature, K
T_B	boiling temperature, K
V	droplet volume, m^3
x	mol fraction in liquid
y	mol fraction in vapour
Y	mass fraction in liquid

Greek Letters

α, β	parameters of the gamma distribution
γ	distribution origin, kg/kmol
ς_C	fraction of lignin converted to char
η	dimensionless radial coordinate (=r/R)

η	Dynamic viscosity, centipose
θ	distribution mean (= mean mol mass), kg/kmol
λ	thermal conductivity, W/m.K
χ_G	ratio N_G /total mol flux N
χ_j	ratio N_j /total vapour mol flux
σ	distribution standard deviation, kg/kmol
Ψ	$= \theta^2 + \sigma^2$ (2nd moment) of f (I)
ρ	gas density, kg/m^3

Subscripts

A	air
C	char
F	fuel
G	pyrolysis gas
j	index for a fuel fraction
L	liquid phase
PY	pyrolyzing component
R	at the droplet surface
0	initial value
∞	ambient value

TABLE OF CONTENTS

LIST OF TABLES

LIST OF FIGURES

CHAPTER 1

Introduction

1.1 GENERAL

Biomass pyrolysis oil is a liquid obtained from the fast pyrolysis of biomass. Fast pyrolysis refers to the rapid thermal decomposition of biomass or organic compounds in the absence of oxygen to produce liquids, gases and char. At a temperature of around 500 °C, much of the biomass is transformed into vapour, which then may be cooled, condensed and recovered as a liquid bio-oil product. Bio-oil is currently being produced in limited quantities by two Canadian companies: Ensyn Technologies Inc., Ottawa and Dynamotive Energy Systems Corporation, Vancouver. The main components of pyrolysis oils are carboxylic acids, aldehydes, ketones, water and pyrolytic lignin. Pyrolytic lignin, comprising lignin decomposition products such as phenols, guaiacyl- and syringyl-based compounds and lignin oligomers, is a high molecular weight mixture resulting from the partial pyrolysis of the original lignin in the wood.

The potential of biomass pyrolysis oil as a substitute for petroleum fuels in diesel engine, boiler, and turbine applications has resulted in an interest in studying the behaviour of single bio-oil droplet evaporation/combustion. Since the fuel oils are usually introduced into the burner as sprays of droplets, it is reasonable to expect that the collective gasification of

individual droplets would influence the bulk spray vaporization, which in turn determines the burner performance. Therefore, the evaporation behaviour of a single droplet has an important role in understanding of the combustion and/or ignition characteristics of the droplets in spray combustion. Pyrolysis oils exhibit complex evaporation and combustion behaviour: typically the initial liquid heating period is followed by bubbling and/or "micro-explosions", after which the heavy non-volatile residue remaining pyrolyzes to a highly porous, irregularly-shaped char particle or "cenosphere". The bubbling / disruptions indicate internal boiling, which can occur because of the differences in composition between the surface and interior of the droplet. After the initial heating period, the droplet surface layer loses the light components of the fuel and becomes capable of being heated to higher temperatures. The lighter inner core then has a lower bubble point than the surface, so that vapour bubbles can be formed by internal vaporization of the lighter components.

In modelling of a single droplet evaporation of liquid fuel, the physical problem is that of a cold droplet which is exposed to a hot environment and begins to vaporize. The heat flux from the hot surrounding atmosphere is transferred into the droplet by conduction, convection and radiation; much of the heating is used to heat the droplet, and some for the evaporation of light components on the droplet surface. The concentration of the fuel vapour is a maximum at the droplet surface and reduces towards the surroundings; hence, a mass flux occurs away from the droplet surface (see Figure 1.1). Within time an equilibrium liquid temperature and evaporation rate are established at the droplet surface.

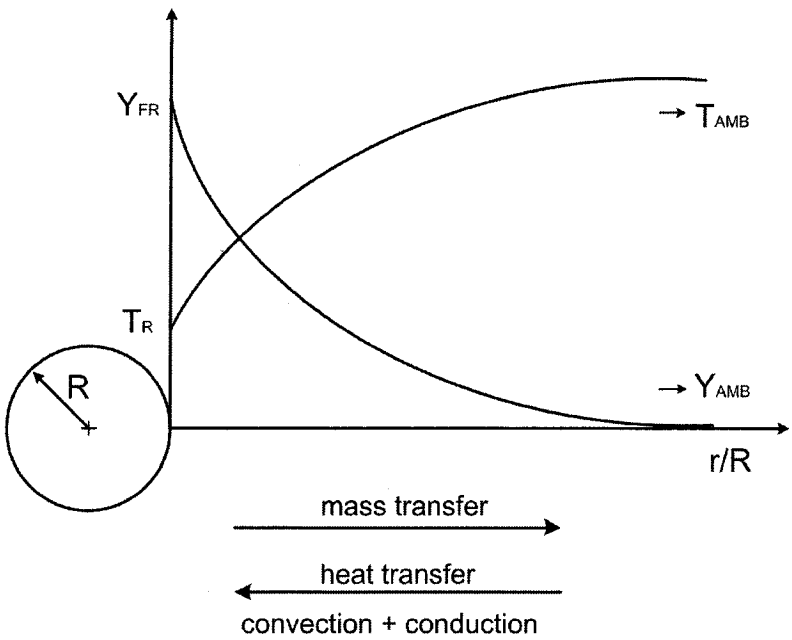

Figure 1.1: Basic process occurs during the quasi-steady evaporation of a single liquid droplet of radius R

For a multi-component fuel droplet, such as biomass pyrolysis oils, the vapour phase composition and evaporation rate depend on the liquid composition at the droplet surface, which in turn are controlled by liquid internal mixing. Mixing inside the liquid droplet can be described by two limiting models:

1. Diffusion-Limited Model: This model assumes that bulk internal mixing doesn't exist so that the transport inside the droplet occurs by molecular diffusion only.
2. Well-mixed Model: This model assumes complete mixing inside the droplet: the internal circulation is fast enough so that the concentration and temperature profiles remain uniform.

Both limiting cases, explained above, will be the interest of this thesis.

1.2 OBJECTIVE

The objective of the research reported in this thesis is to investigate experimentally and analytically the evaporation behaviour of biomass pyrolysis oils. The scope of research includes experimental tasks, as outlined below:

1. Understand the nature of bubbling/boiling.
2. Investigate the nucleation of bubbles inside the liquid.
3. Describe the processes of liquid-phase mixing
4. Deduce the kinetics of the lignin pyrolysis reaction
5. Determine the physical properties of the fuel

The analytical task, on the other hand, was to extend a model for wood pyrolysis oil droplet evaporation and pyrolysis developed by Hallett and Clark (2006). This model assumed a well-mixed liquid, a reasonable assumption due to the vigorous bubbling during much of the evaporation process; however, this assumption is questionable during the period prior to the start of bubbling. Therefore, the model is extended to cover this period more accurately with a simplified diffusion-limited liquid phase calculation, based on that of Law and Law (1981) as extended to a continuous mixture form by Hallett (2000). The model and experimental results obtained by using the suspended droplet/moving furnace technique will be tested against each other.

1.3 PRESENTATION OF THESIS

Following a literature review in Chapter 2, Chapter 3 reports on the development of a mathematical model for single droplet evaporation using the diffusion-limited model, and a review of the previous model. The experimental apparatus and procedure will be presented in

Chapter 4. Experimental and numerical results and discussion will be reported in Chapter 5. Finally, Chapter 6 provides a summary of conclusions and recommendations for future research.

CHAPTER 2

Literature Survey

2.1 INTRODUCTION

The current research project is based on the evaporation of biomass pyrolysis oil as a single droplet. Single droplet evaporation concepts have been used in analyses of the evaporation/combustion behaviour of the fuel. These concepts, which have been studied in the past by many researchers, involve both experimental and mathematical studies. Experimental studies of droplet evaporation/combustion have two techniques, which are i) the suspended /moving furnace technique; ii) the free falling single droplet technique. Mathematical model concepts for multicomponent fuels are i) multicomponent droplet evaporation; ii) continuous thermodynamics for modelling mixtures. In this chapter, the previous researches on these concepts as well as on the composition and behaviour of biomass pyrolysis oil are reviewed in separate sections.

2.2 BIOMASS PYROLSIS OILS

Biomass pyrolysis oils, also known as bio-oils or pyrolysis oils, are dark brown organic liquids with a distinctive smoky odour, obtained from rapid heating and pyrolysis of biomass. Pyrolysis oils are multicomponent mixtures comprising different sized molecules derived primarily from depolymerization and fragmentation reactions of three key biomass building

blocks: cellulose, hemicellulose, and lignin. The potential of these fuels as a substitute for petroleum fuels in engine and boiler applications has resulted in several researches on their chemical composition, physical properties, homogeneity, stability, and miscibility being carried out. The following is a list of previous research results, with brief explanations of objectives, and findings.

2.2.1 Chemical Composition

Sipilä et al. (1998) compared the chemical composition analyses of pyrolysis oils based on different feedstocks (hardwood oil, Scots pine oil, and wheat straw oil) and pyrolysis processes. The pyrolysis liquids mainly comprised water, volatile acids, ketones, aldehydes, and pyrolytic lignin (defined as a mixture of high molecular weight species resulting from partial pyrolysis of the original lignin). Those analysed differed in their ability to dissolve in water. Water-soluble fractions, 60-80 % of the oils, were extracted by diethylether, and the analysis for hardwood pyrolysis oil showed that the diethylether-soluble part of the water fraction contained guaiacyl and syringyl lignin-derived compounds, and the diethylether insolubles contained levoglucosan and cellobiosan, known as degradation products of cellulose and hemicelluloses. The water-insoluble fraction, pyrolytic lignin, in the pyrolysis oil varied from 20 to 40 wt %, and the highest proportion was obtained from hardwood pyrolysis oil (Ensyn, Canada). Hardwood pyrolysis oil has a water content of 20-25% and a moderate density of 1.2 kg/dm^3 ; similar density values were also determined by **Peacocke et al. (1994), Maggi and Delmon (1994), Czernik et al. (1995), Oasmaa and Czernik (1999), Oasmaa and Peacocke (2001), and Oasmaa et al. (2001).**

Oasmaa et al. (2003) investigated the effects of extractives (fatty acids, fatty alcohols, terpenes, resin acids, and terpenoids) on the phase separation of pyrolysis oils. They reported that during storage some changes occurred, including oxidation/degradation/polymerization of resin acids, and evaporation of volatile compounds. Phase separation results from the significant polarity/solubility and density differences between extractives and the highly hydrophilic pyrolysis liquid compounds. After a certain storage time in a phase separation tower the liquid was recovered from the bottom of the tower as "bottom" and "top" phases. The amount of water phenolics, syrup-like "sugar" fraction (levoglucosan and cellobiosan), aldehydes (acetaldehyde, 2-furaldehyde, 5-methylfurfurale, glycolaldehyde), ketones (1-hydroxy-2-propanone, 1-hydroxy-2-butanone, 2-cyclopenten-1-one, 1-acetyloxypropan-2-one, and 5H-furan-2-one), and carboxylic acids was significantly lower in the top phase than in the bottom phase, which caused a clear polarity difference between the two phases.

Water in pyrolysis liquids, which results from the original moisture in the feedstock, also has effects on phase separation. This was investigated by **Oasmaa and Czernik (1999),** who reported that the oil water content varied in a wide range, from 15-30%, depending on the feedstock and pyrolysis process conditions. As water was added to oils obtained from birch, pine, and poplar, phase separation occurred at water concentrations of 27 %, 23-25 %, and 31-wt % respectively. The researchers reported information on the properties of pyrolysis oils as follows:

- The average molecular weight of the bio-oil was determined to vary from 370 to 1000 g/mol.

- A distillation process was performed on bio-oils and it was observed that the slow heating of the oil during distillation results in polymerization of some reactive components. This left 35-50 % of the starting material as residue.
- The aging rate for hot-filtered poplar pyrolysis oil was correlated by a relation obtained from experimental results.

Oasmaa et al. (2003) investigated the physicochemical composition of pyrolysis oils based on three kinds of forestry residue feedstock (stem wood, needles, and bark). The researchers reported that the forestry residue pyrolysis liquid separates immediately after condensation to a liquid bottom phase (80-90wt %) and a viscous top phase (10-20 wt %). The water-soluble fraction (carboxylic acids, aldehydes, alcohols, ketones, and water (22 wt %)) was 80 wt % and the water-insoluble fraction was 20 wt % of the original liquid. The composition of the bottom phase (main product) was reported in the form of mass fractions: volatile acids 8-10 wt %; aldehydes and ketones 10-15 wt %; water 25-30 wt %; "sugar" constituents 30-35 wt %; water-insoluble, mainly lignin-based constituents 12-20 wt %; and extractives (2-6 wt %).

Scholze et al. (2000) presented the results obtained for various pyrolytic lignins of pyrolysis oils from different fast pyrolysis processes (eight pyrolytic lignin samples). The mass average (M_w) and the number average (M_n) of the molecular weight of pyrolytic lignins are reported. Out of eight pyrolytic lignin samples the Ensyn pyrolytic lignin (hardwood pyrolytic lignin) displayed the lowest molecular weight distribution (M_w=649 g/mol and M_n=376 g/mol by Refractive Index (RI) detector, or M_w =621 g/mol and M_n =305 g/mol by ultraviolet (UV) detector). Subsequently, the average molecular weight of pyrolytic lignin from different feedstocks was determined to be between 650 and 1300 g/mol. The results

indicated that in softwood pyrolysis oils more than 90% of the lignin units are guaiacyl units, while in hardwood pyrolysis oil syringyl units dominate (60%-80%). It was also claimed that the lignin fraction in pyrolysis liquids is mainly trimers and tetramers of hydroxyphenyl (H), guaiacyl (G), and syringyl (S) compounds.

The lignin distribution in pyrolysis oils was approximately fitted to experimental results by **Scholze and Meier (2001)**; similar distributions are further reported by **Czernik et al. (1994), and Diebold and Czernik (1997).**

The thermal conductivity of liquid pyrolysis oils was found to be between 0.35 and 0.43 W/mK , which is higher than for heavy fuel oils (0.177 W/mK at 100 °C) and significantly less than water (0.667 W/mK) **(Peacocke et al., 1994).** Similar results by **Oasmaa and Peacocke (2001)** supported these data.

2.2.2 The "Aging" Process of Pyrolysis Oils

Biomass oils contain compounds that, during storage or handling, can react with themselves to form larger molecules. These reactions results in undesirable changes in physical properties, such as an increase of viscosity and water content with corresponding decrease of volatility. Since the changes progress slowly over time, the process is called "aging". **Oasmaa and Kuoppala (2003)** studied the reasons for the instability of pyrolysis oils, and the aging of forestry residue and pine pyrolysis liquids. The high molecular mass fraction of water-insoluble (lignin-derived) material increased because of polymerization and

condensation reactions of aldehydes and ketones, which in turn slowly increased the viscosity of pyrolysis oil. Observed chemical changes during the "aging" process were:

- Decrease in volatile aldehydes and ketones.
- Formation of water as a byproduct.
- Decrease in heating value.
- Increase in flash point.
- Increase in pour point.
- Increase in the density of the liquid.

Similar effects of "aging" were also reported by **Czernik et al. (1994),** and the effects of additives on the aging rate and viscosity of pyrolysis oils were reported by **Diebold and Czernik (1997), Boucher et al. (2000), Czernik and Bridgwater (2004), and Shaddix and Hardesty (1999)**.

2.2.3 Evaporation/Combustion Behaviour

D'Alessio et al. (1998), Wornat et al. (1994), and Shaddix and Hardesty (1999) studied the combustion, and **Hallett and Clark (2006)** studied the evaporation of biomass pyrolysis oil droplets. Experimental observations showed that the initial liquid heating period is followed by bubbling and/or "micro-explosions", after which the heavy non-volatile residue remaining pyrolyzes to a highly porous, irregularly shaped char particle or "cenosphere". **Czernik and Bridgwater (2004)** reported pyrolysis oil applications in burner, diesel engines, turbines, and Stirling engines. It was reported that the combustion behaviour of a single droplet demonstrates a multistep process comprised of the following phases: ignition,

quiescent burning, droplet micro-explosion, disruptive sooty burning of droplet fragments, and formation and burnout of cenosphere particles.

2.3 EXPERIMENTAL WORK

Experimental studies of droplet evaporation/combustion have performed by two main techniques:

1. a single droplet suspended on the end of a fine quartz fibre or thermocouple;
2. a freely falling single droplet.

2.3.1 Suspended Droplet Studies

This technique is considered as the simplest type of droplet experiment. A fuel droplet placed on the end of a fine filament evaporates and/or ignites in the hot environment produced by a heated chamber or a hot air stream. A motion picture camera and an optical system are usually used to observe the evaporation/combustion behaviour of the droplet.

Kobayasi (1954) performed experiments on eight different fuel droplets (heavy oils, gasoline, kerosene, n-heptane, ethyl alcohol, etc.). The observed droplet diameter changes and the ignition times of the fuels were presented. Furthermore, the evaporation behaviour of heavy oil droplets was examined in this study, and it was reported that after evaporation of the lighter components, a viscous semi-solid residue remains. Vapour bubbles were formed by internal vaporization and by liquid-phase cracking in the droplet (This is similar behaviour to that observed for pyrolysis oils). **Nishiwaki (1954)** studied the effects of a uniform airflow on the droplet diameter changes and the ignition/evaporation times of water,

ethanol, and methanol droplets. The researcher performed some of the earliest evaporation and combustion experiments on fuel droplets using the suspended droplet/moving furnace technique. A liquid fuel droplet was suspended on the end of a filament fibre. An electric furnace mounted on rails was moved over the suspended droplet, and the evaporation rate and the dimensions of the droplet were obtained from shadow photographs of fuel droplets taken by using a motion-picture camera. Fine thermocouple wires measured the temperature of the single droplet. The suspended droplet technique with similar apparatus has been used by **Araya and Tsunematsu (1987), Bergeron and Hallett (1989), D'Alessio et al. (1998), Hallett and Clark (2006)**, and many others**. Lin and Chen (2002)** studied the drying/evaporation process of milk droplets and other foods by using a similar method; however, instead of a furnace, hot air was provided to evaporate the droplet. The droplet temperature was measured by a K type thermocouple.

Okajima and Kumagai (1982) devised a system to investigate the combustion behaviour of suspended fuel droplets in a uniform airflow under zero gravity (10^{-5}g) and normal gravity conditions (1g-2g), the purpose being to eliminate natural convection. Zero gravity experiments were made in a 5 m drop tower, carefully designed to absorb the shock given to the falling assembly using rubber cushions. A single fuel droplet was suspended on the end of a silica filament mounted in a falling assembly with airtight covers, an optical system, an igniter, and a small wind tunnel. High gravity experiments were performed by pulling up the assembly using a cord through a pulley system. Both zero gravity and high gravity experiments were conducted during this free fall period. **Xu et al. (2002)** also investigated the combustion of fuel droplets under microgravity conditions. Experiments were conducted in a drop shaft, which can generate good microgravity conditions. Platinum-rhodium

thermocouple wires supported the fuel droplets, and measured the droplet inside temperature. A heater was used to heat the droplet instead of a hot chamber. A CCD camera was used in the experiments to picture the whole process.

The advantages of this experimental technique are:

1. Suspended droplet experiments can be easily set up and performed.
2. The droplet is stationary and hence easily observed, something that is much more difficult with falling droplets in a drop tube furnace.

The disadvantages of this experimental technique are:

1. Because of the thickness of the quartz fibre, it is difficult to suspend a droplet much smaller than 1 mm in diameter, which is much larger than the size in spray evaporation/combustion.
2. Suspending the droplet distorts its shape from spherical.
3. Heat conduction through the suspending fibre can affect the droplet behaviour.

2.3.2 Free Falling Droplet Studies

This method is performed by injecting single droplets directly into an environment contributing to evaporation or combustion.

Okajima and Kumagai (1982) conducted combustion experiments under a zero gravity condition. They developed a technique to make the relative velocity of a freely falling droplet zero to the freely falling chamber. A single fuel droplet was first suspended on a silica filament, and then by pulling the filament upward with a rapid acceleration, the droplet was

released. As the droplet reached the highest point of its trajectory, the chamber began to fall freely. The history of the droplet size was photographed by a movie camera. **D'Alessio et al. (1998)** performed combustion experiments both using suspended furnace and freely falling droplet methods. The procedure used in this study was that the small droplets were generated by an atomizer and injected downwards in a drop-tube furnace heated by cylindrical ceramic heaters. **Wornat et al. (1994)** conducted experiments in Sandia National Laboratories in a setup, which was detailed by **Shaddix and Hardesty (1999).** The fuel was pumped by a syringe pump through an inner capillary tube, and the fuel droplets were released downwardly into the centerline of a laminar flow reactor. A flow burner provided the high-temperature gas environment for the combustion experiments and a video camera was used to record two positions of the droplet to calculate the droplet velocity.

The advantage of this experimental technique is:

1. Small droplet sizes can be used in the experiments.
2. No disturbance due to suspending fibre

The disadvantages of this experimental technique are:

1. Experimental method is more complex.
2. The droplet is in motion and hence observing the droplet by a camera would be more complicated.
3. Droplets are subjected to forced convection by their motion relative to the gas.

2.4 MATHEMATICAL MODELS

2.4.1 Droplet Evaporation

The theory of fuel droplet vaporization/combustion has been intensively developed during the past several decades. The classical droplet vaporization model is described in many textbooks and by many researchers in the literature **(e.g. Hallett (1997), Spalding (1979), Kanury (1975), Sirignano and Law (1978), and Abramzon and Sirignano (1989))**. The physical problem of droplet vaporization is that of a single droplet which is suddenly exposed to a hot environment and starts evaporating. The droplet, which is at a relatively low temperature in the early stages of the droplet lifetime, begins to heat up, and the temperature of the droplet increases rapidly until it reaches an equilibrium. During the initial heating period, much of the heat transfer to the surface is used to heat the droplet, because of the low vaporization rate. However, as the equilibrium state is approached, the temperature becomes constant and almost all the energy supplied to the droplet surface is used for the vaporization of fuel. At the droplet surface, an equilibrium between the fuel vapour and liquid composition will exist, and the fuel vapour will diffuse to the surroundings away from the droplet; hence, a mass flux occurs away from the droplet surface. In this research, the pressure is close to atmospheric pressure; therefore, air absorption by the liquid was neglected.

The classical theory of the droplet is based on the following assumptions:

- Spherical symmetry: Although the real droplets are nearly symmetrical, the fields of vapour concentration and temperature around them become distorted by natural and forced convection (or by the suspending quartz fibre in some experiments as mentioned before), which are ignored in the theory.

- Quasi-steady evaporation: The vapour field is assumed to adjust to a new steady state condition almost instantaneously after the droplet temperature and/or radius change. These adjustments are defined by transients terms ($\partial/\partial t$) in the equations; however, due to the significant difference between the density of liquid and gas phases, the liquid transport processes are much slower than those of the gas phase. Vapour phase mass and thermal diffusivities are of the order of $10^{-5}\ m^2/s$ **(Law, 1982)**, and are much higher than the liquid phase thermal and mass diffusivities of 10^{-7} or $10^{-9}\ m^2/s$ **(Law, 1982)**. Therefore, the transient terms can be dropped from the vapour phase governing equations.
- Constant gas phase transport properties.
- Constant pressure
- Pure fuel
- No chemical reaction
- Liquid-phase temperature and concentration uniform through the droplet but time varying.

2.4.2 Multi-Component Droplets

Commercial petroleum fuels contain hundreds of components, each of which has a different boiling point. Earlier experiments and theoretical results all indicate that the evaporation and combustion of the droplets of such mixtures may differ both quantitatively and qualitatively from those of single component droplets **(Law et al., 1977)**. **Law (1976)** indicated that a theoretical analysis for the multi-component droplet presents several complexities absent in a similar analysis for the single component droplet:

- The phase-change process at the multi-component fuel droplet surface and the transport of fuel vapour mixture in the gas phase need to be properly described.
- The numerical efforts are complicated by the stiffness of the coupled governing equations because thermal diffusion is much faster than mass diffusion in the liquid.

The intensity of liquid mixing and internal motion controls the rate of components exposed to the droplet surface, which in turn affects the vapour phase composition and evaporation rate of the droplet. Mixing inside the liquid droplet can be described by two limiting cases for the transport of mass and heat in the liquid:

1. Well-mixed Model
2. Diffusion-Limited Model

The well-mixed model is based on the assumption of rapid internal mixing. For low viscosity mixtures where the internal circulation is fast enough, the concentration and temperature profiles are uniform but vary in time. The process of vaporization is similar to batch distillation: the more volatile components are continuously brought to the surface and vaporized first; thus, the droplet becomes less volatile as the light components are removed. The liquid motion inside the droplet can be caused by shear of the liquid as it emerges from the atomizer and/or by natural or forced convection in the surrounding gas.

The diffusion-limited model is relevant for a very viscous fluid mixture in which internal motion does not exist, and it assumes that the transport within the droplet occurs only by molecular diffusion. After vaporization begins, the concentration profile varies steeply at the droplet surface, but the interior core of the droplet remains at its initial condition due to the

low liquid-phase mass diffusion rates until approached by the receding surface. Therefore, the liquid temperature and composition are not uniform.

Wood et al. (1960), in one of the earliest studies of multicomponent fuels, studied the burning rate coefficient for a two-component fuel and showed that the droplet diameter squared varied linearly with time. The researchers assumed the existence of uniform composition within the liquid at every instance and a quasi-steady vapour phase as in the classical droplet theory to simplify the droplet model. The results indicated that the composition of the liquid phase changes as a batch distillation process in which the liquid and the vapour are in equilibrium with respect to composition and temperature.

The existence of internal mixing was studied by **El-Wakil et.al. (1956).** The researchers performed experiments on single-component droplets to show that enough internal circulation exists even in a stationary droplet to cause mixing of the fluid.

Law (1976) studied the problem of unsteady combustion of a multi-component fuel droplet in a stagnant, unbounded atmosphere. The model assumed that the composition and temperature within the droplet were uniform but time-varying, and a quasi-steady vapour phase heat and mass transfer model was developed by considering constant transport properties. The results indicated that the components vaporize approximately sequentially in the order of their relative volatilities and the vaporization rate is insensitive to the mixture composition during pure vaporization in hot environments. The researcher reported that the well-mixed model is relevant for less viscous mixtures when internal circulation is so fast

that the droplet temperature and compositions are maintained spatially uniform although time-varying. **Sirignano and Law (1978)** studied both limiting cases of internal mixing in a single-component fuel droplet: the diffusion-limited model and the well-mixed model. The model was based on the quasi-steady vapour phase assumption. They compared the results obtained from both limiting cases and concluded that the droplet vaporization time can be predicted with good accuracy regardless of the mode of internal heat transfer. **Law and Law (1981)** studied the diffusion-limited model in a binary droplet using quasi-steady vapour phase assumptions as in classical droplet evaporation, and calculating the constant vapour-phase transport properties at reference temperature and concentration values. The researchers reported that due to the extremely slow rate of the liquid-phase mass diffusion, the droplet liquid concentration profile remains at an almost constant shape during much of the droplet lifetime; hence, the quasi-steady assumption can be applied to the liquid-phase in order to simplify the multi-component droplet evaporation modelling.

Aggarwal (1987) studied vaporization of a single component fuel droplet and a multi-component fuel droplet by considering both limiting cases of internal mixing. Moreover, transient heating effects in the gas-phase were introduced. The differences between these two models were relatively large for the single-component case compared to the multicomponent case, and consequently it was suggested that internal circulation is less important for the multicomponent case. **Faeth and Olson (1968)** compared the effects of constant and time-varying properties on the predicted temperature profiles of two different vapour concentrations at the droplet surface. The results showed that constant property assumptions produce a very large error in predicted temperatures.

Bergeron and Hallett (1989) studied the auto-ignition of single droplets of two-component mixtures. In the model, a well-mixed liquid phase was assumed and transient effects in the vapour-phase were introduced. The same assumptions for the liquid and vapour phase were also used by **Hallett and Ricard (1992)** to develop a mathematical model for the auto-ignition of a multi-component (seven-component) single fuel droplet, which predicted ignition delay times as a function of composition for mixtures.

Tong and Sirignano (1984) developed a transient diffusional model, accounting for liquid-phase internal circulation, for the vaporization of a two-component droplet. The results compared the infinite diffusivity (i.e. well-mixed) model and the spherical diffusion-limited model. A quasi-steady convective gas phase was assumed to simplify the model. The researchers recommended the spherical diffusion model for transient diffusion in the liquid phase for the stagnant situation where there is no relative gas motion.

Abramzon and Sirignano (1989) studied the evaporation of a fuel droplet including the effects of transient convection, Stefan flow, internal mixing, and liquid heating. They assumed quasi-steady gas phase heat and mass transfer.

2.4.3 Continuous Thermodynamics

Most of the fuels used for industrial process are complex liquid mixtures, containing hundreds or thousands of components. In calculations, it is impractical to obtain the concentration of every one of the hundreds of species in a commercial fuel, and therefore alternative methods are required. In earlier treatments of this problem, the 'pseudo-

components method', based on representing each group of components of similar properties by one "pseudo-component", has been used. An alternative solution to describe the mixture properties is the method of continuous thermodynamics, which treats the mixture composition as a probability density distribution rather than as a series of discrete components, with the distribution giving the composition as a function of a property such as species molecular weight or boiling point. The main advantage of this method is that instead of dealing with a large number of individual components, one only needs the parameters of the distribution function (mean, standard deviation) to make calculations for the fuel. This concept was introduced more than sixty years ago by **Katz and Brown (1933),** who presented a method for calculation of the vapour pressure of petroleum fractions, in which the complex mixture composition was expressed in terms of true boiling point.

In Continuous Thermodynamics, the fluid is described by a continuous distribution function f(I), where I is the distribution variable for the mixture, which can be any convenient physical property, such as molecular weight, boiling point temperature, or carbon number.

Prausnitz (1983) developed a method to calculate phase equilibria for complex mixtures using the concept of pseudo-components whose properties are given by the characterization data. Moreover, the researcher presented an alternative to the pseudo-component method in the form of phase-equilibrium calculations using continuous thermodynamics. **Chou and Prausnitz (1986)** studied continuous or semi-continuous mixtures, and applied continuous thermodynamics principles to multi-stage absorption and distillation. A Gaussian distribution

method is used to solve phase-equilibrium. **Briano and Glandt (1983)** modelled the thermodynamic relations in continuous distribution function form.

Tamim and Hallett (1995) developed a model for the evaporation of droplets of multi-component liquids in which the mixture composition, properties, and vapour-liquid equilibrium are described by the methods of continuous thermodynamics. The liquid-phase was approximated as a well-mixed liquid, and the transport equations for the droplet vapour phase included transient effects. Transport equations for the parameters of the distribution function describing the mixture composition were derived and solved numerically. The resulting solutions describe the changes in liquid and vapour composition with time as well as the variation of vapour composition in space. **Hallett (2000)** simplified this theory to a quasi-steady model, and also adapted the Law and Law (1981) model to a continuous mixture, and compared the model with the well-mixed model. **Abdel-Qader and Hallett (2005)** developed a continuous thermodynamics theory to compare the two limiting cases of liquid-phase mixing, the well-mixed and diffusion-limited case for evaporating droplets. A mixing factor was included to allow an approximate treatment of internal circulation as in **Talley and Yao (1986)**. The results were reported for both single component droplets and binary droplets, and also compared to the model developed in **Hallett (2000)**. **Hallett and Clark (2006)** developed a numerical model based on continuous thermodynamics for the evaporation of biomass pyrolysis oil, with the assumptions of a well-mixed liquid and a quasi-steady vapour phase for simplicity of calculation. Pyrolytic lignin, the heaviest component of the fuel, was assumed to pyrolyze as well as evaporating.

CHAPTER 3

Mathematical Model

3.1 INTRODUCTION

The mathematical model reported in this thesis is based on a model developed by Hallett and Clark (2006) in order to describe the evaporation of a biomass pyrolysis oil droplet and its pyrolysis to gas and char. The earlier model assumes a well-mixed liquid, which is reasonable due to the vigorous bubbling during much of the evaporation process. However, this assumption is questionable during the pre-bubbling period, when mixing is by diffusion alone and hence is slow. The main objective here is to gain some insight into the onset and location of bubbling, which requires information about how the liquid composition varies with position inside the droplet. A complete description of this requires solution of the diffusion equation in the liquid phase as was done by Abdel-Qader and Hallett (2005). For a continuous thermodynamics solution with two distribution functions, they had to solve six diffusion equations together with flux matching conditions at the droplet surface. For the pyrolysis oil model, we have four distributions and would therefore have to solve twelve equations along with an equal number of flux matching conditions. Since this is a major computational effort, a simplified model for a diffusion-limited liquid phase, developed by Law and Law (1981) and extended by Hallett (2000) to a continuous mixture form, is used with some modifications to extend the previous model to cover the pre-bubbling period more

accurately. In this chapter, the following sections will be a description of the present model, including a brief description of the diffusion-limited model, the well-mixed model, and derivation of the liquid composition equations.

3.2 LIQUID-PHASE LIMITING CASES

Law and Law (1981) have developed a liquid-phase mass diffusion-controlled, quasi-steady solution for evaporation and combustion of droplets. The model is based on the assumptions that the concentration changes are limited to a thin surface layer and that the concentration profiles are approximately quasi-steady. Owing to the slow rate of liquid-phase mass diffusion, concentrations vary steeply close to the droplet surface, but rapidly approach to their initial values further inside and remain at that condition until approached by the receding surface.

To simplify the model, the following assumptions were made (Hallett & Clark, 2006),

i. Spherical symmetry of the droplet and surroundings is assumed; therefore, only radial transport is possible.

ii. A quasi-steady vapour phase and uniform (but time-varying) properties are assumed. This assumption predicts that concentration and temperature variables of the vapour-phase adjust to a new steady state almost instantaneously. Hence, the transient terms ($\partial/\partial t$) can be dropped from the transport and governing equations. This assumption leads to an analytical vapor-phase solution similar to "classical" droplet evaporation theory.

iii. Evaporation in pure air, $y_{F\infty} = 0$

iv. No chemical reaction is included in the model (pure evaporation).

These assumptions are standard common assumptions in most modeling work of droplet evaporation.

The well-mixed model was detailed in the earlier paper (Hallett and Clark, 2006). Briefly, the fuel is assumed to consist of four chemical groups (carboxylic acids, aldehydes / ketones, water, and pyrolytic lignin), and the continuous thermodynamics technique is used to represent each chemical group in the pyrolysis oil. In continuous thermodynamics, the molar concentrations of species in each chemical group j are described by a distribution function $f_j(I)$. Since several distributions are required to model pyrolysis oil in order to be able to represent different chemical groups, the subscript j is used. The vapour and liquid phase mol fraction of a particular species i is given by

$$y_i = y_{Fj} f_j(I) dI_j \quad ; \qquad x_i = x_{Fj} f_{Lj}(I) dI_j \tag{3.2-1}$$

The fuel composition of each chemical group is represented by a gamma distribution function, with mean θ_{L_j}, standard deviation σ_{L_j}, and origin γ_j, and the distribution variable I was chosen as species molecular weight. Evaporation produces corresponding vapour phase distributions with mean θ_j and standard deviation σ_j. The gamma distribution describing the vapour and liquid phases is

$$f_j(I) = \frac{(I-\gamma)^{\alpha_j - 1}}{\beta_j^{\alpha_j} \Gamma(\alpha_j)} exp\left[-\left(\frac{I-\gamma}{\beta_j} \right) \right] \tag{3.2-2}$$

where α_j and β_j are the distribution parameters, $I = \gamma_j$ is the origin, and $\Gamma(\alpha)$ is the gamma function. Distribution parameters are different for liquid and vapour, but the origin γ_j is assumed to be the same for both phases.

The mean and variance are

$$\theta_j = \alpha_j \beta_j + \gamma_j; \qquad \sigma_j^2 = \alpha_j \beta_j^2 \tag{3.2-3}$$

The distribution function has the property that

$$\int_0^\infty f_j(I)dI = 1 \tag{3.2-4}$$

$$\theta_j = \int_0^\infty f_j(I)IdI \tag{3.2-5}$$

$$\psi_j = \int_0^\infty f_j(I)I^2 dI = \theta_j^2 + \sigma_j^2 \tag{3.2-6}$$

The quantity θ_j is the mean molecular weight of distribution j.

Quasi-steady behaviour is assumed for the vapour phase, leading to a solution similar to classical droplet evaporation theory.

$$N = \frac{c\bar{D}_j}{R} ln(1 + B_j); \qquad B_j = \frac{y_{FjR} - y_{Fj\infty}}{\chi_j - y_{FjR}} \tag{3.2-7}$$

Pyrolytic lignin is assumed to comprise high molecular weight species. This component vaporizes very little, and remains liquid at high temperature, where it is assumed to pyrolyze

to gas and char. Therefore, the mol flux N includes pyrolysis gas as well as vapor. The mol fraction of each vapor component and of pyrolysis gas in the total mol flux N are defined as

$$\chi_j = N_j/N; \qquad \chi_G = N_G/N \tag{3.2-8}$$

where

$$\sum_j^J \chi_j + \chi_G = 1 \tag{3.2-9}$$

At low mass transfer rates, the effects of convection may be introduced by Sherwood number, and mol flux becomes

$$N = \frac{c\bar{D}_j Sh_0}{2R} ln(1+B_j) \tag{3.2-10}$$

The χ_j may be found by writing equation (3.2-7) for j=1 and for j and equating, giving

$$\chi_j = y_{FjR} + \frac{y_{FjR} - y_{Fj\infty}}{(1+B_1)^{\bar{D}_1/\bar{D}_j} - 1} = y_{FjR} + \frac{y_{FjR} - y_{Fj\infty}}{exp(2NR/c\bar{D}_j Sh_0) - 1} \tag{3.2-11}$$

Vapor pressure and properties, required for each chemical group as simple functions of molecular weight in continuous mixture theory, were developed from standard correlations. Phase equilibrium is described by a continuous mixture form at the droplet surface using Raoult's law together with the Clausius-Clapeyron equation for individual component vapour pressures. Details may be found in Hallett and Clark (2006).

3.3 LIQUID-PHASE EQUATIONS

The liquid is assumed to be well-mixed-uniform in composition and temperature after bubbling starts. The mol balance equation on the droplet for the well-mixed case is the same as in the earlier work. Full details are given by Hallett and Clark (2006), but the equations required for later use in the present model are reproduced here. The rate of conversion of liquid by evaporation (first term) and pyrolysis (second term) is:

$$\frac{d}{dt}(c_L V_L) = -NA\left[(1-\chi_G)+\frac{\chi_G}{(1-\zeta_C)}\frac{\theta_G}{\theta_{LPY}}\right] \tag{3.3-1}$$

where χ_G is the pyrolysis gas mol fraction, c_L is the liquid molar density, A is the droplet surface area, θ_G is the mean mol mass of the pyrolysis gases, θ_{LPY} is the mean of the lignin distribution function, and ζ_C is fraction of lignin converted to char. A mol balance on the droplet for a single species i gives

$$\frac{d}{dt}(x_i c_L V_L) = -N_i A - N_{Pi} A \tag{3.3-2}$$

where the first term represents evaporation and the second is the rate of pyrolysis of species i if applicable. The vapour flux is given as

$$N_i = N y_{iR} - c D_i \left.\frac{\partial y_{Fi}}{\partial R}\right|_R \tag{3.3-3}$$

This is substituted in Eq. (3.3-2), distribution functions are introduced (Eq. (3.2-1)), the resulting expression is integrated over the distribution variable I, and the derivative in Eq.

(3.3-3) is evaluated from the expression of concentration variation in the vapour phase. For a fuel fraction which does not pyrolyze (ie anything except lignin), N_{Pi} is omitted. The result is an expression for the variation of the liquid composition with time

$$\frac{d\bar{x}_j}{dt} = \frac{NA}{c_L V_L}\left[\bar{x}_j(1-\chi_G) - \chi_j + \frac{\bar{x}_j \chi_G}{(1-\zeta_C)}\frac{\theta_G}{\theta_{LPY}}\right]; \; j \neq PY \tag{3.3-4}$$

Weighting equation Eq. (3.3-2) by I and I^2 respectively, integrating over I and expanding the resulting expression yields the equation for the variation of the distribution parameters with time:

$$\frac{d\bar{\theta}_{Lj}}{dt} = \frac{NA}{\bar{x}_j c_L V_L}\left[\chi_j \bar{\theta}_{Lj} + \frac{\theta_{j\infty} y_{Fj\infty} - \theta_{jR} y_{FjR}(1+B_j)}{B_j}\right] \tag{3.3-5}$$

while a similar equation holds for the liquid second moments $\overline{\Psi}_{Lj}$. For details, please refer to Hallett and Clark (2006).

In the Law and Law (1981) model, the quasi-steady solution for the liquid concentration profile of a single species *i* inside the droplet is given in terms of mass fraction

$$Y_i = Y_{i0} + (Y_{iR} - Y_{i0})exp(-\eta) \tag{3.3-6}$$

where subscripts *R* and *0* refer to values at the droplet surface and at the initial condition respectively. Y_{i0} is the mass fraction value that the equation gives as η goes to infinity, and is assumed equal to initial mass fraction value. The coordinate η is

$$\eta = \eta_0(1-(r/R)) \tag{3.3-7}$$

where

$$\eta_0 = \gamma \cdot \hat{m}_F \cdot Le_L = \left(\frac{\lambda C_{PL}}{C_P \lambda_L}\right) \cdot \left(\frac{GR}{\rho D_j}\right) \cdot \left(\frac{\lambda_L}{C_{PL} \rho_L D_{Lj}}\right) = Le \frac{\rho D_j}{\rho_L D_{Lj}} \left(\frac{GR}{\rho D_j}\right) \tag{3.3-8}$$

where

$$G = \frac{\rho D_j}{R} ln(1 + B_j) \tag{3.3-9}$$

After simplifying, and rearranging Eq. (3.3-8), and by assuming that the vapour phase $Le=1$, it can be rewritten for each component as

$$\eta_{j0} = \frac{\rho D_j}{\rho_L D_{Lj}} ln(1 + B_j) \tag{3.3-10}$$

where ρ is the gas density, ρ_L is the liquid density, both of which are assumed to be constant, D_j is the gas diffusivity, and D_{Lj} is the liquid diffusivity, which will be given later in section 3.5, and the transfer number B_j is given by Eq. (3.2-7). Equation (3.3-6) may then be written in terms of mol fraction to conform to the rest of the model by substituting the expression $Y_i = x_i M_i / M$ into equation (3.3-6), where M is the mixture mol mass, calculated as $M = \theta_L = \sum_j x_{Fj} \theta_{Lj}$,

$$\frac{x_{Fi}}{\theta_L} = \frac{x_{Fi0}}{\theta_{L0}} + \left(\frac{x_{FiR}}{\theta_{LR}} - \frac{x_{Fi0}}{\theta_{L0}}\right) exp(-\eta_0 (1 - r/R)) \tag{3.3-11}$$

Since $x_F = 1$, the sum of equation (3.3-11) gives the change of mean molecular weight

$$\frac{1}{\theta_L} = \frac{1}{\theta_{L0}} + \left(\frac{1}{\theta_{LR}} - \frac{1}{\theta_{L0}}\right) exp\left(-\eta_0 (1 - r/R)\right) \tag{3.3-12}$$

Substituting the distribution function for the mol fraction as in Eq. (3.2-1), and integrating over the distribution with weighting factor I^n *(n=0, 1, 2)* gives an equation as follows

$$\phi_j = \phi_{j0} + (\phi_{jR} - \phi_{j0}) exp\left(-\eta_{j0} (1 - r/R)\right) \tag{3.3-13}$$

where ϕ_j represents $\frac{x_{Fj}}{\theta_L}$, $\frac{x_{Fj}\theta_{Lj}}{\theta_L}$, $\frac{x_{Fj}\psi_{Lj}}{\theta_L}$ and the overall liquid mean $\frac{1}{\theta_L}$.

In the original Law and Law (1981) model, the solution for Y_{iR} (mass fraction at the surface) was obtained by combining the liquid and vapour phase solutions, but the solution did not conserve component mass in the droplet. Therefore, in this research, the quantities at the surface were obtained by assuming that Eq. (3.3-13) gives the same average concentrations as an overall balance on the droplet. The total number of mols of component i in the droplet is

$$n_i = 4\pi \int_0^R r^2 \bar{c}_L \bar{x}_i dr = 4\pi \int_0^R r^2 \rho_L \frac{x_i}{\theta_L} dr \tag{3.3-14}$$

$$n_i = \bar{\bar{x}}_i \cdot \bar{c}_L \cdot V \tag{3.3-15}$$

where $\bar{c}_L = \rho_L / \bar{\theta}_L$

and $\bar{\bar{x}}_i = \bar{x}_j \cdot \bar{f}_{Lj}(I) dI$ (3.3-16)

$\bar{c}_L$ and $\bar{x}_i$ are quantities averaged over the droplet. Substituting Eq. (3.3-16) into Eq. (3.3-14), and integrating over the distribution variable I yields

$$\frac{1}{3}R^3\bar{c}_L\bar{x}_j = \int_0^R r^2 \rho_L \frac{x_j}{\theta_L} dr \tag{3.3-17}$$

Performing the same procedure with a weighting factor of I and I^2 gives an expression in general form

$$\frac{1}{3}R^3\bar{\phi}_j = \int_0^R r^2 \phi_j dr \tag{3.3-18}$$

Substituting equation (3.3-13) into equation (3.3-18), integrating and rearranging to solve for ϕ_{jR} gives

$$\phi_{jR} = \left(\bar{\phi}_j / 3 - \phi_{j0}/3\right) / \left[\frac{1}{\eta_{j0}} - \frac{2}{\eta_{j0}^2} + \frac{2}{\eta_{j0}^3}\left(1 - exp\left(-\eta_{j0}\right)\right)\right] + \phi_{j0} \tag{3.3-19}$$

The averaged liquid phase values, $\bar{x}_{Fj}$, $\bar{\theta}_{Lj}$, and $\bar{\Psi}_{Lj}$, required in this equation are calculated in Eq. (3.3-4) and (3.3-5), while the values with subscript 0 are the (known) initial values. The surface quantities determined can now be used to define the profiles of x_{Fj}, θ_{Lj} and σ_{Lj} in the droplet (Eqs. 3.3-11 - 3.3-13).

3.4 DETERMINING THE ONSET AND LOCATION OF BUBBLING

The bubble point of the liquid varies corresponding to the liquid composition. Therefore, the liquid composition profile, obtained by Eq. (3.3-13) between the droplet center and surface,

is used to estimate the mixture bubbling point inside the droplet at different positions. Afterward, the bubble point of the liquid is compared to the liquid temperature within the droplet and bubbling is assumed to start at the time and position that the droplet temperature reaches the mixture bubbling point. Since liquid fuels have large Lewis numbers, the liquid-phase thermal diffusion is more rapid, approximately 2 orders of magnitude, than liquid-phase mass diffusion. Therefore, it is reasonable to assume that the liquid temperature is uniform within the droplet.

The vapour phase mol fraction, mean and variance at the droplet surface in continuous mixture form were calculated by using x_{FjR}

$$y_{FRj} = x_{FjR} \int_0^\infty f_{Lj}(I)(P_{vj}(I)/P)dI \tag{3.4-1}$$

$$y_{FjR}\theta_{jR} = x_{FjR} \int_0^\infty f_{Lj}(I)\left(P_{vj}(I)/P\right)IdI \tag{3.4-2}$$

$$y_{FjR}\sigma_{jR}^{\ 2} = x_{FjR} \int_0^\infty f_{Lj}(I)\left(P_{vj}(I)/P\right)(I-\theta)^2 dI \tag{3.4-3}$$

The parameters of the liquid distribution function f_{Lj} (Eq. 3.2-2) can be calculated by using θ_{LjR} and ψ_{LjR} values. The component vapour pressure is given by the Clausius-Clapeyron equation:

$$P_{vj}(I) = P_{ATM}\ exp\left[\frac{s_{FGj}}{\overline{R}}\left(1-\frac{T_{bj}(I)}{T}\right)\right] \tag{3.4-4}$$

where s_{FG_j} is the entropy of vaporization (kJ / kmol K), $\overline{R}$ is the universal gas constant, and $T_{bj}(I)$ is the boiling point correlation function defined as

$$T_{bj}(I) = a_{Bj} + b_{Bj} I \tag{3.4-5}$$

where $\mathbf{a_B}$ and $\mathbf{b_B}$ are the boiling point correlating coefficients. Substituting Eq. (3.4-4) and (3.4-5) into Eq. (3.4-1) and integrating the resulting expression gives

$$y_{FRj} = x_{FjR} \frac{P_{ATM}}{P} \frac{exp\left[\left(s_{FGj}/\overline{R}T_R\right)\left(T_R - a_{Bj} - \gamma_j b_{Bj}\right)\right]}{\left(1 + \left(s_{FGj}/\overline{R}T_R\right) b_{Bj}\beta_{Lj}\right)^{\alpha_{Lj}}} \tag{3.4-6}$$

For more details on the vapour-liquid equilibrium equations, please refer to Tamim and Hallet (1995). In order to calculate the bubble point of the mixture y_{FR} is set to 1 in Eq. (3.4-6) and T_R solved iteratively. The liquid mol fraction profile within the droplet $x_F(r)$ was used in the calculations.

The present model assumes a diffusion-limited liquid phase during the pre-bubbling period, and calculates the liquid and vapour phase values using the equations described in this chapter. By the time bubbling is predicted to start, the diffusion-limited model switches to the well-mixed model, developed by Hallett and Clark (2006).

3.5 LIQUID DIFFUSIVITY

The liquid phase diffusivities required for the calculation of liquid mol fraction and distribution mean and variance at the surface (Eq. (3.3-19)), were determined by using the Wilke-Chang correlation (Reid et al., 1986, page 598). Since the components of the fuel vary

widely in diffusivity, for the accuracy of the solutions the diffusivity of each species was used in the calculations. The method for calculating diffusivity shown here parallels that developed by Abdel-Qader and Hallett (2005) for a continuous mixture. For a single discrete component i the diffusivity can be estimated using the Wilke-Cheng correlation (Reid et al., 1986, page 598).

$$D_{Li} = 7.4 * 10^{-12} \frac{(\phi M)^{1/2} T}{\eta_m V_i^{0.6}} \tag{3.5-1}$$

where D_{Li} is in (m^2/sec), M is the molecular weight of the mixture excluding component i, T is the temperature, η_m is the mixture viscosity in cP, V_i is the pure component molar volume, and ϕ is the association factor for the solvent. For hydrocarbons and other polar molecules, $\phi = 1$ (Reid et al., 1986, 598), and ϕM becomes the mixture mean molecular weight.

$$\phi M = \sum_{j=1}^{N} x_j M_j = \theta_L \tag{3.5-2}$$

The molar volume of the component i (V_i) at normal boiling point is

$$V_i = \frac{1}{c_{Li}} \tag{3.5-3}$$

where c_{Li} is the component molar density. Substituting Eq. (3.5-2) and Eq (3.5-3) into Eq (3.5-1) yields:

$$D_{Li} = 7.4 * 10^{-12} \frac{\theta_L^{1/2} Tc_{Li}^{0.6}}{\eta_m} \tag{3.5-4}$$

In order to solve this equation the liquid mixture viscosity is required. The recommended method for finding a liquid mixture viscosity from the viscosity of the components is that of Grunberg and Nissan (Reid et al., 1986, page 474)

$$\ln \eta_m = \sum_{i=1}^{N} x_i \ln \eta_i + \sum_{i \neq j}^{N} \sum^{N} x_i x_j G_{ij} \tag{3.5-5}$$

where η_i is the viscosity of component i, N is the total number of components in the mixture and G_{ij} is a binary interaction parameter determined from a group contribution method. The binary interaction parameter term is smaller than the first term of equation (3.5-5) and is small for components of similar molecular weight (Reid et al., 1986, page 475), and in a mixture with many components the individual species mole fraction x_i are small; therefore, the second term can be neglected, and the equation in continuous mixture form for x_F=1 becomes

$$\ln \eta_m = \int_0^{\infty} f_L(I) \ln \eta(I) dI \tag{3.5-6}$$

The simplest method to calculate the component viscosity is by using the Orrick and Erbar correlation (Reid et al., 1986, page 456). For a single discrete component i, the liquid viscosity can be estimated as

$$\ln\left(\frac{\eta_i}{\rho_L M_i}\right) = A + \frac{B}{T} \tag{3.5-7}$$

where M_i is the component molecular weight and T is the liquid temperature. A and B parameters for each component were written in the general form

$$A = a_1 + a_2 I, \qquad B = b_1 + b_2 I \tag{3.5-8}$$

A and B parameters, M_i and coefficients a_1, a_2, b_1, b_2 for each component distribution are given in Appendix A, Table A.2.

Substituting equations (3.5-8) into (3.5-7) yields

$$\ln \eta_i = \ln \rho_L + \ln I + a_1 + \left[a_2 + \frac{b_2}{T}\right] I + \frac{b_1}{T} \tag{3.5-9}$$

In order to find an expression for liquid mixture viscosity, equation (3.5-9) will be substituted into (3.5-6) and integrated over I to yield

$$\ln \eta_m = \ln \rho_L + a_1 + \frac{b_1}{T} + \left[a_2 + \frac{b_2}{T}\right] \theta_L + \int_0^\infty f_L(I) \ln I \, dI \tag{3.5-10}$$

Substituting the gamma distribution (Eq. 3.2-2) gives

$$\ln \eta_m = \ln \rho_L + a_1 + \frac{b_1}{T} + \left[a_2 + \frac{b_2}{T}\right] \theta_L + \frac{1}{\Gamma(\alpha_L)} \int_0^\infty t^{\alpha_L - 1} \exp(-t) \ln(\beta_L t + \gamma) dt \tag{3.5-11}$$

where

$$t = \frac{I - \gamma}{\beta} \tag{3.5-12}$$

For $\gamma = 0$, the equation can be integrated in closed form, and becomes

$$ln\,\eta_m = ln\,\rho_L + a_1 + \frac{b_1}{T} + \left[a_2 + \frac{b_2}{T}\right]\theta_L + ln(\beta_L) + \Psi(\alpha) \tag{3.5-13}$$

where $\Psi(\alpha)$ is the digamma function, which can be calculated using an asymptotic formula found in Abramovitz and Stegun (1970)

$$\psi(\alpha_L) = ln(\alpha_L) - \frac{1}{2\alpha_L} - \frac{1}{12\alpha_L^2} + \frac{1}{120\alpha_L^4} - \frac{1}{252\alpha_L^6} + \ldots \tag{3.5-14}$$

For non-zero gamma, the integration must be carried out numerically. The viscosity of each chemical group was calculated and substituted into Eq. (3.5-5) to obtain the liquid mixture viscosity. The diffusivity was then calculated (Eq. (3.5-4)) using the mean molecular weight for each distribution rather than as described by Abdel-Qader and Hallett (2005) by integrating the diffusivity over the distribution function. The reason is that computational problems, in particular a very large gamma function, occur with the heavier components of the pyrolysis oil.

Properties Correlations

For the calculation and correlation of properties required for the model, such as vapour and liquid specific heat, vapour thermal conductivity and diffusivity, critical temperature and pressure, liquid density, boiling point, and enthalpy of vaporization, for each of the four chemical groups, please refer to Hallett and Clark (2006).

CHAPTER 4

Experimental Apparatus and Technique

The main purpose of the experiments is to understand the pyrolysis oil droplet evaporation behaviour and the nature of bubbling/boiling, to investigate the nucleation of bubbles inside the liquid, and to measure some physical properties of the fuel. In this chapter, the experimental apparatus and technique, and the methods used in chemical analyses will be explained.

4.1 GENERAL

The experiments were performed by using the suspended droplet/moving furnace technique in which the droplet is placed on the end of a quartz fibre and a preheated electric furnace moves rapidly to enclose the droplet and begin evaporation. Kobayasi (1954) and Nishiwaki (1954) performed some of the earliest evaporation and combustion experiments by using this technique and the same apparatus has been used by Araya and Tsunematsu (1978), and D'Alessio et al. (1998) among many others. This technique was selected because the experiments can be easily set up and performed; moreover, the suspended droplet is easy to observe during the experiment, since it is stationary. The alternative technique, free falling droplets, wasn't preferred because of the difficulty of observing the droplet, performing the experiments, and the effect of forced convection. The test set up is illustrated in Figure 4.1 and 4.2 in detail.

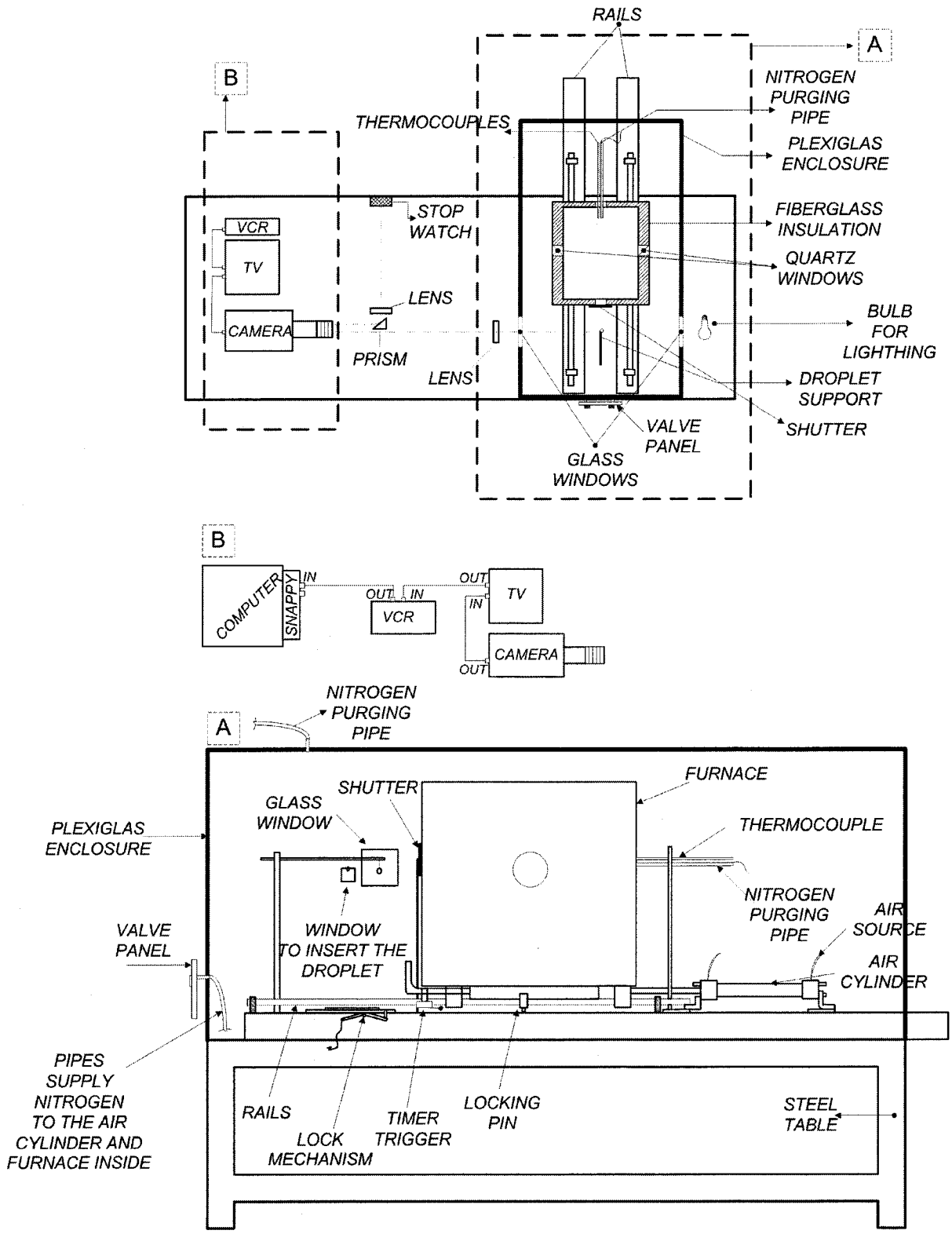

Figure 4.1: Test setup

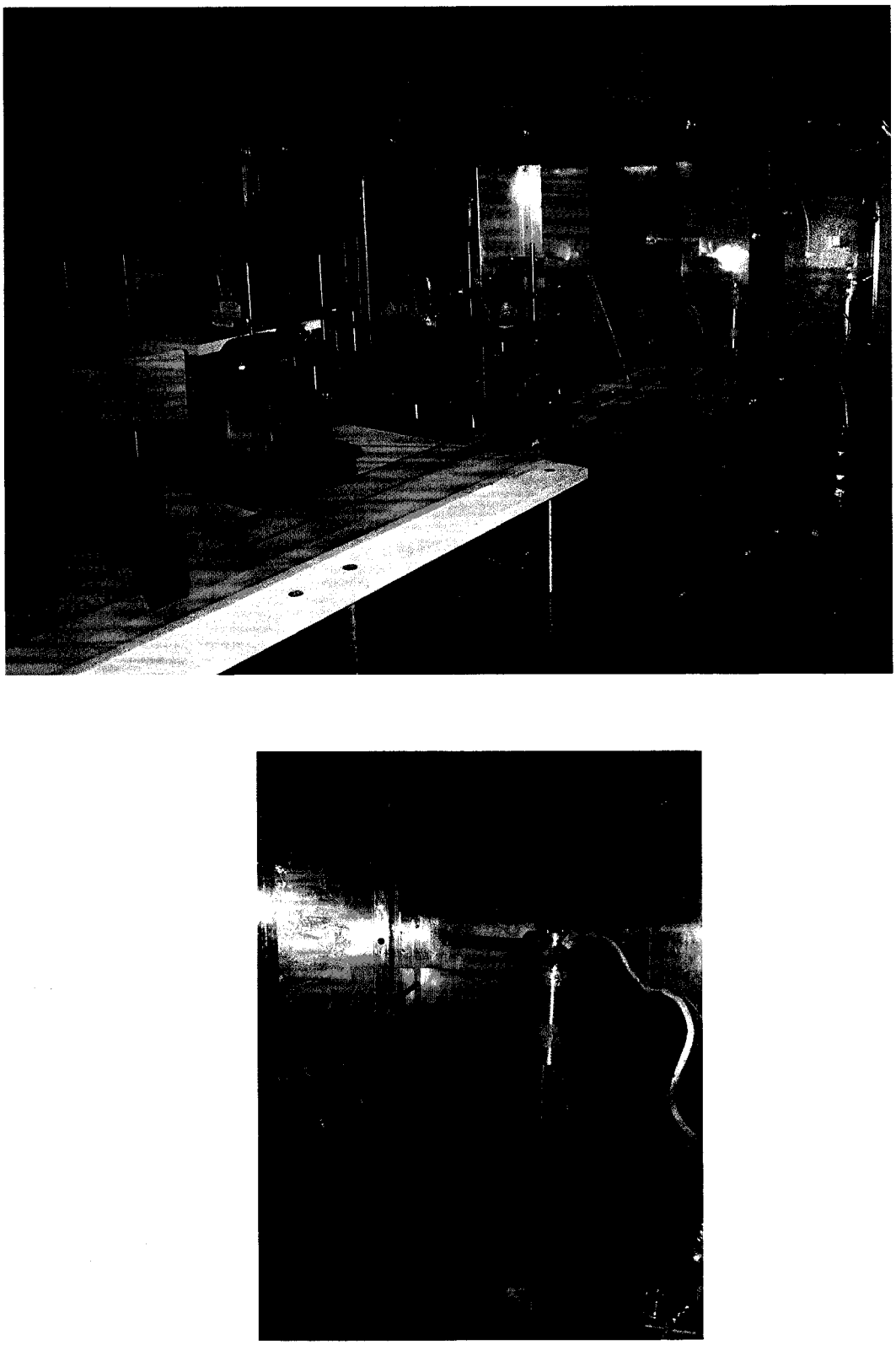

Figure 4.2: Test setup

4.2 Experimental Apparatus

4.2.1 The Furnace

Briefly, the features of the furnace used in this research are:

(i) Constructed of 50 mm thick Fibrefrax Duraboard lightweight refractory board.

(ii) Heated by two semi-cylindrical heating elements of 125 mm diameter.

(iii) Two quartz windows of 5 cm diameter are mounted on opposite sides of the furnace to observe the droplet during the experiments.

(iv) Vertical slits of 45x13 mm in size are located on the front and back wall. One serves as a droplet support entrance, and the other as an entrance for a nitrogen purging tube and a thermocouple. A shutter blocks off the front droplet entrance until the furnace is about to move over the droplet and fibreglass insulation is used to cover the back wall entrance.

In this study, experiments were performed at 723, 1023 and 1123 K furnace temperatures. The electric furnace temperature was regulated by controlling the power supply voltage with a variable transformer. A K-type thermocouple, which is arranged to occupy the same position in the furnace that the droplet will occupy after the furnace has moved, is used to measure the furnace temperature. An air cylinder is used to move the preheated furnace mounted on rails rapidly over the suspended droplet to achieve a step change in temperature and begin evaporation. The furnace is locked into its position by a spring-loaded pin which drops into a hole in the guide rail after the furnace moves over the droplet.

Most droplets in spray combustion evaporate inside vapour clouds rather than burning individually; therefore, in order to simulate the behaviour of a droplet in a spray, the entire experiment was enclosed in a nitrogen-filled containment made of Plexiglas. Additionally, a purging nitrogen flow was introduced to the furnace and the Plexiglas enclosure before each experimental run, and during the experiment a nitrogen flow was introduced to the enclosure near the furnace entrance to prevent combustion and ensure pure evaporation at high temperatures.

4.2.2 Droplet Suspension and Imaging System

A 0.18-0.22 mm quartz fibre, with a 0.58-0.61 mm bead, was used to suspend the droplet. The quartz fibres are made from a piece of quartz rod, and melted at one end to form a bead. The beads are measured by a micrometer to make sure that they all have the same diameter. Pyrolysis oil droplets were formed by a 5 μl syringe in diameters of 1.4, 1.56, and 1.7 mm, and placed on the end of the quartz fibre, which is securely fixed to the support by being placed between two small plates that are tightened together with a screw.

A 50 mm video camera and two lenses were used to record the evaporation behaviour of the droplet together with a timer, which is started by a trigger as the droplet enters the furnace. The droplet was backlit by two 50 W halogen bulbs. Before the beginning of a series of experiments, a scale together with the bead and the droplet is also photographed to calibrate the droplet diameter size. The recorded images were transferred to individual computer files by a digital video capture device, Snappy Video Snapshot, and the droplet diameters were measured physically by counting the number of pixels in the images. The horizontal

diameter was measured, and the small deviations from a perfectly spherical shape were neglected. In some experiments, a 0.025 mm (0.001") K type thermocouple wire was used as the suspending fibre instead so as to measure the droplet temperature, with a 0.6 mm ceramic bead on the tip to hold the droplet. The thermocouple wire was inserted into a 1/8" ceramic thermocouple insulator tube, and connected to a data acquisition system.

Experiments performed before by Kobayasi (1954) and by Hallett and Clark (2006) showed that the droplet evaporation behaviour depends on suspending fibre material and diameter. The quartz fibre used for most experiments in this study is similar in thermal conductivity and specific heat to liquid fuels, and should therefore not affect droplet heating significantly. However, the supporting fibre may have acted as a nucleation site to initiate internal boiling at the bubble point of the mixture. Unsupported droplets in spray combustion, on the other hand, may be able to experience some superheat owing to the absence of internal nucleation sites.

In the earlier experiments conducted by Hallett and Clark (2006) the use of 0.125 mm (0.005") diameter thermocouples to suspend the droplets showed a significant shortening of the droplet lifetime owing to heat conduction along the thermocouple wire. They therefore added a crude correction to the computer model to account for this effect. The correction assumes conduction along the wire over a distance corresponding to a boundary layer thickness around the droplet; this distance was fitted in earlier work to experimental data for pure fuels. In this research, the thermocouple wire was selected as thin as possible 0.025 mm (0.001") to reduce this effect. In order to assess the error, experiments were performed with

pure *n*-hexadecane and compared with calculations using the model with and without correction. Fig. 4.3 shows the results of these tests. The measured temperatures lie below the bubble point of the fuel, as they should. Predictions and measurements agree very closely during the initial heating period; however, there is a small discrepancy within about 10°C during the equilibrium vaporization period. Since the calculated thermocouple correction is small, the main reason for this difference is probably that the droplet in conjunction with the ceramic bead is not centered on the thermocouple tip, and as a result an error on the temperature readings occurs.

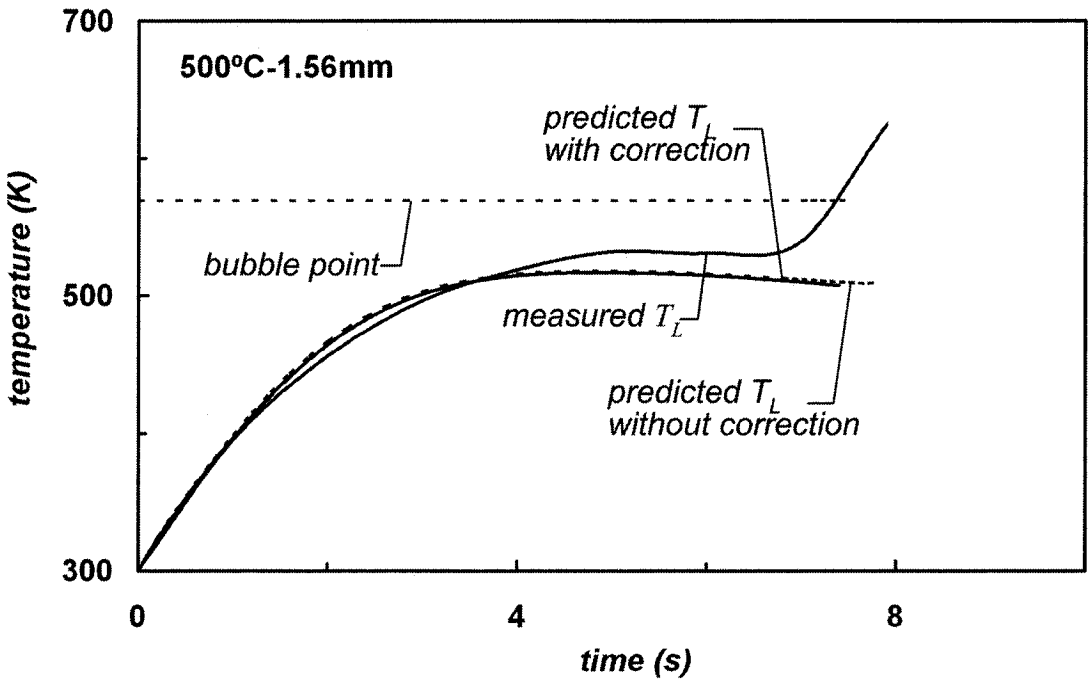

Figure 4.3: Predicted droplet temperature and boiling point compared with temperature measured by a 0.025mm (0.001") thermocouple supporting the droplet, for a 1.56mm n-hexadecane droplet evaporating at 773 K. The predictions include an estimate of the additional heat transfer to the droplet through the thermocouple.

Possible Error Sources in the Experiments

1. Errors in Droplet Diameter Measurements

- The droplet diameter was measured physically by counting pixels; therefore, the resolution of the computer screen limit the accuracy of the total number of pixels counted, which in turn affects the accuracy of the measured droplet diameter. The estimated error in measured diameter is $\pm$ 0.03 mm.

- If the lenses and/or the camera are not focussed correctly, it will result in a larger image; the pixels will appear more spread out, which in turn gives inaccurate measurements. One problem encountered with these experiments was that the variation of refractive index with temperature of the gas inside the furnace could shift the point of focus and blur the image.

- Lightning improves imaging significantly. If the position of the bulbs is not adjusted properly, it will cause the image to blur and cause difficulties in measuring the diameter accurately. At 1123 K furnace temperature, the inside of the furnace was very bright due to the radiation from the furnace walls, causing the images to appear transparent and more spread out. Therefore, the droplet diameters were measured with a lower accuracy.

2. Errors in Temperature Measurements

- The K-type thermocouple used to measure the furnace temperature was calibrated at ice point using a voltmeter and data acquisition board and gave accurate readings. K-

type thermocouples offer a low standard error, less than ± 2.2 °C or 0.75% (www.omega.com). The thermocouple was connected to a digital temperature readout with a precision of ± 1 °C during the experiments.

- Another source of error is the air current caused by the moving furnace, which can disturb the droplet but not significantly.

4.3 Chemical Analyses

Complete chemical analyses of these fuels are not available: most composition information in the literature is in the form of mass fractions of selected components, mass fractions of water-insoluble and soluble groups, or listings of components without quantitative concentrations. In this research, the fuel is assumed to comprise four chemical groups: organic acids, aldehydes and ketones, pyrolytic lignin (lignin decomposition products: phenols, guaiacyl- and syringyl-based compounds, and lignin oligomers), and water, as in earlier work by Hallett and Clark (2006).

Pyrolysis liquids contain an abundance of water (15-35 wt %) due to the moist feed and the water formed during pyrolysis. The water content of the pyrolysis oil used in our experiments is reported as 30 wt% of the fuel by the supplier company, Ensyn Technologies Inc. The water-insoluble fraction of the fuel, "pyrolytic lignin", was measured using the method detailed in Oasmaa et al. (2001). Pyrolysis oil was added slowly to distilled water using the oil-water ratio=1:10 and mixed for at least two hours. Afterwards, the solution was filtered using 0.45 μm filters; the precipitate remaining on the filter, which contains the substances

insoluble in water, was dried in a vacuum oven at 20° C and weighted. The experiments were repeated 5 times and the average value was used in the calculations.

CHAPTER 5

Results and Discussion

Droplet evaporation experiments were conducted to understand the nature of bubbling/boiling, to determine the pyrolysis oil droplet evaporation behaviour, and to measure some physical properties of the fuel. Experiments were performed at atmospheric pressure and results were obtained for pyrolysis oil droplets in diameters of 1.4, 1.56 and 1.7 mm at 773, 1023 and 1123 K furnace temperature. The model calculations, expanded from the earlier model to gain some insight into the pre-bubbling period, were compared against the experimental results. In this chapter the results for the experiments and the model will be presented.

5.1 FUEL PROPERTIES

In this research, the same distribution parameters for the distribution functions describing the different chemical groups in the fuel were used as in Hallett and Clark (2006), who selected these functions based on more detailed composition information for an earlier sample of pyrolysis oil and on information in the literature. However, the mol fractions of the fuel components in this work are different than assumed in the earlier work. The mol fraction of pyrolytic lignin was found using the methods described in Chapter 4 to be 30 wt % of the liquid. The water content of the fuel was reported as 30 wt% by the supplier company, Ensyn

Technologies Inc. The mol fraction of carboxylic acids and aldehydes were estimated by using the same ratio as used earlier by Hallett and Clark (2006). The distribution functions and assumed composition of pyrolysis oil are given in Figure 5.1 and Table 5.1.

The density of the pyrolysis oil was determined by measuring its mass and volume and using hydrometers; consequently, the density was found to be 1.12 kg /m^3, which is the average of 10 trials. The pyrolytic lignin density was set to 2000 kg/m^3 in order to force the mixture density to equal the calculated value.

For modelling purposes of pyrolytic lignin, rate parameters were roughly chosen as **E=200 kJ/mol** and **K =1x10^{15} s^{-1}**, and the char yield from pyrolysis was found as ς_C **= 0.5.** Our choice will be justified in Section 5.7.

5.2 DROPLET HISTORY

5.2.1 Visual Observations

Figure 5.2 presents a sample of video recordings of droplet evaporation on a quartz fibre at 1023 K. During the transient heating period no significant change was observed (Picture 1); however, at a time roughly corresponding to the end of this period, the droplet began to show vigorous bubbling and disruption (Picture 2), swelling to about twice its original size and collapsing again 5-6 times per second. In time the liquid became more viscous, hence bubbling became less intense and the droplet surface appeared to "skin over" (Picture 3). The droplet then stopped bubbling but still moved around erratically on the quartz fibre. When motion had stopped altogether, the droplet had became a highly porous, irregularly-shaped

char particle or "cenosphere" (Picture 4). At low temperatures the residue remaining had a smooth, round and glossy appearance with a somewhat porous interior and sticky surface. Apparently, the droplet had simply dried out, leaving unconverted lignin and perhaps additional material from polymerization. However, at high temperatures, the residue remaining was clearly char or "cenosphere" with a highly porous interior, and irregular shaped and a much smaller remaining mass (Figure 5.3). Changes in viscosity during heating suggest polymerization, which is known to occur when pyrolysis oils are heated (Oasmaa et al. (1999), Oasmaa et al. (2003), Boucher et al. (2000), Diebold et al. (1997), Czernik et al. (1994)). This would restrict bubble growth and internal mixing; it would also tend to prevent the escape of vapour, causing the droplet to "balloon" and swell.

Figure 5.4-5.6 illustrates the measured droplet diameters for droplets on quartz fibre, and indicates these fluctuations as mean and standard deviation at different furnace temperatures. The bubble sizes were estimated from the images by counting the pixels of the droplet image physically, and each time that the droplet swelled and collapsed was counted as a bubble. At 1123 K furnace temperature, the inside of the furnace was very bright owing to the radiation from the furnace walls; therefore, the droplet images were not good enough to determine the bubbling rate of the droplet. Consequently, the number of bubbles during the large disruption period could not be exactly specified. As mentioned previously in Chapter 4, furnace environment also causes the images appear transparent and more spread out. Hence, some error on the droplet diameter measurements in Figure (5.6) should be expected.

5.2.2 Temperature History

Figures 5.7-5.9 display the average and standard deviations of temperature records from droplet evaporation experiments on thermocouples, with events from the droplet history as observed from experiments using a quartz fibre suspension plotted below. Plotted temperature measurements are the mean and standard deviations of 10 trials. As demonstrated in an earlier chapter (Chapter 4), for 0.001" thermocouple wires the thermocouple effect is negligible, allowing direct comparison between quartz fibre and thermocouple measurements. After the droplet enters the furnace, it begins to heat up until the liquid temperature reaches a nearly constant value while the light components evaporate. After the lighter components disappear the droplet temperature rises sharply and pyrolysis begins.

As mentioned earlier in Chapter 4, in the experiments conducted by thermocouple wire approximately 10° error at the equilibrium temperature was detected. It was observed from the visual recordings that the reason for this error is the location of ceramic bead on the thermocouple: the off-center ceramic bead causes the thermocouple to measure the temperature not exactly at the droplet center. The results for the experiments conducted with pyrolysis oil using the thermocouple wire (Figure 5.10) are consistent with the result obtained from the experiments performed with pure n-hexadecane (Figure 4.2-1), and confirm that the effect of the ceramic bead is confined to the final equilibrium temperature, not the heat-up period. However, the internal mixing, bubbling and the error due to the ceramic bead contributed to the measured temperatures being higher than the predicted ones. Reasons for the possible incorrect calculation of the bubble point which will be discussed

later cause the droplet temperature to be higher than the bubble point. Nevertheless, the measurements are close to the bubbling point and the predicted liquid temperature, and superheating is not evident.

Experiments performed with pyrolysis oil droplets of different diameters showed that the shape of the liquid temperature history doesn't change regardless of changes in droplet size, although of course larger droplets undergo changes more slowly. However, the effect of the ceramic bead on the final equilibrium temperature increases slightly for droplet sizes smaller than 1.56 mm (Figure 5.11).

5.3 MODEL PREDICTIONS

Figures 5.12-5.14 compare the predicted droplet evaporation and temperature histories with the experimental timelines. The light components - aldehydes, acids, and water - evaporate simultaneously, and during this period the temperature remains nearly constant. The slow but steady rise of droplet temperature occurs as a result of fractional distillation of the acid and aldehyde groups out of the water: the more volatile components evaporate first and leave the less volatile in the liquid droplet. The bubbling period corresponds to the evolution of light components, especially water, and the amount of disruption decreases when most of the aldehyde has been evaporated. Comparing model and experiment results, the period of the evaporation agrees well with the observed bubbling and disruption period, confirming that this results from the evolution of light species.

The effects of the distillation of light components can also be seen in the changes in composition of the individual distributions in the liquid, shown in Figure (5.15). During the first stage of the model the concentrations in the liquid are non-uniform and therefore the graph shows the average, while during the well-mixed stage concentration becomes the average by definition. The average molecular weights $\bar{\theta}_{Lj}$ of the acid and aldehyde groups remaining in the liquid rise nearly linearly and the standard deviations decrease as vaporization progress, which also contributes to a steady increase in temperature. Evaporation of the light fractions decreases the width of the distribution ($\bar{\sigma}_{Lj}$) steadily. The composition of the acid group shows initially little change, but later the average rises sharply as a result of the distillation of both the water and aldehyde groups, and for the same reason its standard deviation decreases sharply. The lignin and water compositions are not shown in Figure 5.15 because they both have nearly constant and uniform values of $\bar{\theta}_{Lj}$, the water because it is a pure component, and the lignin because it essentially doesn't evaporate at all. However, water dominates the process thermally because of its very high enthalpy of vaporization, and this keeps the temperature close to the boiling point of water until the volatile components have evaporated. The lignin remaining evaporates very little because of its high molecular weight, so that the temperature then rises sharply and pyrolysis begins, converting lignin to char and gas. The predicted droplet evaporation and temperature histories agree well with the visual observations and temperature measurements, and confirm that the temperature rises as a result of the evaporation of light fractions.

The bubbling / disruptions indicate internal boiling, which can occur because of the differences in composition between the surface and interior of the droplet. After the initial

heating period, the droplet surface layer loses the light components of the fuel and becomes capable of being heated to higher temperatures. The lighter inner core then has a lower bubble point than the surface, so that vapour bubbles can be formed by internal vaporization of the lighter components. The slow rate of diffusion in the liquid means that large concentration differences can occur during initial heating; however, after bubbling begins, it should cause fairly vigorous mixing.

Fig. 5.16-5.18 represent the gas and vapour evolution rates from the droplet presented as droplet volumes per second to allow rough comparison with bubbling. The difference in predicted concentrations between the present model and well-mixed model causes a sudden increase in the results at the time bubbling begins. During the initial heating period most of the heat arriving at the droplet surface is used for droplet heating; therefore vaporization is slow. During the bubbling period, for a 1.56 mm pyrolysis oil droplet evaporating at 773 K, from visual observations of the bubbling rate (6-7 per second) and bubble volume, the vapour flux associated with the bubbles was estimated at roughly 25 droplet volumes / sec. The bubble volume was estimated by measuring the diameter physically on the images and multiplying this volume by bubbling rate. The fluxes in Figure 5.16 are substantially larger, suggesting that most evaporation still takes place from the droplet surface. Lower bubbling rates later on correspond to reduced vapour production rates because of the removal of light components, although ongoing polymerization of the fuel, as indicated by the increasingly viscous nature of the surface, would also be expected to decrease vapour pressures. At higher temperatures, vapor is being evolved more quickly and this results in an increase on the rate of bubbling, and the vapour flux. The results are evident in Figure 5.17 and 5.18. From the

visual observations, the vapor flux associated with the bubbles was estimated at roughly 55 and 65 droplet volumes / sec at 1023 and 1123 K furnace temperatures.

5.4 LIQUID PHASE COMPOSITION PROFILE

Figure (5.19) shows that the evaporation of the lightest component – the aldehyde group, which is more volatile than the acid group or the water - increases the mol fraction of the heavier components - water and acids, also lignin - at the surface. The mol fraction of aldehydes varies the most time-wise, because this group is evaporating most rapidly, then comes water, which is evaporating more rapidly than the acids (see Fig. 5.12), and finally the acids vary the least because they aren't evaporating quickly at this point. During the pre-bubbling period, the distribution mean θ_L of the aldehyde and acid groups increases at the surface by the evaporation of light components while the water and lignin compositions remain nearly constant (Fig. 5.20). As vaporization progress, the mol fractions of the light component (aldehydes) keep falling while those of the heavier components increase. Figure 5.21 shows the variation of mean and surface mol fraction with time. Since aldehydes are more volatile, they evaporate much more than the other components during the pre-bubbling period; therefore, the mol fraction of aldehydes falls while the mol faction of water and acid groups increases at the surface. Figure 5.22 shows the liquid distribution mean and standard deviation at the droplet surface θ_{LR} and σ_{LR} for aldehydes and acids with time. The more volatile components leave the droplet at a fast rate and leave in the mixture the less volatile components, which leads to the decrease in σ_{LR} (narrower distribution).

The Law and Law (1981) model is based on the assumptions that the concentration changes are limited to a thin surface layer and that the concentration profiles are approximately quasi-steady. Owing to the slow rate of liquid-phase mass diffusion, concentrations vary steeply close to the droplet surface, but rapidly approach to their initial values when moving inward and remain at that condition until approached by the receding surface. Comparing the present model with their solution based on these assumptions, the difference in mol fraction and liquid distribution values between the droplet center and surface was found to be less than those found by Law and Law (1981). The main reason is their analytical solution did not conserve component mass in the droplet, but in present model mass conservation was assumed. However, the present model predictions were found to be reasonable comparing to the numerically calculated composition profiles by Abdel-Qader and Hallett (2005).

5.5 MODEL BEHAVIOUR

The present model assumes a liquid-phase mass diffusion-controlled solution during the pre-bubbling period, and calculated the liquid and vapour phase concentration as described in Chapter 3. By the time bubbling starts, the model switches to the earlier model, developed by Hallett and Clark (2006) with the assumption of well-mixed liquid phase. In this section, the results calculated by the present and the earlier model were compared.

Figure 5.23 shows that the present model temperature history is slightly higher at the equilibrium temperature than the earlier model. After the start of bubbling at 2.26 sec, the temperature histories predicted by the present model become identical to those of the well-mixed model. However, this difference between the two models was not observed at higher

temperatures, because the droplet starts bubbling after a very short initial heating period and the present model runs for a very short time. At all furnace temperatures (Figures 5.24-5.25), the predicted droplet temperature of the present model rises earlier than that of the well-mixed model. Figure 5.26 shows that the present model predicts the evaporation rate of aldehydes higher than that of earlier model, and relatively the water mol fraction is smaller while that of acids remains the same. Small differences in the mol fraction during the pre bubbling period effects the temperature history as well as the liquid distribution values (Figure 5.27). Consequently, the changes from the earlier model are found to be small because the differences in concentration between the centre and surface are small.

5.6 THE LOCATION AND TIMING OF BUBBLING

The intensity of liquid mixing and internal motion has an important role on the overall droplet lifetime. Internal circulation can be produced during the initial, violent atomization process or arise as a result of the natural or forced convective gas flow which is induced by shear stress at the droplet surface. In our experiments, while generating the droplets by a syringe and suspending them on a suspending fibre, some small degree of internal circulation would occur. However, for modeling purposes, it is assumed that the internal circulation does not exist during the initial heating period, but that after the vigorous bubbling and disruption begins the fuel becomes well-mixed. In case of the absence of internal circulation, non-uniform temperature and species profiles exist within the droplet. Nonetheless, the liquid-phase thermal diffusivity is almost 2 orders of magnitude larger than the mass diffusivity (Le>>1), which makes the uniform temperature assumption within the droplet reasonable. These assumptions together with the ideal mixture phase equilibrium assumption were used

to model the pre-bubbling period in order to gain some insight into the onset and location of bubbling. After the droplet was exposed to the hot environment, the liquid temperature and differences in composition between the surface and interior of the droplet increased, which in turn causes the inner core to have a lower bubble point than the surface (Fig. 5.28-5.30). The droplet will start bubbling where and when the droplet temperature reaches the bubble point, in other words, at the intersection point of those two temperature curves. The pyrolysis oil includes polar components such as water and aldehyde group, which makes the ideal mixture phase equilibrium assumption inaccurate. Because of this, comparing the visual observations and the model results, the predicted time at which bubbling began was found to be over-predicted. Therefore, a crude correction was applied by subtracting approximately 22° degrees from the bubble point temperatures, this correction being the value that made the predicted onset of bubbling agree with the experiments at 500°C. Subtracting the same correction from the bubble point at all experimental conditions is reasonable, because the temperature and composition of the droplet at the onset of bubbling are similar for the different experiments. Figure 5.28 shows the predicted results. The difference between the predicted and measured bubbling time results vary within a range of 0.1-0.4 s for three different furnace temperatures. At high temperatures and smaller droplet sizes, the predicted results are relatively more accurate. Comparing the model and experiment results, agreement of the overall droplet evaporation lifetimes was achieved.

5.7 PYROLYSIS RATE

For modelling purposes, pyrolytic lignin is assumed to pyrolyze to gas and char according to a single first-order reaction:

$$\frac{dL}{dt} = -KL\,exp(-E/RT) \qquad (5.7\text{-}1)$$

where L is the fraction of original lignin unconverted. Each kg of lignin produces ς_C kg of char and $(1-\varsigma_C)$ kg of gas. The pyrolysis rate parameters K and E and the char yield ς_C were estimated as described by Hallett and Clark (2006) from measurements of the residue mass remaining after droplet evaporation at different temperatures. Some droplets were withdrawn from the furnace and the residue mass measured shortly after the bubbling ceased, while others were left in the furnace five times longer ("long term exposure") at low temperatures and three times longer at high temperatures; the intention of this was to try to mark the temperature range at which pyrolysis goes from being slow to rapid. For predictions the end of bubbling period was defined as the time at which the light components had disappeared plus 6 seconds, estimated by comparing the experimental timeline with the predicted droplet evaporation history.

As shown in Figure 5.31, below 673 K the residue mass is large and does not change with increasing exposure, indicating that the droplet is simply "drying out" and not pyrolyzing. However, at 673 K the mass significantly drops with longer exposure, indicating that slow pyrolysis is beginning. Above about 873K the difference caused by longer exposure decreased and the residues became highly porous and hollow. Using the numerical model with these observations, rate parameters were roughly chosen as **E=200 kJ/mol** and **K =1x10^{15} s^{-1}**, and the char yield from pyrolysis was found as ς_C **= 0.5,** obtained from the ratio of the mass of lignin to char. Model predictions of residue in Figure 5.31 show that the chosen rate parameters give reasonable agreement with the measured trends. The literature

gives activation energies for lignin ranging from 20 (Órfão et al., 1999) to 50 (Grønli et al., 2002) to 250 (Avni et al., 1985) kJ/mol. Lower values such as 50 kj/kmol used by Grønli et al. (2002) gave excessively long pyrolysis times at high temperature or too rapid pyrolysis at low temperatures, depending on the value of pre-exponential value K used. Since the pyrolytic lignin in the fuel is chemically different from the lignin in wood, it is reasonable to expect different kinetics.

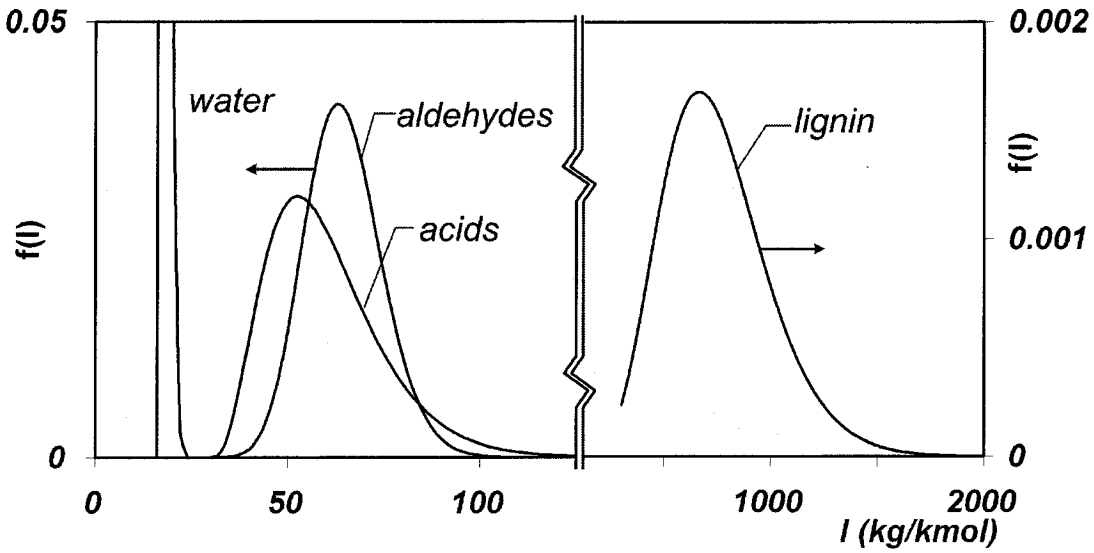

Figure 5.1: Distribution functions used to simulate biomass pyrolysis oils.

Table 5.1: Assumed composition of pyrolysis oils.

Group	θ_{L0}	σ_{L0}	γ	w_{L0}
aldehydes/ ketones	65	10	0	0.25
carboxylic acids	60	15	30	0.15
water	18	1	16	0.30
Pyrolytic lignin	750	250	0	0.30

Picture 1: The Initial Heating Period

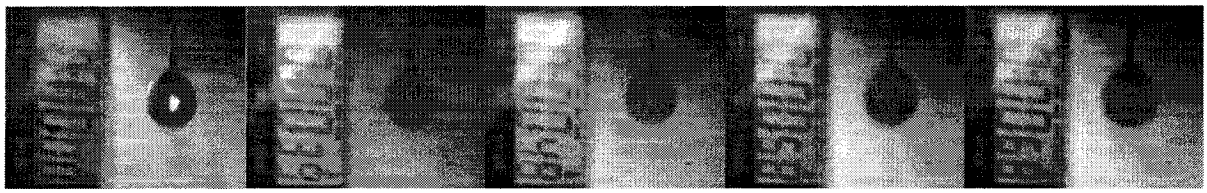

Picture 2: The Bubbling/Disruption Period

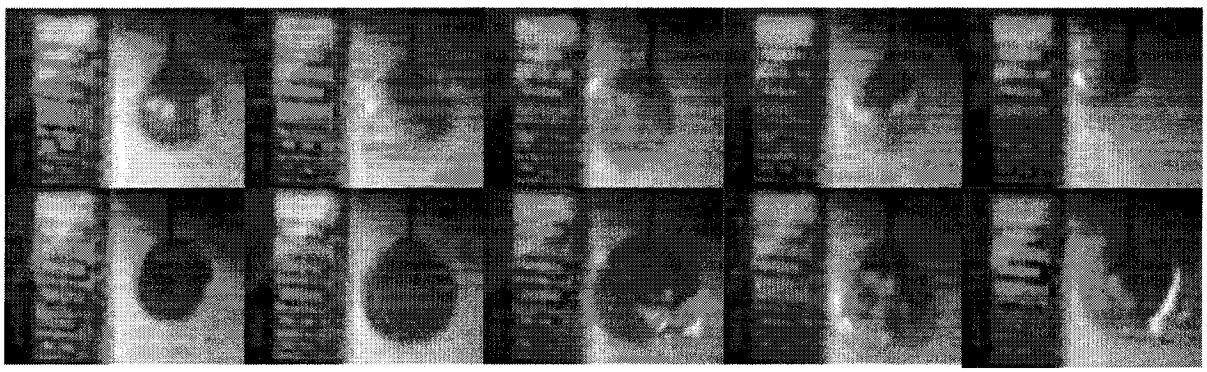

Picture 3: Later Stages

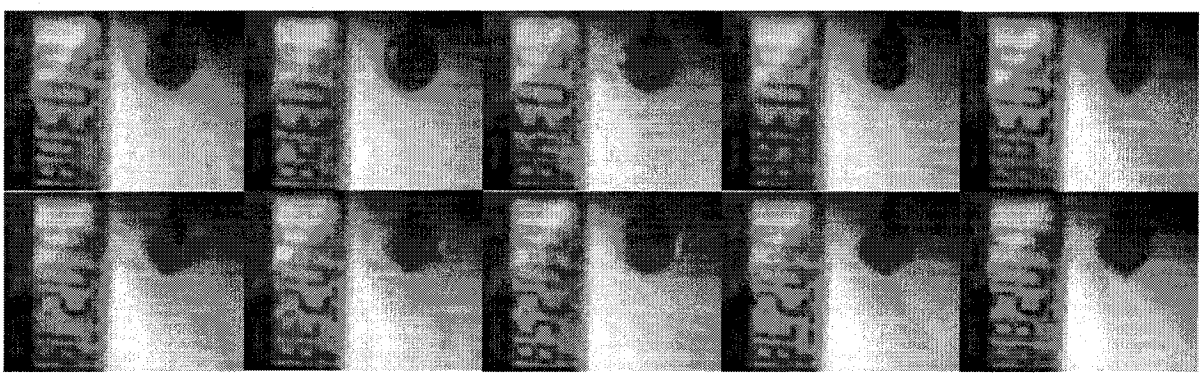

Picture 4: Char Particle / Cenospehere

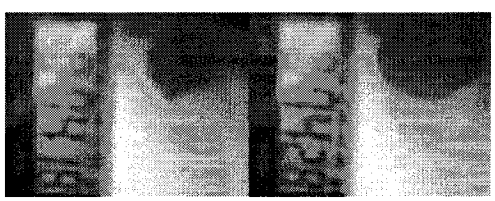

Figure 5.2: Observed evaporation behaviour of a 1.56 mm droplet on quartz fibre at 750 °C.

100 ° C

300 ° C

400 ° C

750 ° C

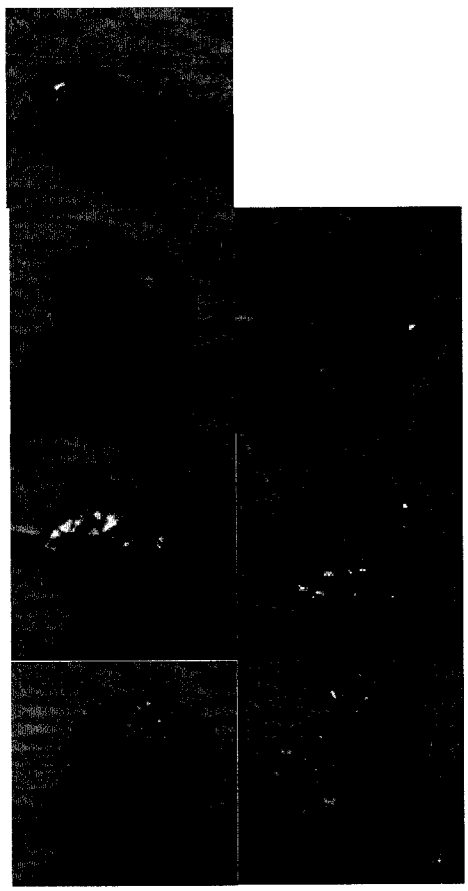

Figure 5.3: Residue remaining at different furnace temperatures for 1.7 mm bio-oil droplet.

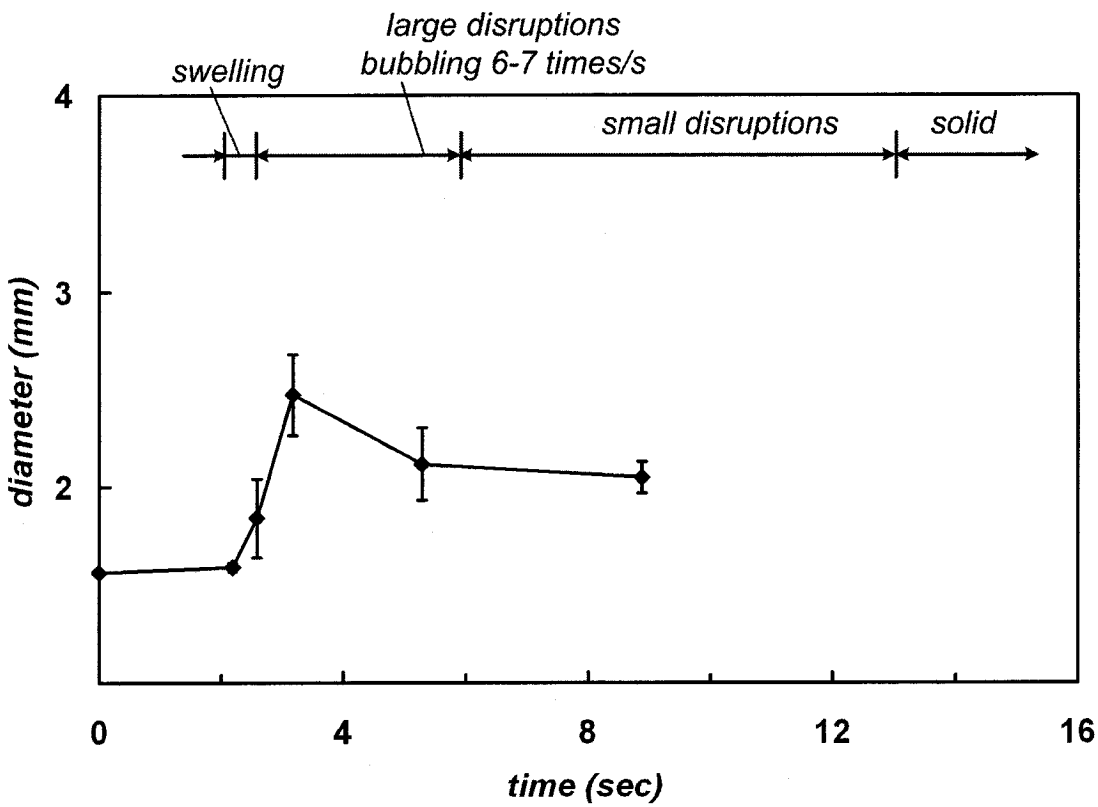

Figure 5.4: Measured droplet diameter and observed behaviour vs. time, 1.56 mm bio-oil droplet on quartz fibre at 773 K. Means and standard deviations of 8-10 trials.

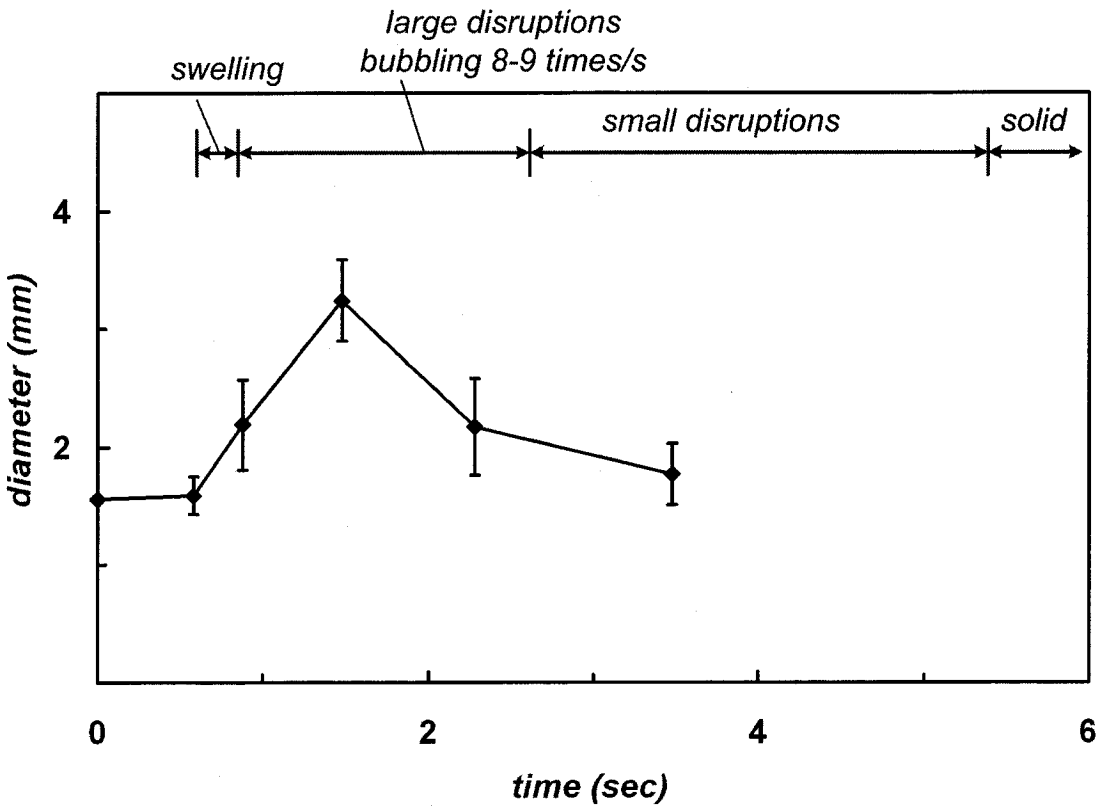

Figure 5.5: Measured droplet diameter and observed behaviour vs. time, 1.56 mm bio-oil droplet on quartz fibre at 1023 K. Means and standard deviations of 8-10 trials.

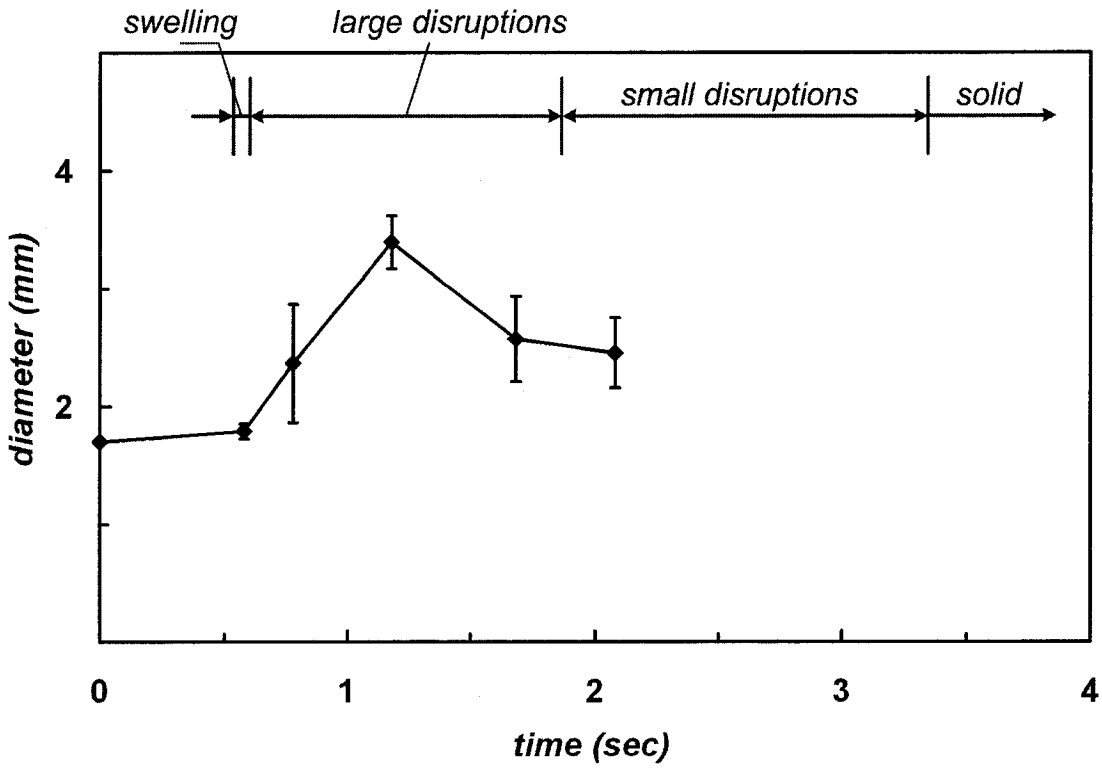

Figure 5.6: Measured droplet diameter and observed behaviour vs. time, 1.7 mm bio-oil droplet on quartz fibre at 1123 K. Means and standard deviations of 8-10 trials.

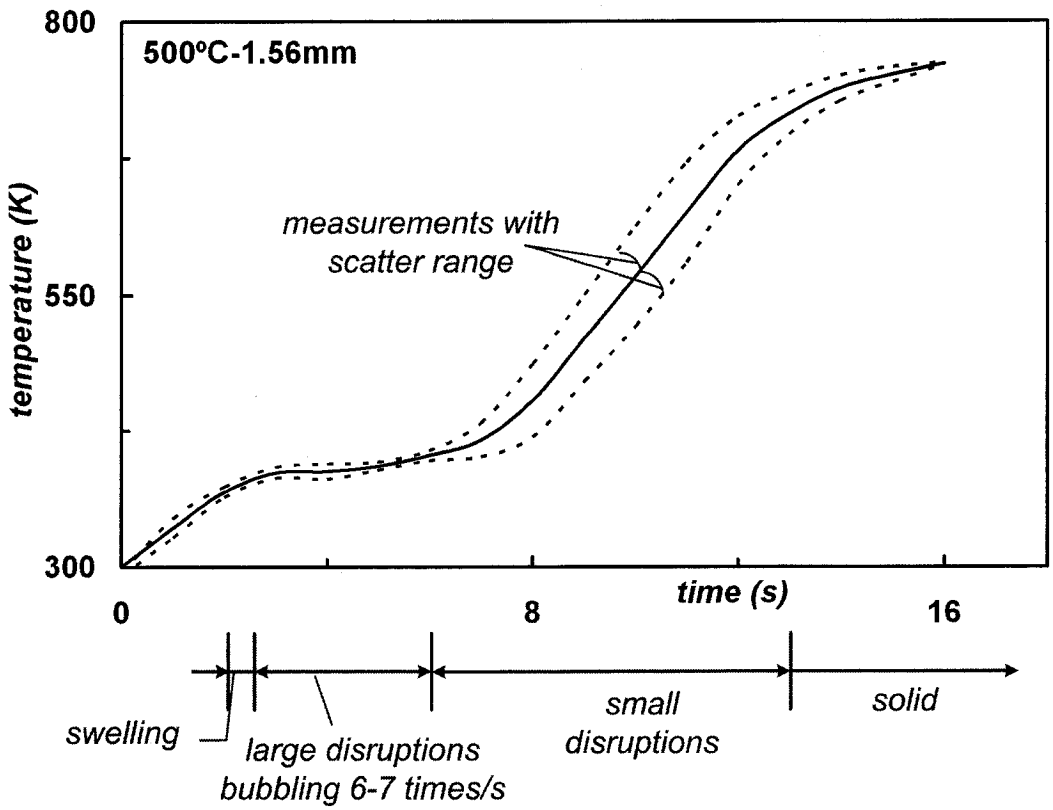

Figure 5.7: Measured temperature for 1.56 mm droplet on 0.001" thermocouple wire at 773 K. Measurements are average and standard deviation of 10 trials. Observed droplet behaviour on quartz fibre at the same conditions plotted below time scale. Initial droplet is at 300K.

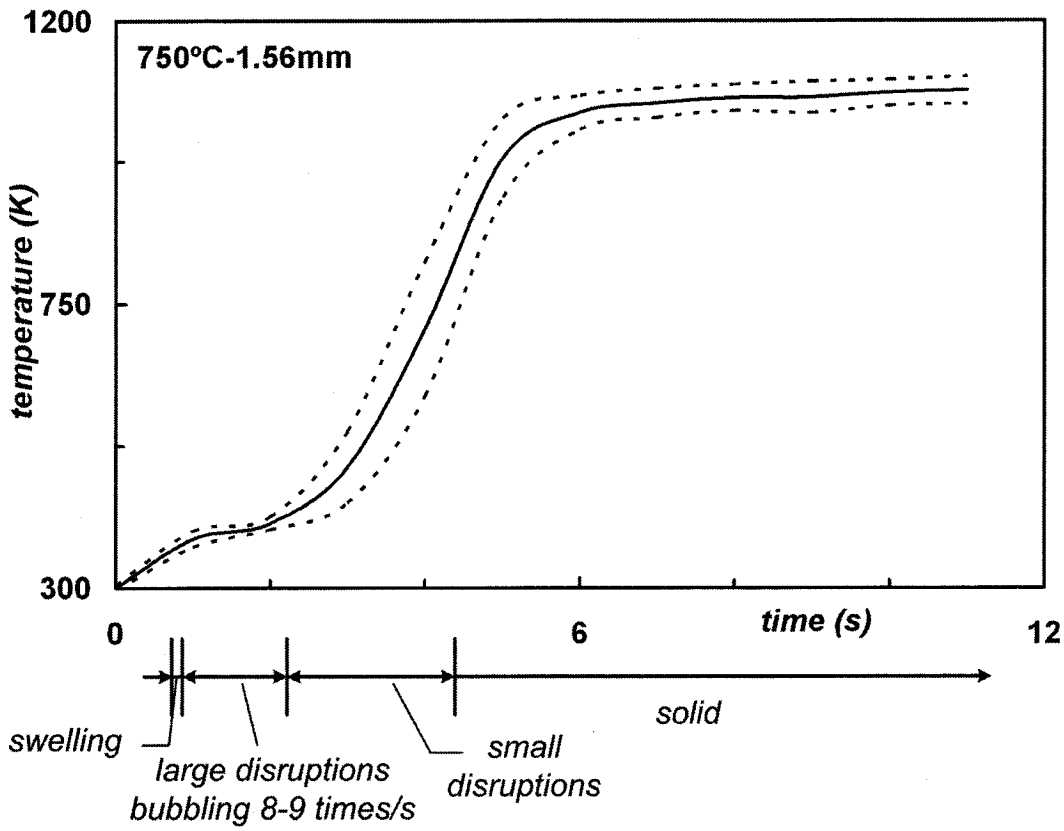

Figure 5.8: Measured temperature for 1.56 mm droplet suspended on 0.001" thermocouple wire at 1023 K. Measurements are average and standard deviation of 10 trials. Observed droplet behaviour on quartz fibre at the same conditions plotted below time scale.

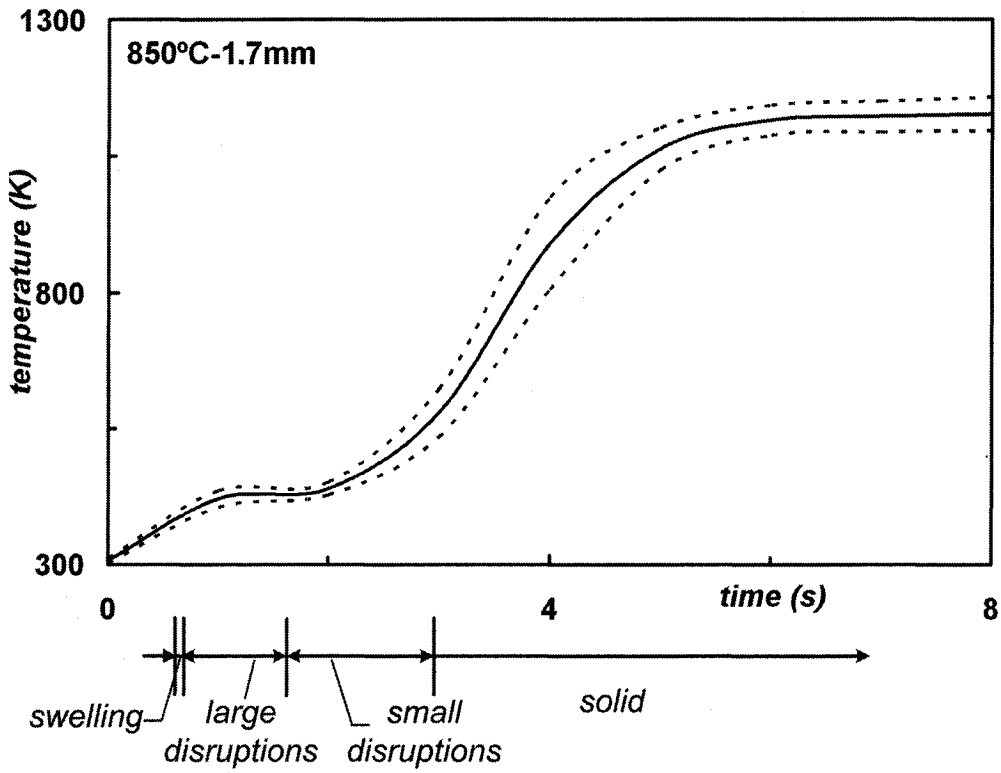

Figure 5.9: Measured temperature for 1.7 mm droplet suspended on 0.001" thermocouple wire at 1123 K. Measurements are average and standard deviation of 10 trials. Observed droplet behaviour on quartz fibre at the same conditions plotted below time scale.

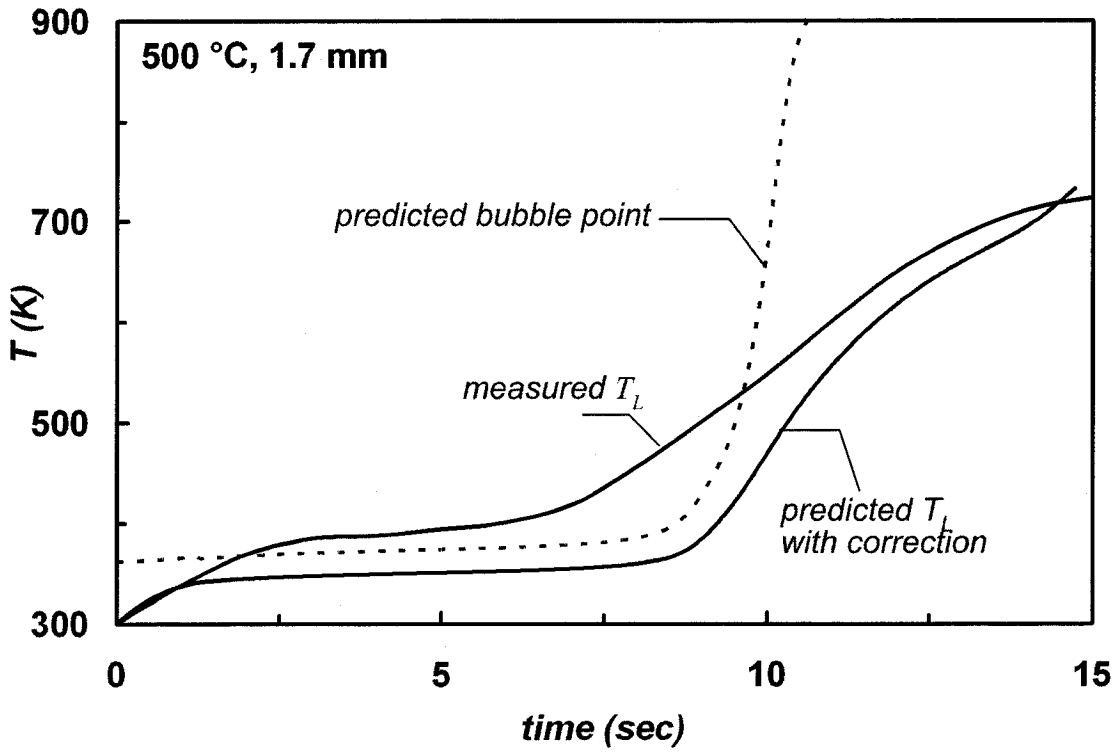

Figure 5.10: Predicted droplet temperature and boiling point compared with temperature measured by a 0.025mm (0.001") thermocouple supporting the droplet, for a 1.7 mm pyrolysis oil droplet evaporating at 773 K. The predictions include an estimate of the additional heat transfer to the droplet through the thermocouple.

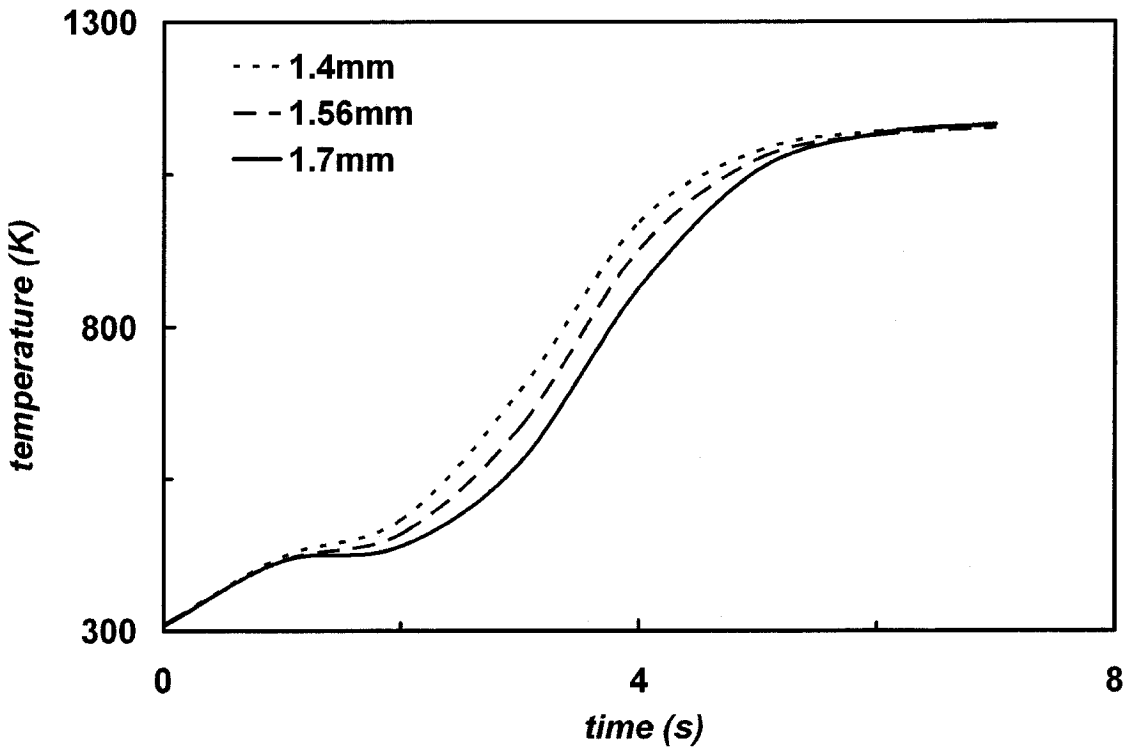

Figure 5.11: Measured temperature for 1.4, 1.56, and 1.7 mm droplets on 0.001" thermocouple wire at 1123K. Measurements are average of 10 trials.

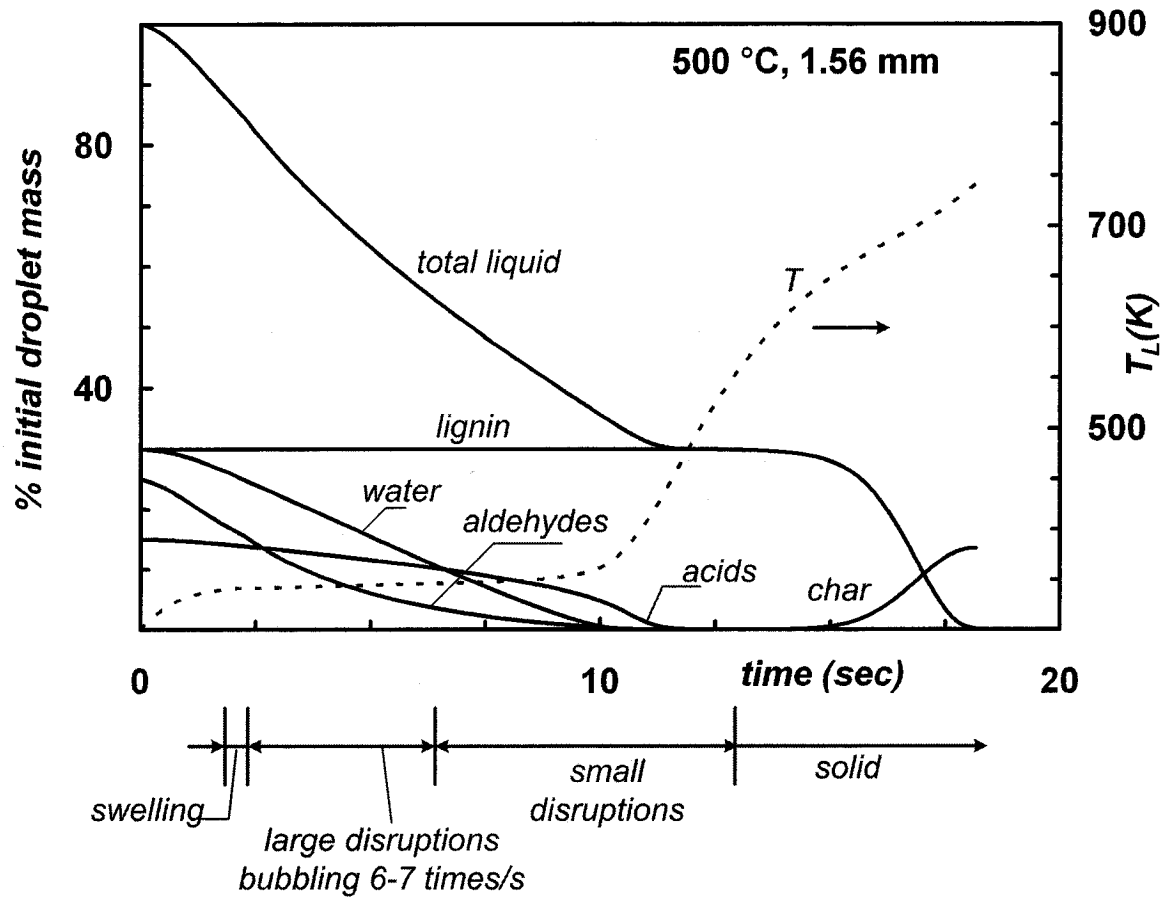

Figure 5.12: Predicted droplet composition (expressed as fractions of initial droplet mass) and temperature as a function of time for a 1.56 mm pyrolysis oil droplet evaporating at 773 K. Observed droplet behaviour plotted below time scale. Initial droplet temperature 300 K.

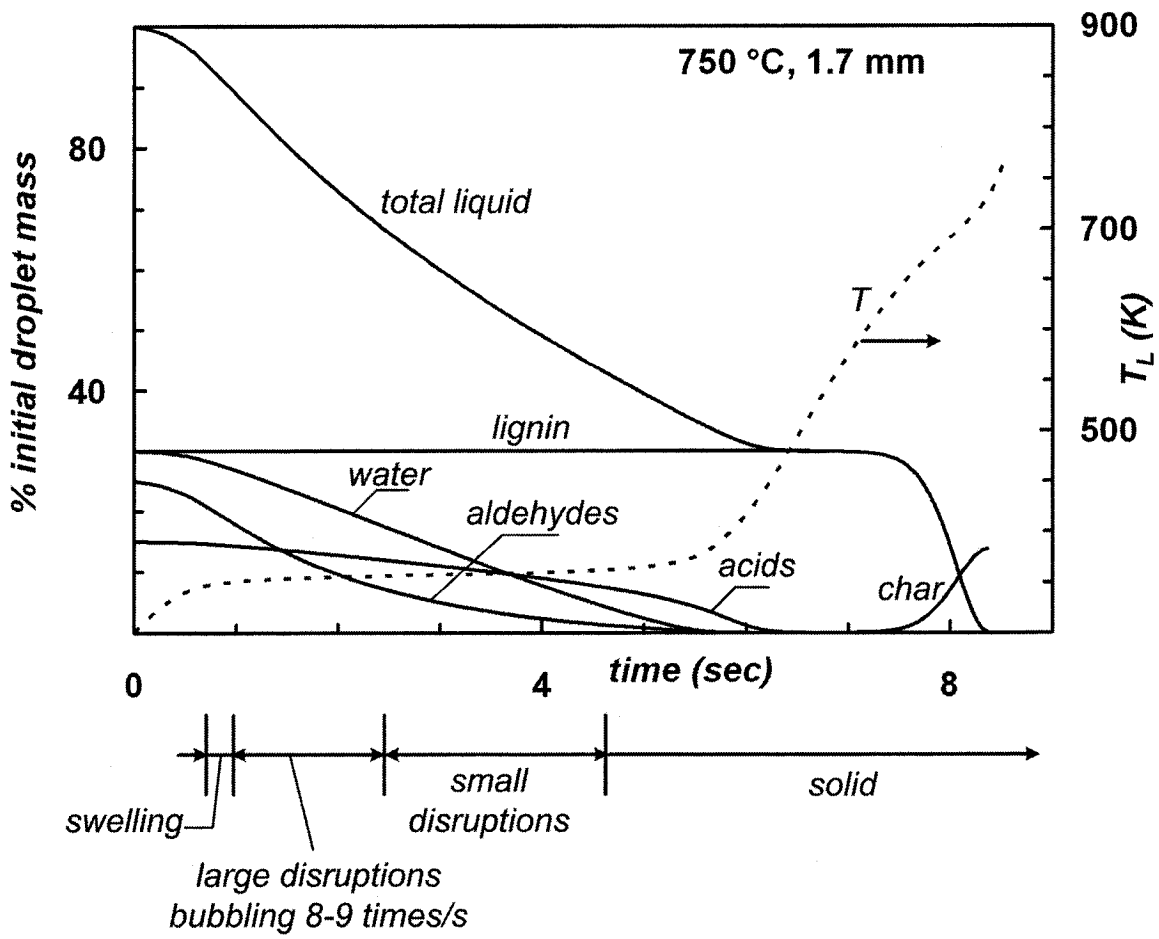

Figure 5.13: Predicted droplet composition (expressed as fractions of initial droplet mass) and temperature as a function of time for a 1.7 mm pyrolysis oil droplet evaporating at 1023 K. Observed droplet behaviour plotted below time scale. Initial droplet temperature 300 K.

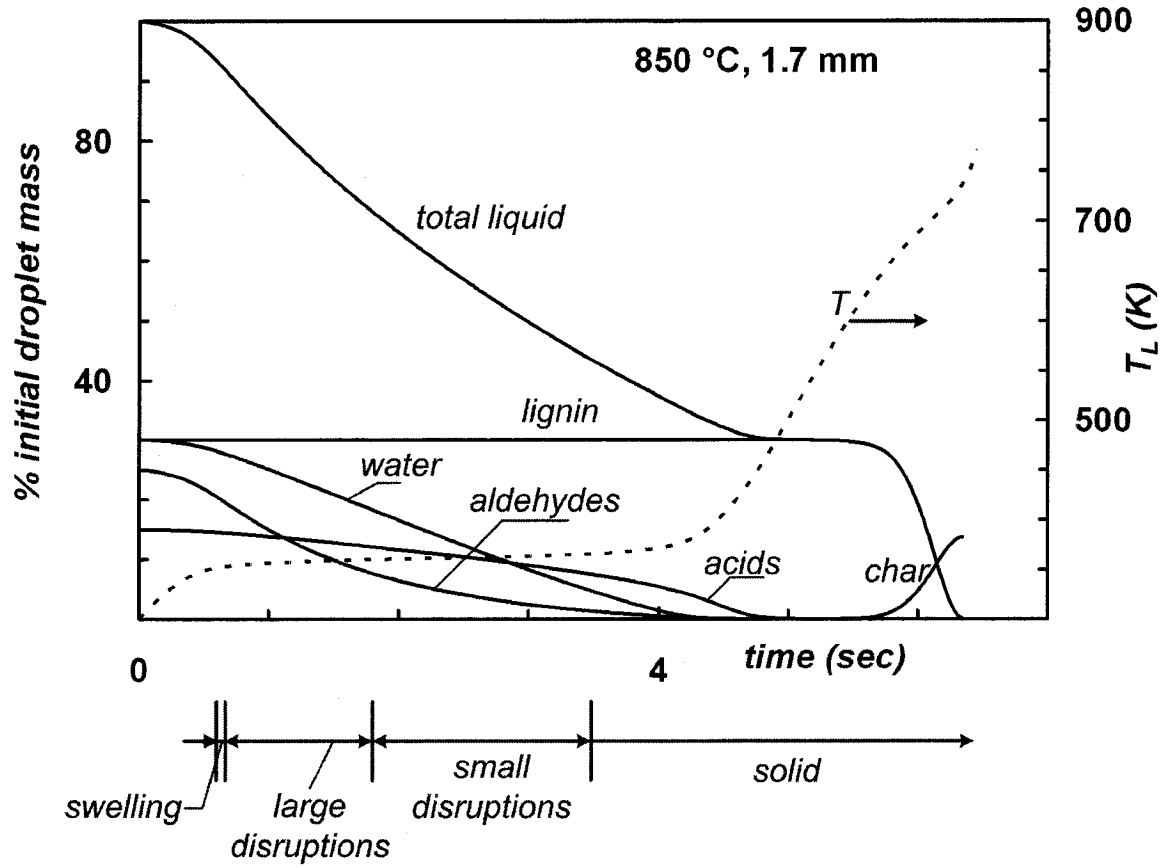

Figure 5.14: Predicted droplet composition (expressed as fractions of initial droplet mass) and temperature as a function of time for a 1.7 mm pyrolysis oil droplet evaporating at 1123 K. Observed droplet behaviour plotted below time scale. Initial droplet temperature 300 K.

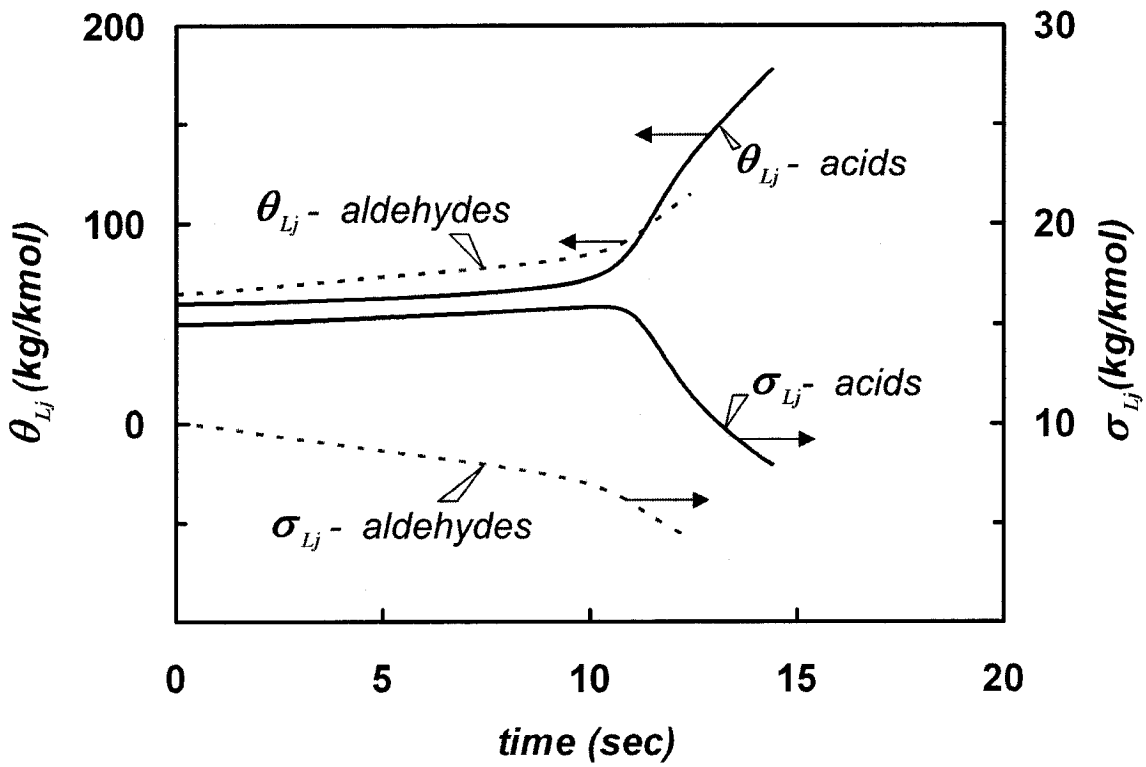

Figure 5.15: Predicted acid and aldehyde fraction distribution parameters θ_{Lj} and σ_{Lj} as functions of time for 1.56 mm pyrolysis oil droplet evaporation at 773 K. Initial droplet temperature 300K.

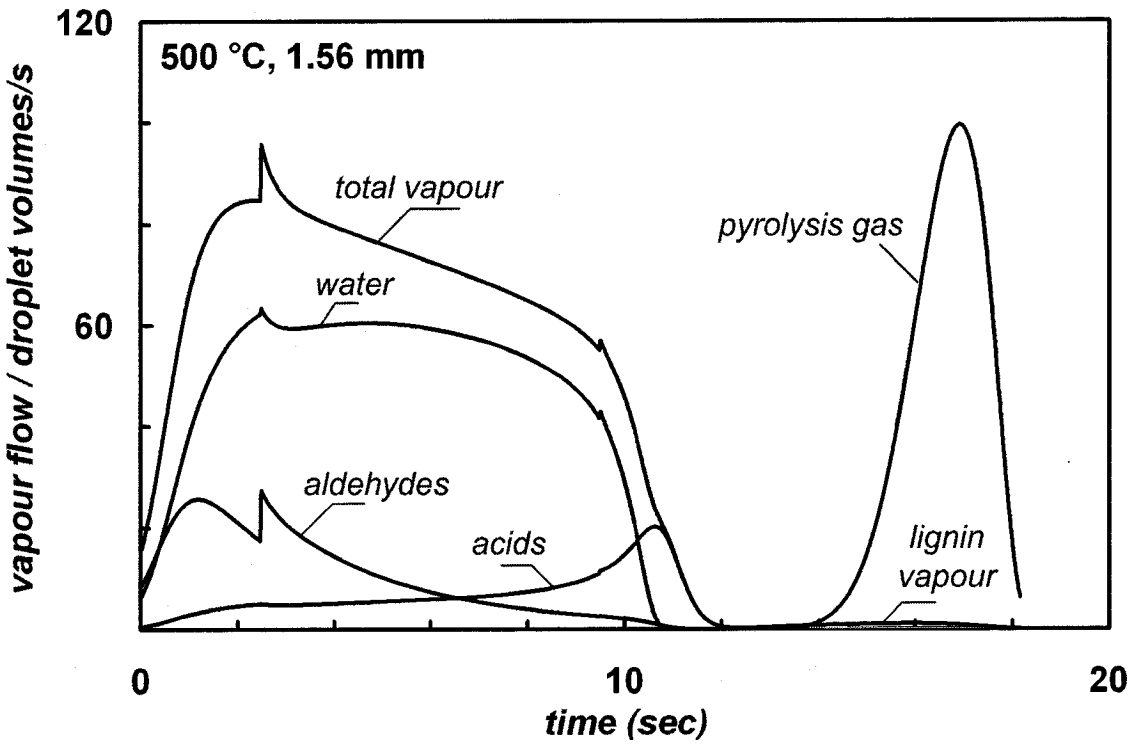

Figure 5.16: Predicted vapour and pyrolysis gas evolution rates, expressed in initial droplet volumes per second, for a 1.56 mm pyrolysis oil droplet evaporating at 773 K. Initial droplet temperature 300 K.

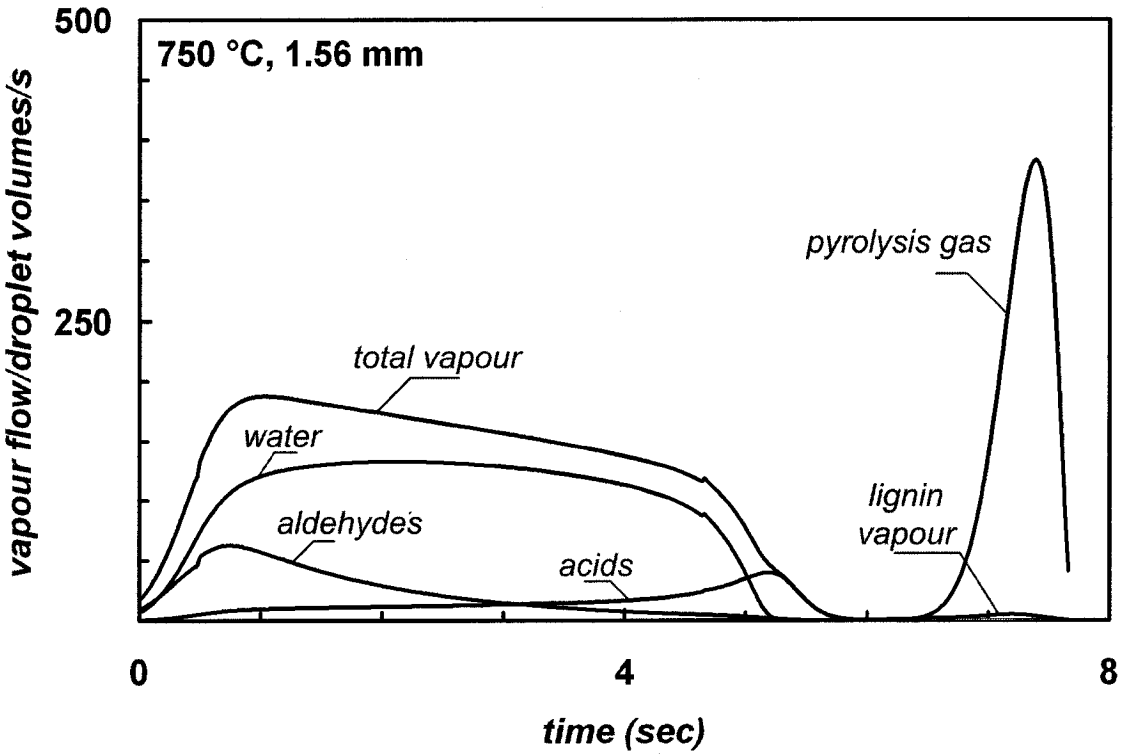

Figure 5.17: Predicted vapour and pyrolysis gas evolution rates, expressed in initial droplet volumes per second, for a 1.56 mm pyrolysis oil droplet evaporating at 1023 K. Initial droplet temperature 300 K.

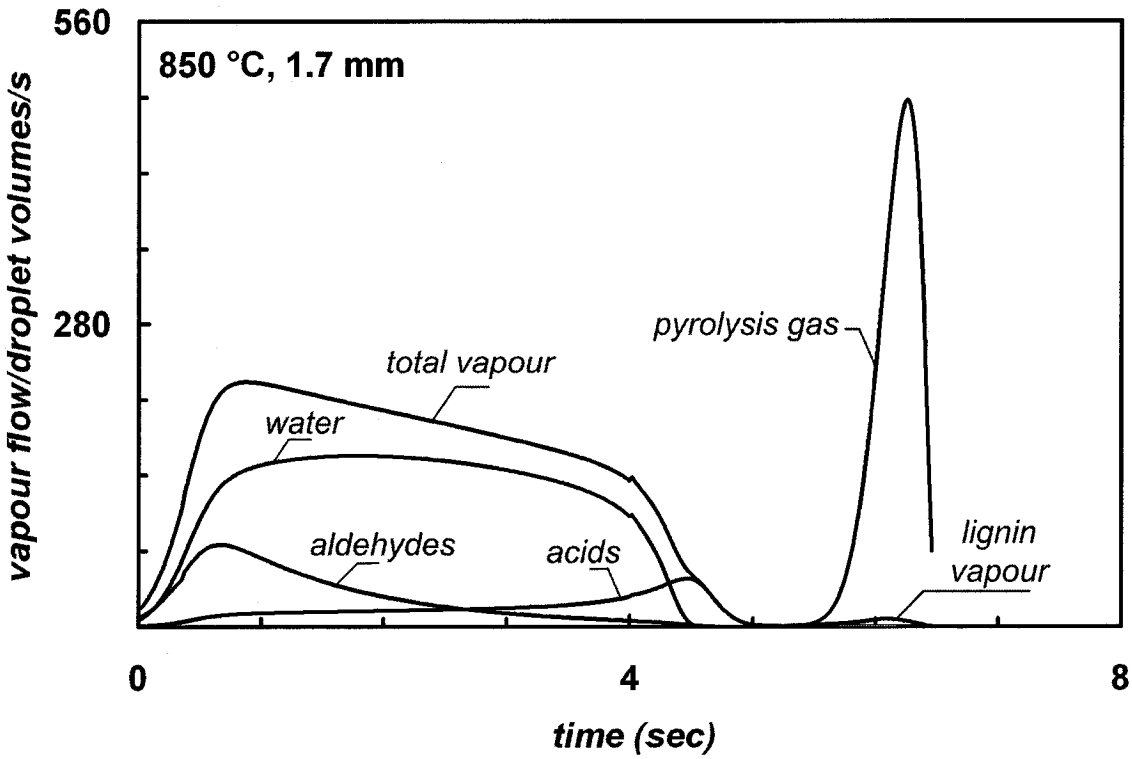

Figure 5.18: Predicted vapour and pyrolysis gas evolution rates, expressed in initial droplet volumes per second, for a 1.7 mm pyrolysis oil droplet evaporating at 1123 K. Initial droplet temperature 300 K.

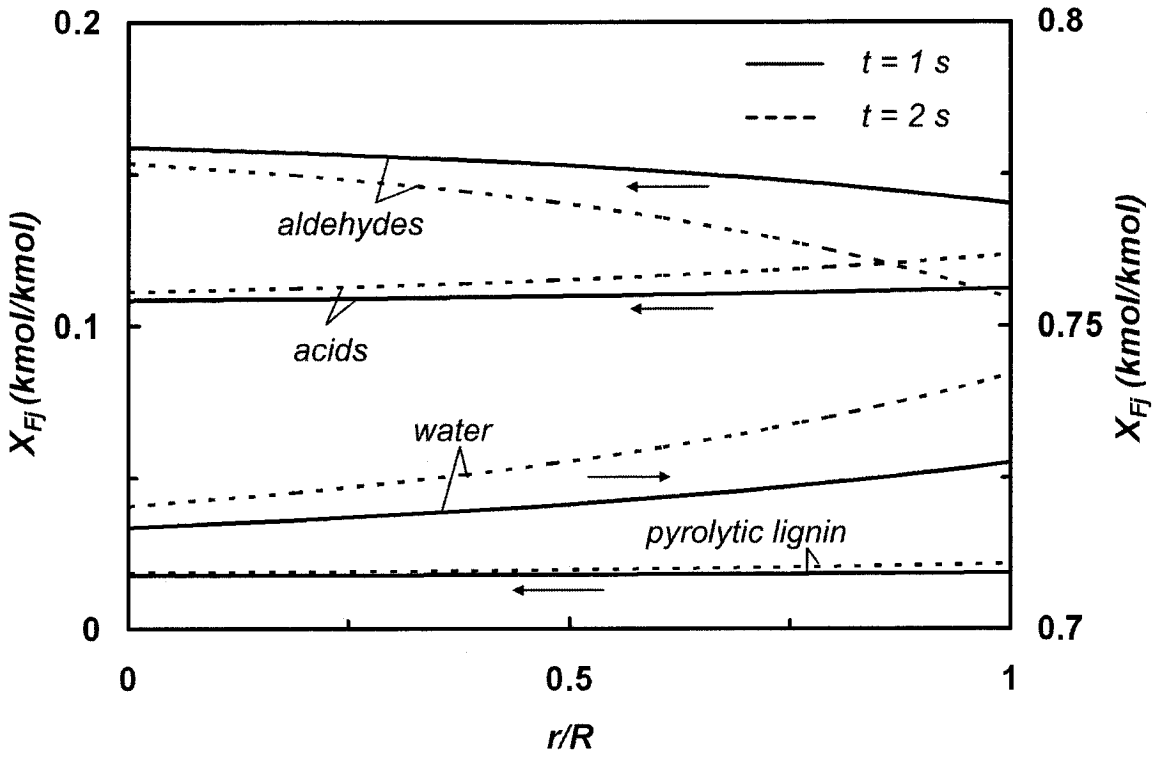

Figure 5.19: Radial profiles of predicted mol fractions x_j within droplet at times t = 1 s and 2 s for each chemical group. 1.56 mm droplet, initial temperature 300 K, ambient temperature 773 K.

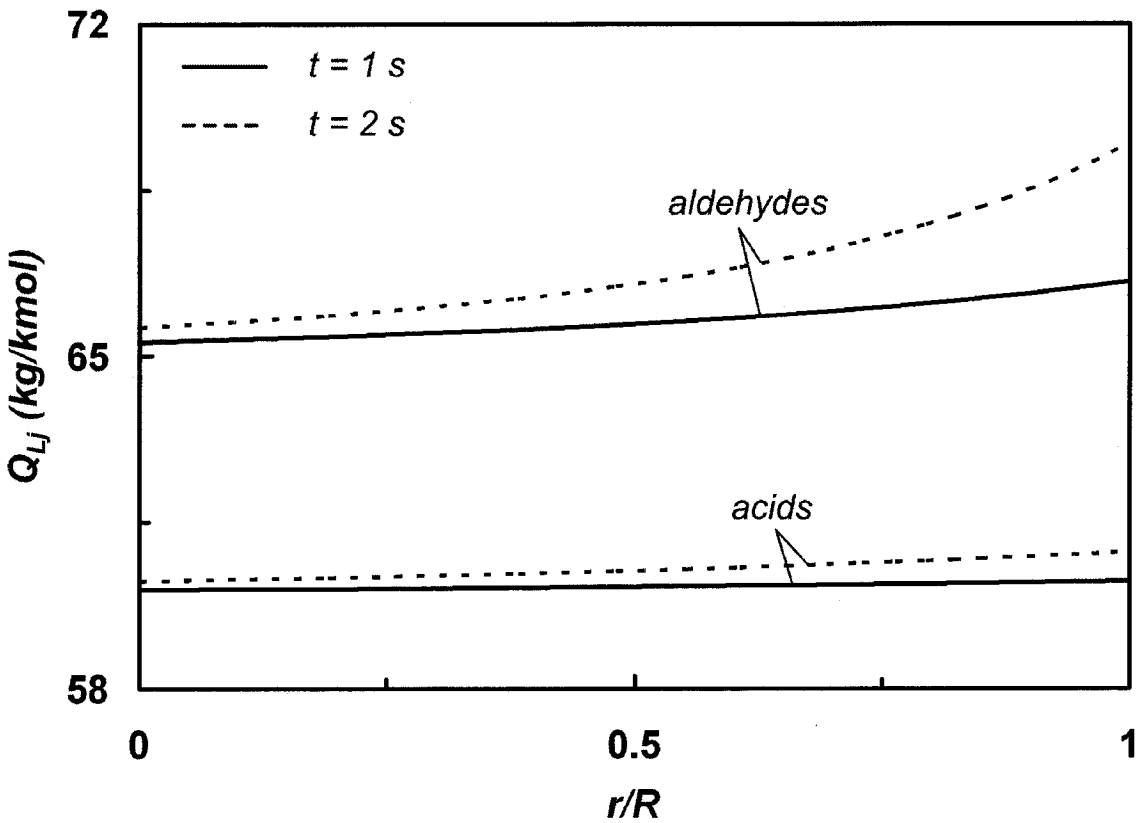

Figure 5.20: Radial profiles of predicted distribution means θ_{Lj} within droplet at times t = 1 s and 2 s for aldehyde and acid fraction. 1.56 mm droplet, initial temperature 300 K, ambient temperature 773 K.

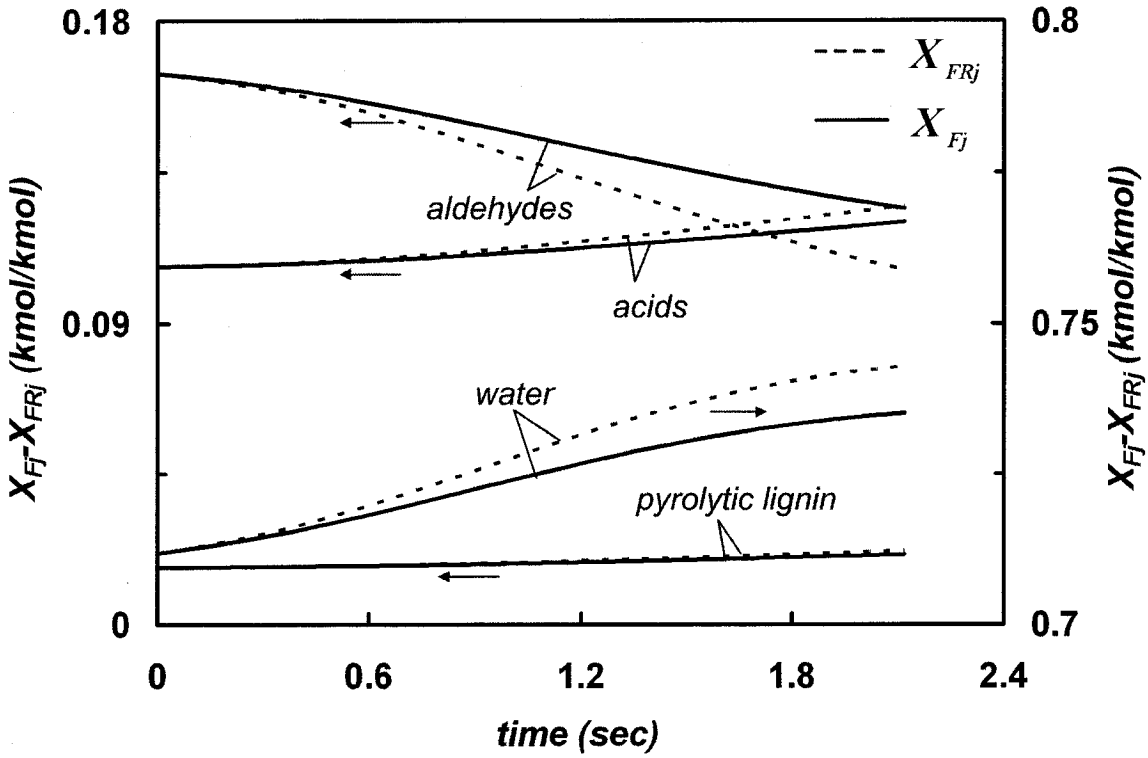

Figure 5.21: Predicted mean and surface mol fraction x_{Fj} and x_{FjR} against time. 1.56 mm droplet, initial temperature 300 K, ambient temperature 773 K.

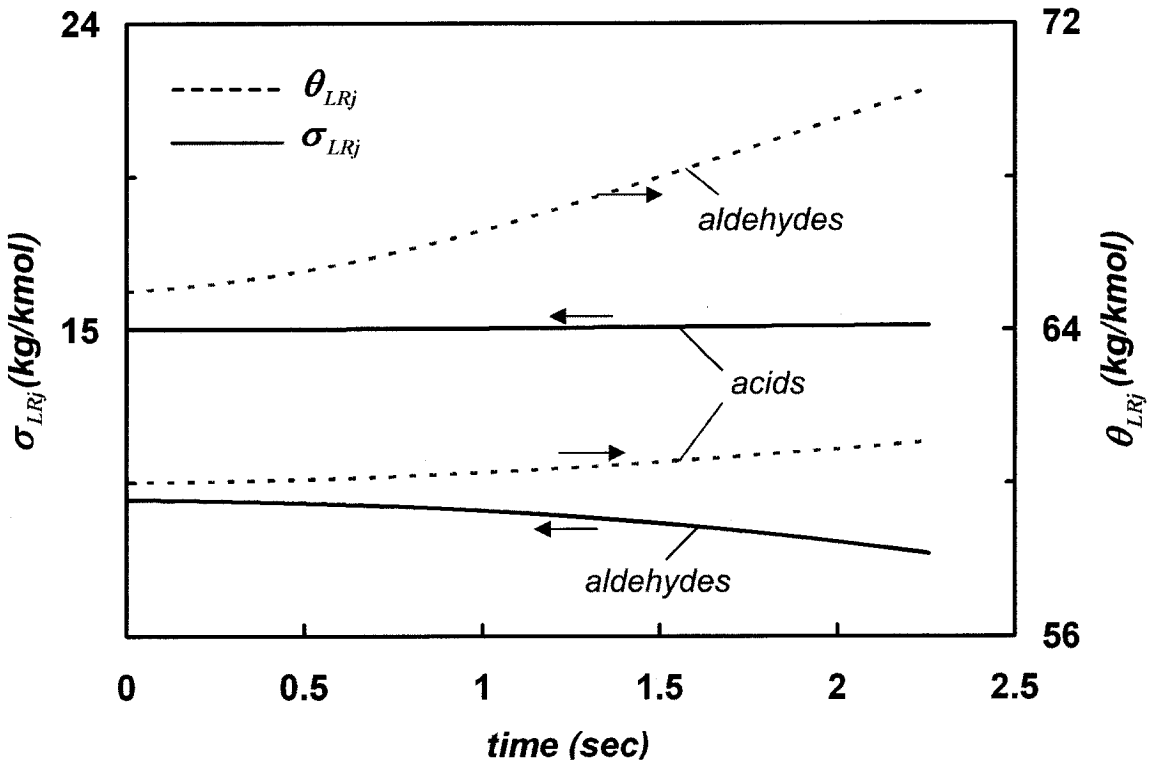

Figure 5.22: Liquid distribution means θ_{LjR} and standard deviations σ_{LjR} at the droplet surface for the aldehyde and acid fraction. 1.56 mm droplet, initial temperature 300 K, ambient temperature 773 K.

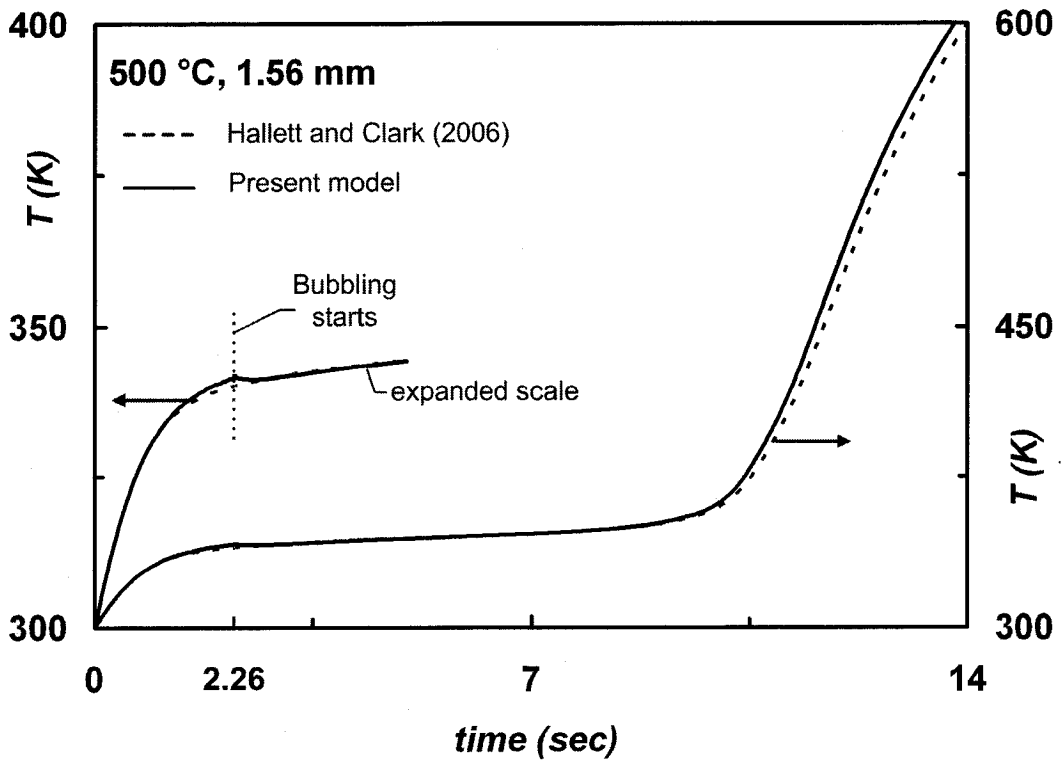

Figure 5.23: Droplet temperature vs. time for 1.56 mm pyrolysis oil droplet, showing the difference between the present model and the earlier model. Initial temperature 300 K, ambient temperature 773 K. Upper curve shows initial part of temperature history with scale expanded.

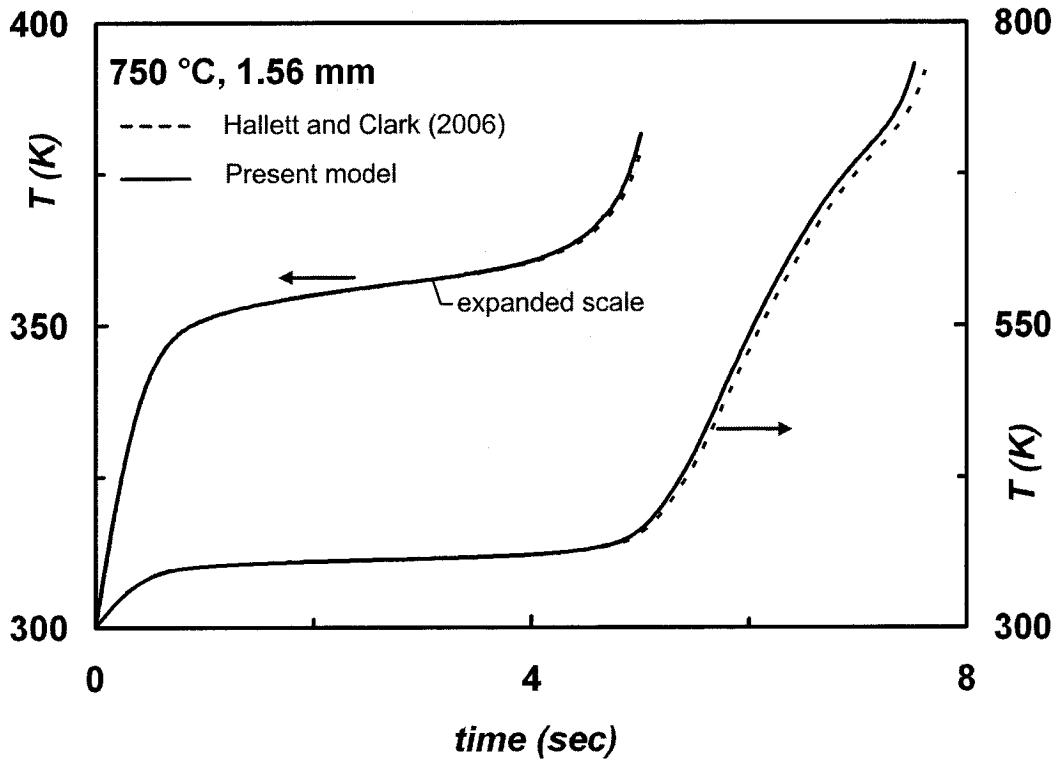

Figure 5.24: Droplet temperature vs. time for 1.56 mm pyrolysis oil droplet, showing the difference between the present model and the earlier model. Initial temperature 300 K, ambient temperature 1023 K. Upper curve shows initial part of temperature history with scale expanded.

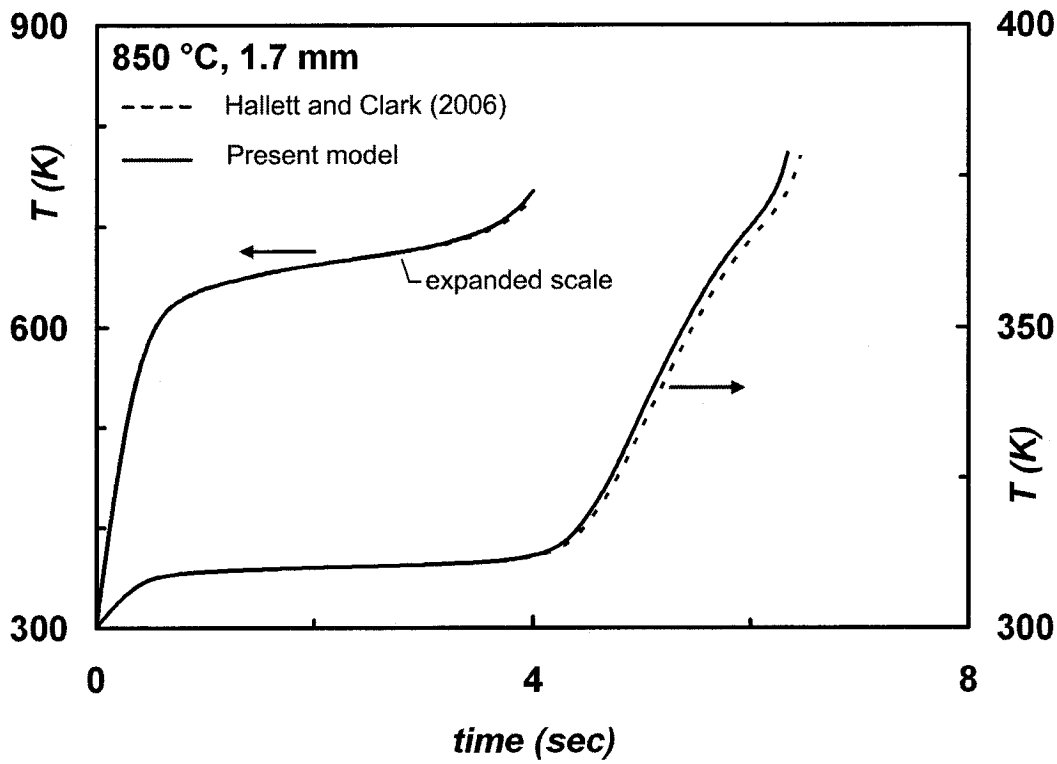

Figure 5.25: Droplet temperature vs. time for 1.7 mm pyrolysis oil droplet, showing the difference between the present model and the earlier model. Initial temperature 300 K, ambient temperature 1123 K. Upper curve shows initial part of temperature history with scale expanded.

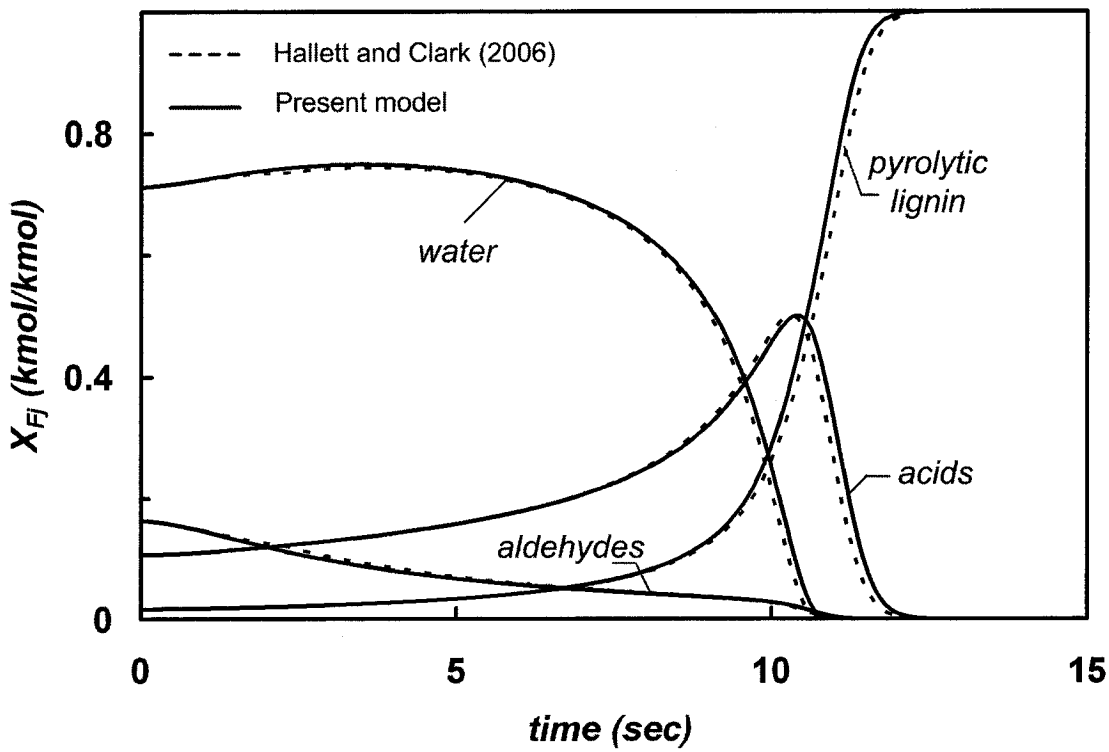

Figure 5.26: Liquid mol fractions x_{Fj} vs. time, showing the difference between the present model and the earlier model. 1.56 mm droplet, initial temperature 300 K, ambient temperature 773 K.

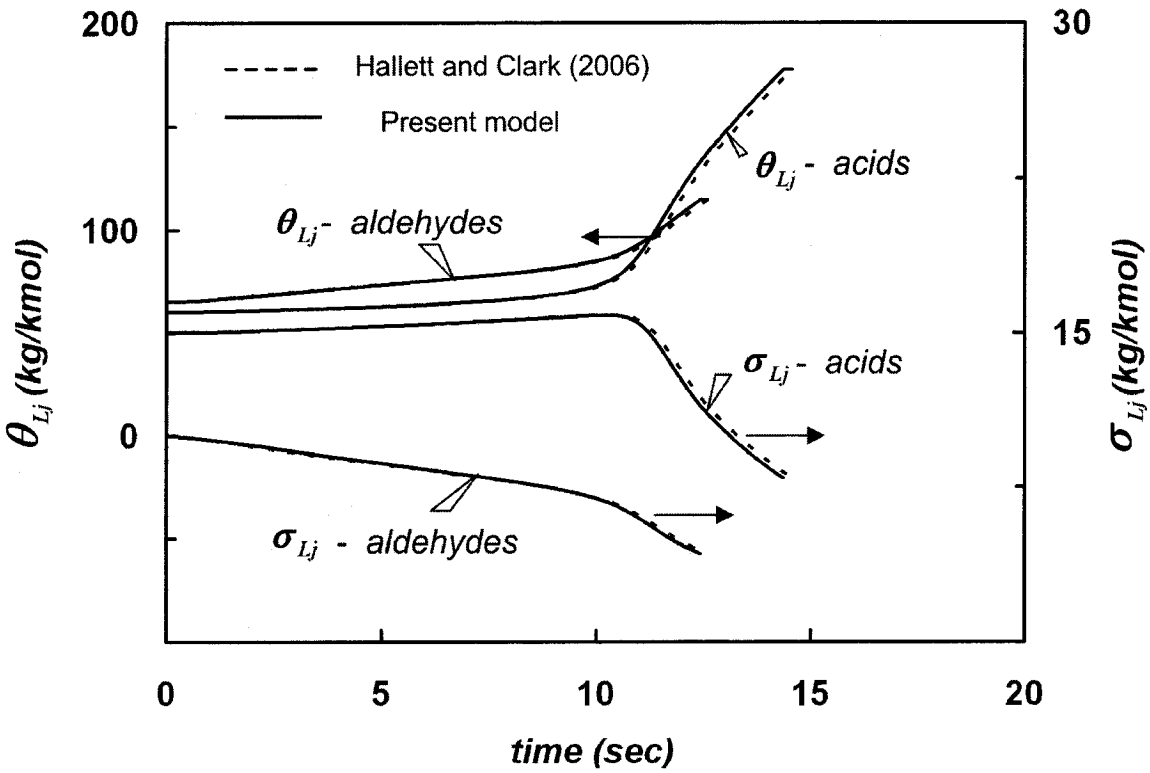

Figure 5.27: Liquid composition means θ_{LjR} and standard deviations σ_{LjR} at the droplet surface for the aldehyde and acid fraction, showing the difference between the present model and the earlier model. 1.56 mm droplet, initial temperature 300 K, ambient temperature 773 K.

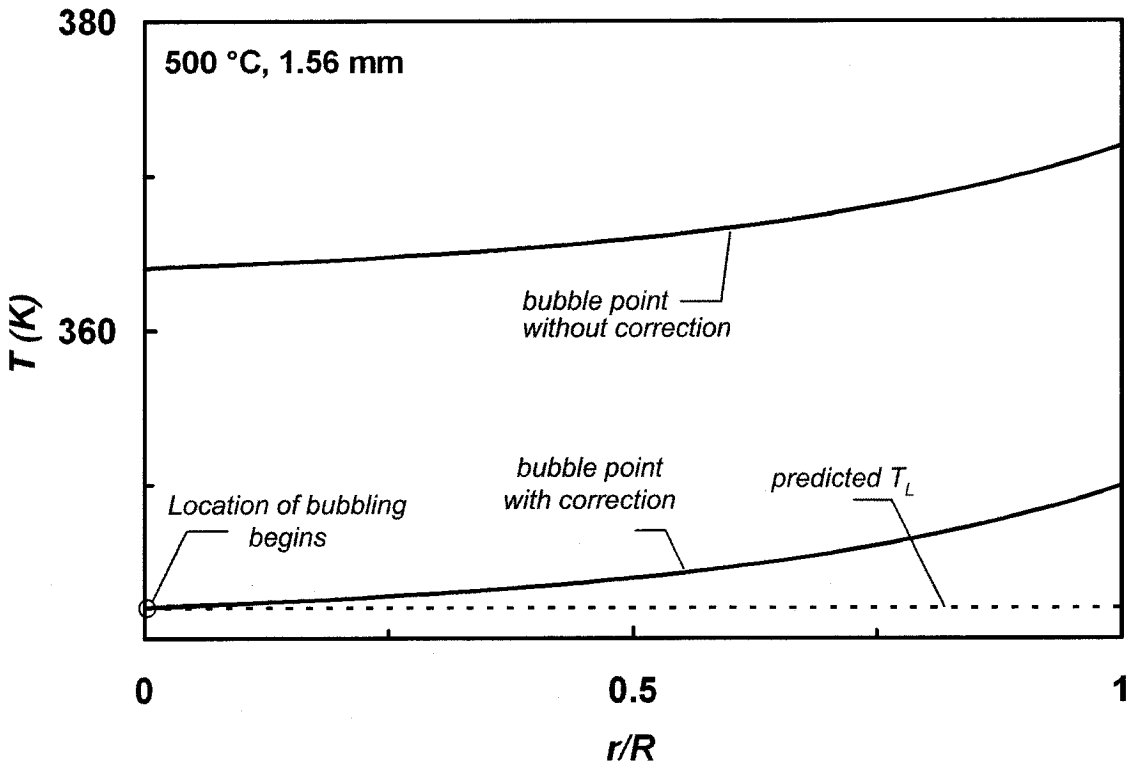

Figure 5.28: Radial profiles of predicted bubble point and droplet temperature. 1.56 mm droplet, initial temperature 300 K, ambient temperature 773 K.

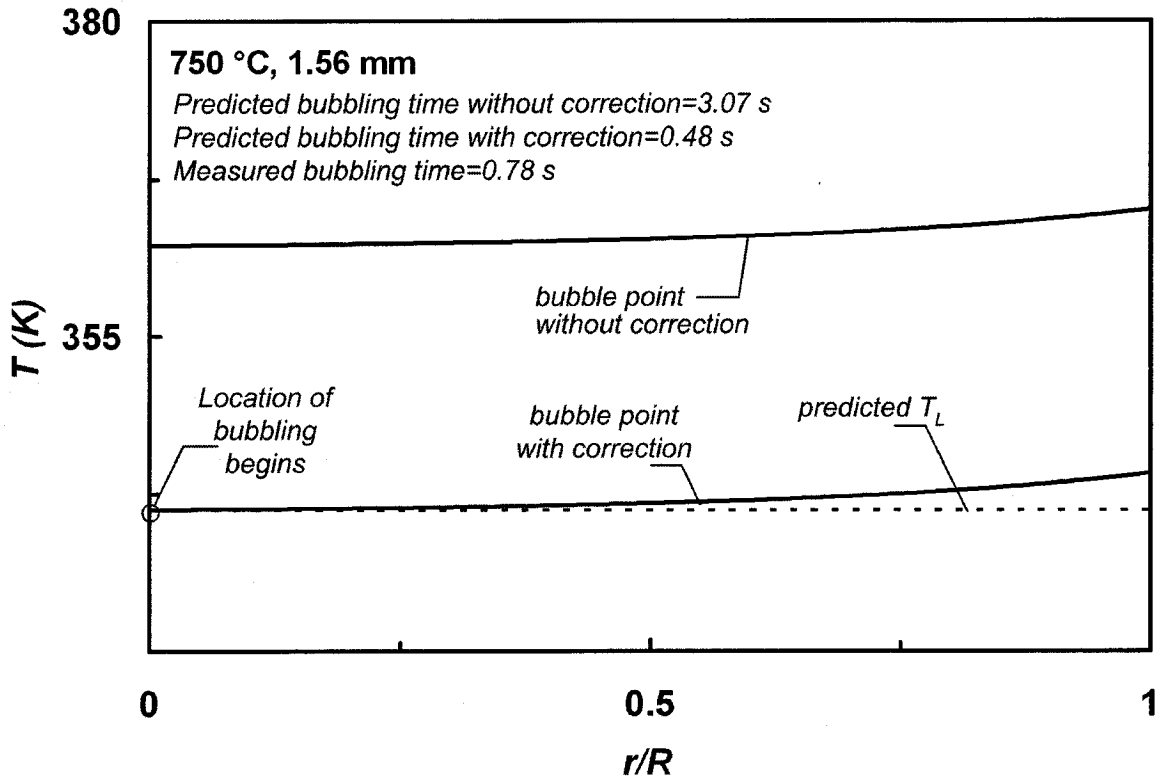

Figure 5.29: Radial profiles of predicted bubble point and droplet temperature. 1.56 mm droplet, initial temperature 300 K, ambient temperature 1023 K.

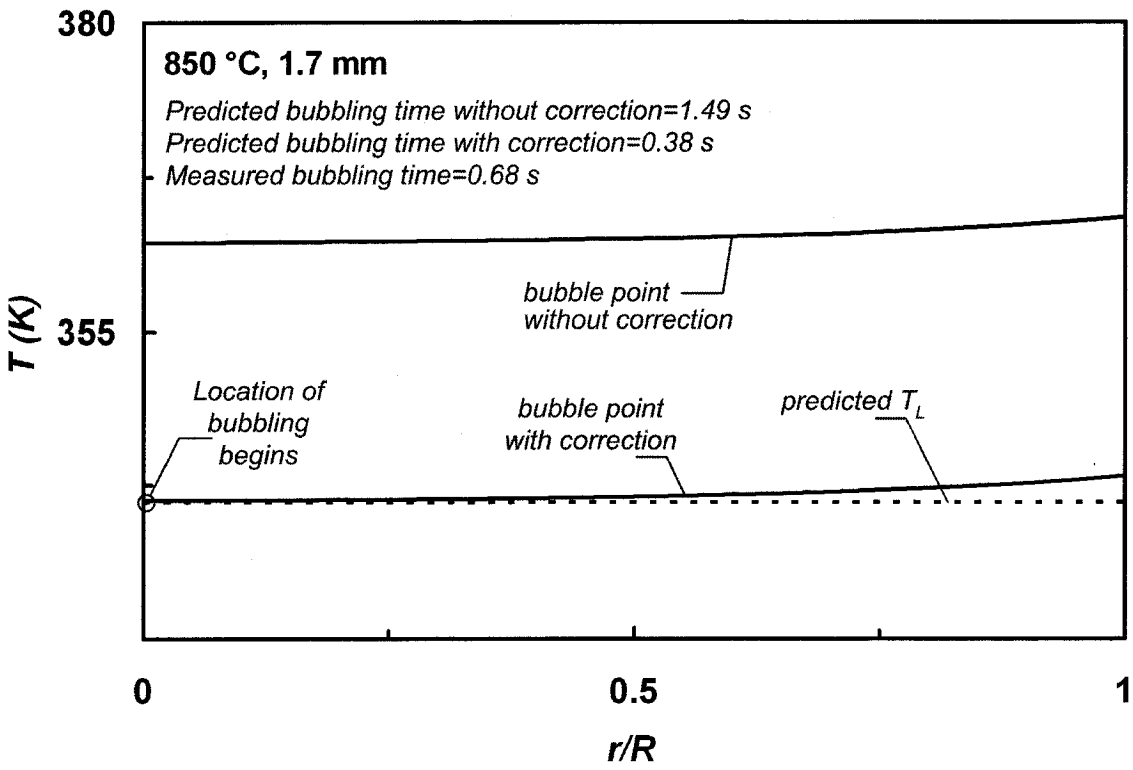

Figure 5.30: Radial profiles of predicted bubble point and droplet temperature. 1.7 mm droplet, initial temperature 300 K, ambient temperature 1123 K.

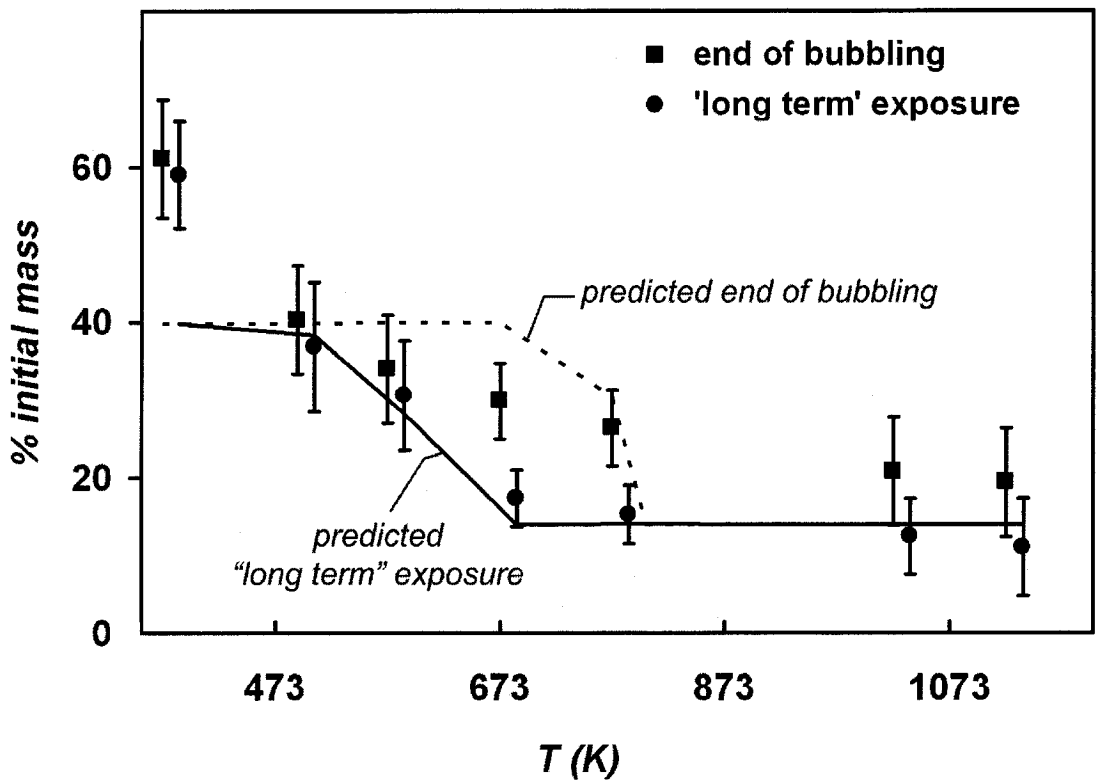

Figure 5.31: Residual mass at the end of the droplet lifetime. Each point is result of 5-6 trials; error bars represent standard deviation. Predictions shown by lines. ■ – droplet withdrawn from the furnace shortly after bubbling ceased; ● -droplet withdrawn after five or three times longer exposure. 1.7 mm droplet, initial temperature 300 K.

CHAPTER 6

Conclusions and Recommendations

6.1 GENERAL CONCLUSIONS

In this research, experiments were performed on the evaporation of pyrolysis oil droplets at high temperatures to analyze their complex behaviour, and to gain some insight into the nature of bubbling. The physical properties of the fuel such as density, thermal conductivity, and pyrolysis rate parameters were determined for modelling purposes. In the mathematical model, the pre-bubbling period was modeled by assuming a diffusion-limited liquid phase, and after bubbling begins the liquid-phase was approximated as a well-mixed liquid. The following conclusions can be drawn from the experimental and numerical investigation:

- The experiments showed that bubbling begins at a time roughly corresponding to the end of initial heating period and the liquid temperature reaches a nearly constant value while the light components evaporate. It suggests the formation of vapour bubbles by internal vaporization of the lighter inner core. Internal mixing of the liquid is fairly vigorous due to the bubbling, making the well-mixed liquid assumption reasonable.

- The model has been shown to give reasonable predictions of the time scales of the major events in the life of a droplet: evaporation of volatile species and pyrolysis of

pyrolytic lignin to char. The model results for the period of the evaporation agree well with the observed bubbling and disruption period, confirming that this results from the evolution of light species.

- The ideal mixture behaviour assumption appears to cause the predicted times for the onset of bubbling to be longer than observed results from the experiments. The cause of this discrepancy appears to be the use of an ideal mixture model for phase equilibrium. Therefore, a crude correction was included in the model to obtain more reasonable bubbling point temperatures. Comparing the model predictions and experiments, good agreement of the temperature and droplet evaporation histories was achieved.

- The present diffusion limited model did not show as dramatic a difference in composition between the droplet surface and center as the analytical solution of Law and Law (1981). However, the predicted results are realistic when compared to the numerical solution of Abdel-Qader and Hallett (2005).

6.2 RECOMMENDATIONS FOR FUTURE WORK

- The ideal mixture behaviour assumption is inaccurate because of the polar components of the fuel such as water and the aldehyde group. Therefore, assuming non-ideal mixture phase equilibrium might help obtain more accurate results for bubble point temperature.

- The effect of a non-uniform temperature profile should be investigated to improve the results for the pre-bubbling period.

List of References

Abramovitz, M. and Stegun, I.A, *Handbook of Mathematical Functions*, Dover, New York (1970).

Abdel-Qader, Z. and Hallett, W.L.H, "The role of liquid mixing in evaporation of complex multicomponent mixtures: modelling using continuous thermodynamics", *Chemical Engineering Science*, **60,** 1629-1640 (2005).

Abramzon, B. and Sirignano, W.A., "Droplet vaporization model for spray combustion calculations", *Int. Journal Heat Mass Transfer*, **32**, 1605-1618 (1989).

Aggarwal, S.K., "Modelling of a dilute vaporizing multicomponent fuel spray", *Int. Journal Heat and Mass Transfer*, **30**, 1949-1961 (1987).

Araya, K. and Tsunematsu, S., "Single droplet combustion of sunflower oil", *SAE* Paper 870590, (1987)

Avni, E., Coughlin, R.W., Solomon, P.R., King, H.H., "Mathematical modelling of lignin pyrolysis", *Fuel,* **64**, 1495-1501 (1985).

Bergeron, C.A., Hallett, W.L.H., "Ignition characteristics of liquid hydrocarbon fuels as single droplets", *Canadian Journal of Chemical Engineering*, **67**, 142-149 (1989).

Boucher, M.E., Chaala, A., Roy, C., "Bio-oils obtained by vacuum pyrolysis of softwood bark as a liquid fuel for gas turbines. Part I: Properties of bio-oil and its blends with methanol and a pyrolytic aqueous phase", *Biomass and Bioenergy*, **19,** 337-350 (2000).

Briano, J.G. and Glandt, E.D., "Molecular thermodynamics of continuous mixtures", *Fluid Phase Equilibria*, **14,** 91-102 (1983).

Brown, A.I. and Marco, S.M, *Introduction to Heat Transfer*, 3rd edition, McGraw-Hill book Company, New York (1986).

Chou, G.F. and Prausnitz, J.M., "Adiabatic flash calculations for continuous or semicontinuous mixtures using as equation of state", *Fluid Phase Equilibria*, **142**, 149-162 (1986).

Czernik, S., Johnson, D.K., Black, S., "Stability of wood fast pyrolysis oil", *Biomass and Bioenergy*, **7**, 187-192 (1994).

Czernik, S., Scahill, J., Diebold, J.P., "The production of liquid fuel by fast pyrolysis of biomass", *ASME Journal of Solar Energy Engineering*, **117**, 2-6 (1995).

Czernik, S., Bridgwater, A.V., "Overview of applications of biomass fast pyrolysis oil", *Energy and Fuels*, **18**, 590-598 (2004).

D'Alessio, J., Lazzaro, M., Massoli, P., Moccia, V., "Thermo-optical investigation of burning biomass pyrolysis oil droplets", *27th Symposium (International) on Combustion/ The Combustion Institute*, 1915-1922 (1998).

Diebold, J.P., Czernik, S., "Additives to lower and stabilize the viscosity of pyrolysis oils during storage", *Energy and Fuels*, **11**, 1081-1091 (1997).

El-Wakil, M.M. and Priem, R.J., Brikowski, H.J., Myers P.S., and Uyehara O.A., "Experimental and calculated temperature and mass histories of vaporizing fuel drops", NACA TN 3490 (1956).

Faeth, G.M. and Olson, D.R., "The ignition of hydrocarbon fuel droplets in air", *SAE* Paper 680465, 1793-1802 (1968).

Faulon, J. L. and Hatcher, P.G., "Is there any order in the structure of lignin?", *Energy and Fuels* , **8**, 402-407 (1994).

Grønli, M.G., Varhegyi, G., Di Blasi, C., "Thermogravimetric Analysis and Devolatilization Kinetics of Wood", *Industrial Engineering Chemistry Research,* **41**, 4201-4208 (2002).

Hallett, W.L.H and Ricard, M.A., "Calculations of the auto-ignition of liquid hydrocarbon mixtures as single droplets", *Fuel*, **71,** 225-229 (1992).

Hallett, W.L.H., "A simple model for the vaporization of droplets with large numbers of components", *Combustion and Flame*, **121,** 334-344 (2000).

Hallett, W.L.H and Clark, N., "A Model for the Evaporation of Biomass Pyrolysis Oil Droplets", *Fuel*, **85**, 532-544 (2005).

Katz, D.L and Brown, G.G., "Vapour pressure and vaporization of petroleum fractions", *Ind.Eng.Chem.*, **25**, 1373-1384 (1933).

Kobayasi, K.,"An experimental study in the combustion of a fuel droplet", *5th Symposium (International) on Combustion/The Combustion Institute*, 141-148 (1954).

Law, C.K.,"Multicomponent droplet combustion with rapid internal mixing", *Combustion and Flame*, **26**, 219-233 (1976).

Law C.K., Prakash, S., Sirignano, W.A.,"Theory of convective, transient, multicomponent droplet vaporization", *Sixteenth Symposium* (1977).

Law, C.K., Law, H.K., "A d^2 - law for multicomponent droplet vaporization and combustion", *AIAA Journal*, **20**, 522-527 (1981).

Law, C.K., "Recent advances in droplet vaporization and combustion", *Prog. Energy Combust. Sci.*, **8** , 171-201 (1982).

Lin, S.X.Q and Chen, X.D., "Improving the glass-filament method for accurate measurement of drying kinetics of liquid droplets", *Institution of Chemical Engineers*, **80**, 401-409 (2002).

Maggi, R., Delmon, B., "Characterization and upgrading of bio-oils produced by rapid thermal processing", *Biomass and Bioenergy*, 7, 245-249 (1994).

Nishiwaki, N., "Kinetics of liquid combustion process: Evaporation and ignition lag of fuel droplets", *5th Symposium (International) on Combustion / The Combustion Institute*, 148-159 (1954).

Oasmaa, A. and Czernik, S., "Fuel oil quality of biomass pyrolysis oils - state of the art for the end users", *Energy and Fuels*, **13**, 914-921 (1999).

Oasmaa, A. and Peacocke, C., "A guide to physical property characterization of biomass-derived fast pyrolysis liquids", *Espoo, Finland: Technical Research Centre of Finland* (2001). VTT Publications 450 (available at http://www.vtt.fi/inf/pdf/publications/1997/P306.pdf).

Oasmaa, A., Leppämäki, E., Koponen, P., Levander, J., Tapola, E.,"Physical characterisation of biomass-based pyrolysis liquids. Application of standard fuel oil analyses", *Espoo, Finland: Technical Research Centre of Finland* (2001). VTT Publications 306 (available at http://www.vtt.fi/inf/pdf/publications/1997/P306.pdf).

Oasmaa, A., Kuoppala, E., Gust, S., Solantausta, Y., "Fast pyrolysis of forestry residue. 1. Effect of extractives on phase separation of pyrolysis liquids", *Energy and Fuels*, **17**, 1-12 (2003).

Oasmaa A, Kuoppala E, Solantausta Y., "Fast pyrolysis of forestry residue. 2. Physicochemical composition of product liquid", *Energy and Fuels*, **17**, 433-443 (2003).

Oasmaa A, Kuoppala E., "Fast pyrolysis of forestry residue. 3. Storage stability of liquid fuel", *Energy and Fuels*, **17**, 1075-1084 (2003).

Okajima, S. and Kumagai, S., "Experimental studies on combustion of fuel droplets in flowing air under zero- and high-gravity conditions ", *19th Symposium (International) on Combustion/ The Combustion Institute*, 1021-1027 (1982).

Órfão, J.J.M., Antunes, F.J.A, Figueiredo, J.L., "Pyrolysis kinetics of lignocellulosic materials", *Fuel*, **78,** 349-358 (1999).

Peacocke G.V.C., Russell P.A., Jenkins J.D., Bridgwater A.V., "Physical properties of flash pyrolysis liquids", *Biomass and Bioenergy*, **7**, 169-177 (1994).

Prausnitz, J.M., "Phase equilibria for complex fluid mixtures", *Fluid Phase Equilibria*, **14**, 1-18 (1983).

Reid, R. C., Prausnitz, J. M. and Poling, B. E., *The properties of gases and liquids*, 4th edition, McGraw-Hill, New York (1986)

Scholze B., Hanser C., Meier D., "Characterization of the water-insoluble fraction from fast pyrolysis liquids (pyrolytic lignin). Part II. GPC, carbonyl groups, and ^{13}C-NMR", *Journal of Analytical and Applied Pyrolysis*, **58-59**, 387-400 (2001).

Scholze B, Meier D., "Characterization of the water-insoluble fraction from pyrolysis oil (pyrolytic lignin). Part I. Py-GC/MS, FTIR, and functional groups", *Journal of Analytical and Applied Pyrolysis*, **60,** 41-54 (2001).

Shaddix C .R. and Tennison P.R., "Effects of char content and simple additives on biomass pyrolysis oil droplet combustion", *27 Symposium (International) on Combustion/ The Combustion Institute*, 1907-1914 (1998).

Shaddix C.R., Hardesty D.R., "Combustion properties of biomass flash pyrolysis oils: final project report", Livermore, California: Sandia National Labs, (1999). Report SAND99-8238.

Sipilä K., Kuoppala E., Fagernäs L., Oasmaa A., "Characterization of biomass-based flash pyrolysis oils", *Biomass and Bioenergy*, **14,** 103-113 (1998).

Sirignano, W.K and Law, C.K., "Transient heating and liquid-phase mass diffusion in fuel droplet vaporization", *Evaporation and Combustion of Fuels*, J.F Zung, editor, Adv. In. Chem., **166**, 3 (1978).

Sirignano, W.A., "Fuel Droplet Vaporization and Spray Combustion Theory", *Progress in Energy and Combustion Science*, **9**, 291-322 (1983).

Taley, D.G. and Yao, S.C, "A semi-empirical approach to thermal and composition transients inside vaporizing fuel droplets", *Twenty-first Symposium (International) on Combustion / The Combustion Institute*, 609-616 (1986).

Tamim, J., Hallett, W.L.H., "A continuous thermodynamics model for multicomponent droplet vaporization", *Chemical Engineering Science*, **50**, 2933-2942 (1995).

Tong, A.Y., and Sirignano, W.A., "Multicomponent droplet vaporization in a high temperature gas", *The American Society of Mechanical Engineers*, 84-WA/HT-171984 (1984).

Wood, B.J., Wise, H., and Inami S.H., "Heterogeneous combustion of multicomponent fuels", *Combustion and Flame*, **4,** 235-242 (1960).

Wornat M.J., Porter B.G., Yang N.Y.C., "Single droplet combustion of biomass pyrolysis

oils", *Energy and Fuels*, **8**, 1131-1142 (1994).

Xu, G., Ikegami, M., Honma, S., Ikeda, K., Nagaishi, H., Dietrich, D.L., Takeshita, Y., "Burning Droplets Composed of Light Cycle Oil and Diesel Light Oil", *Energy and Fuels*, **16**, 366-378 (2002).

Appendix A – Calculation of Liquid Viscosity

The viscosity of each component was calculated by using the Orrick and Erbar method (Reid et al., 1986, page 456). This method employs group contributions to estimate A and B in Eq. (A.1)

$$ln\left(\frac{\eta_i}{\rho_L M_i}\right) = A + \frac{B}{T} \qquad (A.1)$$

In this study, group contributions, given in Table A.1, were used to obtain A and B parameters for each chemical group (ie anything except water).

Table A.1: Orrick and Erbar Group Contributions for obtaining A and B

Group	A	B
C=O	-0.5	350
-COOH	-0.9	770
Carbon atoms	-(6.95+0.21n)	275+99n

where n is the number of carbon atoms, related to the mol weight M_i (see Table A.2). Only straight chain alkyl aldehydes and acids, in other words aldehydes with the chemical formula $CH_3(CH_2)_{n-2}CHO$ and acids with the formula $CH_3(CH_2)_{n-2}COOH$, were considered. A and B parameters for the aldehyde and acid groups were then described as a function of mol weight:

Group contributions for aldehydes:

$A=-(6.95+0.21n) + (-0.5)$ (A.2)

$B= 275+99n + 350$ (A.3)

The molecule weight for aldehydes

$M_i=14n+16$ (A.4)

Substituting Eq. (A.4) into (A.2) and (A.3) into gives

$A= a_1+ a_2I$ (A.5)

$B= b_1+ b_2I$ (A.6)

where a_1= *-7.21,* a_2= *-0.015* , b_1= *511.85,* b_2= *7.07* (see Table A.2)

Group contributions for acids:

$A=-(6.95+0.21n) + (-0.9)$ (A.7)

$B= 275+99n + 770$ (A.8)

The molecule weight for acids

$M_i=14n+32$ (A.9)

Substituting into Eq. (A.4)

$A = a_1+a_2 I$ (A.10)

$B = b_1+b_2 I$ (A.11)

where a_1= *-7.37,* a_2= *-0.015* , b_1= *818.714,* b_2= *7.07* (see Table A.2)

Pyrolytic lignin was assumed to have a dimer structure as shown by Faulon and Hatcher (1994) (Fig. 1 structure (5)), and the parameters A and B were calculated using the group contributions corresponding to this structure.

For water, parameters A and B were calculated using the viscosity values taken from a heat transfer table (Brown and Marco, 1958) at different temperatures and fitting them to the Orrick and Erbar viscosity equation (Eq. (A.1)).

The viscosity of the acid and the aldehyde group were calculated by Eq. (3.5-11) and Eq. (3.5-13). In order to obtain the viscosity of water and pyrolytic lignin Eq. (3.5-7) was used. Finally, the liquid mixture viscosity was calculated by substituting the viscosity of each component into Eq. (3.5-5).

Table A.2: Required parameters for the calculation of liquid mixture viscosity.

	Aldehyde Group	Carboxylic Acids	Water	Lignin
A	- (6.95+0.21n) - 0.5	- (6.95+0.21n) - 0.9	-16.25	-18.18
B	(275+99n) + 350	(275+99n) + 770	1903.63	6030
M_i	14n+16	14n+32	18	750
a_1	-7.21	-7.37	-	-
a_2	-0.015	-0.015	-	-
b_1	511.85	818.71	-	-
b_2	7.07	7.07	-	-

Appendix B

```
!   PROGRAM BIOOIL – (DIFFUSION-LIMITED MODEL&WELL-MIXED MODEL)
!   LAST MODIFIED 28 JULY 2006
!   DEVELOPED FROM WELL-MIXED MODEL
!**********************************************************************
!   VARIABLE NAMES:
!   GAS PHASE: T = TEMPERATURE, K; RHO = MOLAR DENSITY, KMOL/M^3;
!   THETA = MEAN OF DIST'N (IE FUEL VAPOUR MEAN MOLECULAR WEIGHT),
!   KG/KMOL; VAR = VARIANCE OF DIST'N; VARM2 = (VAR + THETA^2) = PSI
!   THETL,SIG2L,PSIL ARE VALUES AT LIQUID SURFACE (= AVERAGE VALUES
!   FOR WELL-MIXED CASE).
!**********************************************************************

    REAL::MF,MASS,MASSINIT,MASSEV,MASSP,NUO,MASSLIG0,MCHAR,
    1MASSCHAR,MASSLIQ,MASSLIQO,MASSCHAO,TESTT,CRITT,NTEMP,MA,MMIX,
    2NN,J,F2

    INTEGER CNTTEM,NITER,NITER1,SWITCHWM
    DIMENSION ALPHLI(8),BETALI(8),ALPHAL(8),BETAL(8),VLGAMA(8),
   1AVLE(8),ABVLE(8),YFINF(8),YFTHIN(8),YFPSIN(8),THINF(8),PSINF(8),
   2SIGINF(8),THETLI(8),SIG2LI(8),PSILI(8),THETL(8),THETLO(8),
   3SIG2L(8),SIG2LO(8),SIGL(8),PSIL(8),PSILO(8),YFR(8),THETR(8),
   4SIG2R(8),SIGR(8),XF(8),XFI(8),XFMI(8),XFO(8),DXFDT(8),DTHLDT(8),
   5DPSLDT(8),PSIR(8),CHI(8),B(8),DBAR(8),AH(8),BH(8),AB(8),BB(8),
   6AT(8),BT(8),AP(8),BP(8),TCTB38(8),A0(8),A1(8),A2(8),A3(8),B0(8),
   7B1(8),B2(8),B3(8),AKT(8),AKC(8),BKT(8),BKC(8),AL(8),BL(8),CL(8),
   8AD(8),BD(8),THETREF(8),THETVS(8),PSIVS(8),SIGVS(8),BPHI(8),
   9RHOLM(8),SFG(8),IPYRO(8),VAPVOL(8),PCMLIQ(8),YFTHTREF(8),HFGR(8),
    1TC(8),SIG2VS(8),XFR(8),TB(8),PSILR(8),SIG2LR(8),THETLR(8),
    2SUMTHETLDR(40),DXFDR(8),DTHTLDR(8),DPSILDR(8),
   3DSIG2LDR(8),ZETA(40),ZLE(40),ZLE2(40),ZETAE(40),TBOILC(40),
    4ZETAD(40),ZLE3(40), ZETAED(40), APO(40), APTP(40),A(40),TBUB(40),
    5TBOIL(40),ALPHALR(5),BETALR(5),ETAO(8),TERM(8),DBARL(8),TERM1(8),
   6CHECKTEMP(40),F1(8),F3(8),F4(8),F5(8),F6(8),GAMMA(8),VISC(8),
    7G1(8),G2(8),G3(8),G4(8),G5(8),DGAMMA(8),VISMIX(8),AV1(8),BV1(8),
    8AV2(8),BV2(8)

    CHARACTER*23 FUEL(8)

    COMMON/PROPER/A0,A1,A2,A3,B0,B1,B2,B3,AT,BT,AP,BP,AD,BD,AKT,AKC,
   1BKT,BKC,AL,BL,CL,AH,BH,CONDK,DBAR,YFAVG,TAVG,RHOAVG,PRES,PATM,
   2RUGC,MF,CPF,CPL,TR,THETLM,VISCK,PRANDTL,SCHMIDT,KDIST,YFR,YFRM,
   3THETR,THETL,XF,TCF,THETREF,TIME,BPHI,CPFG,YFRSUM,CPMIX

  OPEN(4,FILE='C:\FORTRAN\SOURCE\MDOPCONS.DAT',STATUS="OLD")
  OPEN(5,FILE='C:\FORTRAN\SOURCE\CARBOXYL.DAT',STATUS="OLD")
!  OPEN(6,FILE='C:\FORTRAN\SOURCE\ALCOHOL.DAT',STATUS="OLD")
```

```
      OPEN(6,FILE='C:\FORTRAN\SOURCE\FUELH2O.DAT',STATUS="OLD")
      OPEN(7,FILE='C:\FORTRAN\SOURCE\ALDEHYDE.DAT',STATUS="OLD")
      OPEN(8,FILE='C:\FORTRAN\SOURCE\LIGNINB.DAT',STATUS="OLD")
      OPEN(11,FILE='C:\FORTRAN\SOURCE\BIOOIL.TXT',STATUS="OLD")
      OPEN(12,FILE='C:\FORTRAN\SOURCE\BIOV1.TXT',STATUS="OLD")
      OPEN(13,FILE='C:\FORTRAN\SOURCE\BIOCHI.TXT',STATUS="OLD")
      OPEN(14,FILE='C:\FORTRAN\SOURCE\ERRORS.TXT',STATUS="OLD")
!     OPEN(15,FILE='C:\FORTRAN\SOURCE\CTQSPROP.OUT',STATUS="OLD")
      OPEN(16,FILE='C:\FORTRAN\SOURCE\BIOV2.TXT',STATUS="OLD")
      OPEN(17,FILE='C:\FORTRAN\SOURCE\BIOLIQ.TXT',STATUS="OLD")
      OPEN(18,FILE='C:\FORTRAN\SOURCE\BIOVOL.TXT',STATUS="OLD")
      OPEN(19,FILE='C:\FORTRAN\SOURCE\BIOLIQM.TXT',STATUS="OLD")
      OPEN(20,FILE='C:\FORTRAN\SOURCE\PYROGAS.DAT',STATUS="OLD")
      OPEN(21,FILE='C:\FORTRAN\SOURCE\SIG2LR.TXT',STATUS="OLD")
      OPEN(22,FILE='C:\FORTRAN\SOURCE\THETLR.TXT',STATUS="OLD")
!     OPEN(23,FILE='C:\FORTRAN\SOURCE\PSILR.TXT',STATUS="OLD")
      OPEN(24,FILE='C:\FORTRAN\SOURCE\ETA0.TXT',STATUS="OLD")
      OPEN(25,FILE='C:\FORTRAN\SOURCE\DXFDR.TXT',STATUS="OLD")
      OPEN(26,FILE='C:\FORTRAN\SOURCE\DTHETDR.TXT',STATUS="OLD")
      OPEN(27,FILE='C:\FORTRAN\SOURCE\DSIG2LDR.TXT',STATUS="OLD")
      OPEN(28,FILE='C:\FORTRAN\SOURCE\TBOIL.TXT',STATUS="OLD")
      OPEN(29,FILE='C:\FORTRAN\SOURCE\BIOLIQ1.TXT',STATUS="OLD")
!*********************************************************************
!     SET INITIAL CONDITIONS, TIME STEP, ETC.
!     CONTROL VARIABLES:
!*********************************************************************
!     PHYSICAL CONSTANTS, BOUNDARY CONDITIONS
!
      RUGC=8.314
       SIGMA=5.669E-8
      PI=3.14159265
!
!      PATM IS AMBIENT PRESSURE IN ATMOSPHERES
!
      PATM=1.00
      PAMB=PATM*760.
      PRES=101.3*PATM
      YFINFM=0.
      XFTOT=0.
      XLIGNIN=1.0
      DCHIGASDT=0.
      DCHI1DT=0.
      NITERPRE = 0
       MCHAR=12.

!     READ OPERATING CONDITIONS
      READ(4,*)
      READ(4,*)
      READ(4,*)TDROP,TFURN,RDROP,TEND,DTIME0,TIMELIM,IRAD
      READ(4,*)
      READ(4,*)ICONV
```

```
      READ(4,*)
      READ(4,*)KDIST
      READ(4,*)
      READ(4,*)IWIRE
!     READ IN VARIABLES FOR THERMOCOUPLE CORRECTION IF REQUIRED FOR
!     COMPARISON WITH SUSPENDED DROPLET EXPERIMENTS
      IF(IWIRE.EQ.1)THEN
      READ(4,*)
      READ(4,*)DWIRE,ACONWIRE,BCONWIRE,NWIRE,XWIRE
      ENDIF
      AWIRE=NWIRE*3.1416*DWIRE*DWIRE/4./1.E6
!     READ FUEL SPECIFICATIONS
      DO 120 K=1,KDIST
      READ(4+K,*)
      READ(4+K,503)FUEL(K)
      READ(4+K,*)
      READ(4+K,*)ALPHLI(K),BETALI(K),VLGAMA(K),RHOLM(K),IPYRO(K)
      READ(4+K,*)
      READ(4+K,*)XFMI(K),YFINF(K),YFTHIN(K),YFPSIN(K)
      READ(4+K,*)
      READ(4+K,*)AB(K),BB(K),SFG(K)
      READ(4+K,*)
      READ(4+K,*)AH(K),BH(K),TCTB38(K)
      READ(4+K,*)
      READ(4+K,*)AT(K),BT(K),AP(K),BP(K)
      READ(4+K,*)
      READ(4+K,*)A0(K),A1(K),A2(K),A3(K)
      READ(4+K,*)B0(K),B1(K),B2(K),B3(K)
      READ(4+K,*)
      READ(4+K,*)AL(K),BL(K),CL(K)
      READ(4+K,*)
      READ(4+K,*)AKT(K),AKC(K),BKT(K),BKC(K)
      READ(4+K,*)
      READ(4+K,*)AD(K),BD(K),BPHI(K)
      IF(IPYRO(K).EQ.1)THEN
      READ(4+K,*)
      READ(4+K,*)ALIGNIN,ELIGNIN,FRACCHAR
      KPYRO=K
      ENDIF
      YFINFM=YFINFM+YFINF(K)
      XFTOT=XFTOT+XFMI(K)
120   CONTINUE
      TOTALM=0.
      DO 142 K=1,KDIST
      THETLI(K)=ALPHLI(K)*BETALI(K)+VLGAMA(K)
      XFI(K)=XFMI(K)/THETLI(K)
142   TOTALM=TOTALM+XFI(K)
      DO 143 K=1,KDIST
143   XFI(K)=XFI(K)/TOTALM
      READ(20,*)
      READ(20,503)FUEL(KDIST+1)
```

```
      READ(20,*)
      READ(20,*)YFINF(KDIST+1),YFTHIN(KDIST+1),THETR(KDIST+1)
      READ(20,*)
      READ(20,*)AT(K),BT(K),AP(K),BP(K)
      READ(20,*)
      READ(20,*)A0(KDIST+1),A1(KDIST+1),A2(KDIST+1),A3(KDIST+1)
      READ(20,*)B0(KDIST+1),B1(KDIST+1),B2(KDIST+1),B3(KDIST+1)
      READ(20,*)
      READ(20,*)AKT(K),AKC(K),BKT(K),BKC(K)
      READ(20,*)
      READ(20,*)AD(KDIST+1),BD(KDIST+1),BPHI(KDIST+1)
      YFINFM=YFINFM+YFINF(KDIST+1)
503   FORMAT(A23)
      IF(XFTOT.NE.1.0)THEN
      WRITE(*,*)'YOU SILLY $@%&## - XF VALUES DO NOT SUM TO 1'
      GOTO 6000
      ENDIF
6002  XLIGNIN=1.0
      WRITE(11,113)
      WRITE(12,113)
      WRITE(16,113)
      WRITE(17,113)
 113  FORMAT(1X,'QUASI-STEADY CONT. THERM. DROPLET EVAPORATION')

      WRITE(11,104)KDIST
      WRITE(12,104)KDIST
      WRITE(16,104)KDIST
      WRITE(17,104)KDIST
 104  FORMAT(3X,'MULTIPLE DISTRIBUTION MODEL WITH',I2,' DISTRIBUTIONS')

      WRITE(11,115)
      WRITE(12,115)
      WRITE(13,115)
      WRITE(16,115)
      WRITE(17,115)
 115  FORMAT(3X,'WELL-MIXED LIQUID PHASE (BATCH DISTILLATION)',/)

      IF(ICONV.EQ.0)THEN
      WRITE(11,116)
      WRITE(12,116)
      WRITE(13,116)
      WRITE(16,116)
      WRITE(17,116)
!     WRITE(*,116)
      ELSE
      WRITE(11,117)
      WRITE(12,117)
      WRITE(13,117)
      WRITE(16,117)
      WRITE(17,117)
!     WRITE(*,117)
```

```
      ENDIF
116   FORMAT(3X,'NO CONVECTION**')
117   FORMAT(3X,'NATURAL CONVECTION')

      IF(IRAD.EQ.0) THEN
      WRITE(11,112)
      WRITE(12,112)
      WRITE(13,112)
      WRITE(16,112)
      WRITE(17,112)
112   FORMAT(1X,'*******NO RADIATION HEAT TRANSFER**********',/)
      ELSE
      WRITE(11,111)
      WRITE(12,111)
      WRITE(13,111)
      WRITE(16,111)
      WRITE(17,111)
111   FORMAT(1X,'********RADIANT HEAT TRANSFER INCLUDED******',/)
      ENDIF
      IF(IWIRE.EQ.1)THEN
      WRITE(11,159)NWIRE,DWIRE,XWIRE
159   FORMAT(1X,'*****CORRECTED FOR THERMOCOUPLE: ',I1,' WIRES ',
      1F5.3,' MM DIA., BOUNDARY LAYER ',F4.1,' R THICK')
      ENDIF

      WRITE(11,110)TDROP,RDROP*2000.
      WRITE(12,110)TDROP,RDROP*2000.
      WRITE(13,110)TDROP,RDROP*2000.
      WRITE(16,110)TDROP,RDROP*2000.
      WRITE(17,110)TDROP,RDROP*2000.
      WRITE(*,110)TDROP,RDROP*2000.
110   FORMAT(2X,'INIT. LIQUID TEMP. ',F4.0,' K', DROPLET DIAM. ',F7.4,' MM')

      WRITE(*,511)TFURN,PATM
      WRITE(11,511)TFURN,PATM
      WRITE(12,511)TFURN,PATM
      WRITE(13,511)TFURN,PATM
      WRITE(16,511)TFURN,PATM
      WRITE(17,511)TFURN,PATM

      DO 121 K = 1,KDIST
      IF(YFINF(K).GT.0.)THEN
      THINF(K)=YFTHIN(K)/YFINF(K)
      PSINF(K)=YFPSIN(K)/YFINF(K)
      SIGINF(K)=SQRT(PSINF(K)-THINF(K)*THINF(K))
      ENDIF
121   CONTINUE

      DO 122 K = 1,KDIST
  !   WRITE(*,504)K,FUEL(K),ALPHLI(K),BETALI(K),VLGAMA(K)
      WRITE(11,504)K,FUEL(K),ALPHLI(K),BETALI(K),VLGAMA(K)
```

```
      WRITE(12,504)K,FUEL(K),ALPHLI(K),BETALI(K),VLGAMA(K)
      WRITE(13,504)K,FUEL(K),ALPHLI(K),BETALI(K),VLGAMA(K)
!     WRITE(15,504)K,FUEL(K),ALPHLI(K),BETALI(K),VLGAMA(K)
      WRITE(16,504)K,FUEL(K),ALPHLI(K),BETALI(K),VLGAMA(K)
      WRITE(17,504)K,FUEL(K),ALPHLI(K),BETALI(K),VLGAMA(K)
!     WRITE(*,512)XFI(K),YFINF(K),THINF(K),SIGINF(K)
      WRITE(11,512)XFI(K),YFINF(K),THINF(K),SIGINF(K)
      WRITE(12,512)XFI(K),YFINF(K),THINF(K),SIGINF(K)
      WRITE(13,512)XFI(K),YFINF(K),THINF(K),SIGINF(K)
      WRITE(16,512)XFI(K),YFINF(K),THINF(K),SIGINF(K)
      WRITE(17,512)XFI(K),YFINF(K),THINF(K),SIGINF(K)
!
!     INITIAL DISTRIBUTION FUNCTION - LIQUID PHASE
!
      ALPHAL(K) = ALPHLI(K)
      BETAL(K) = BETALI(K)
      THETLI(K)=ALPHLI(K)*BETALI(K)+VLGAMA(K)
      SIG2LI(K)=ALPHLI(K)*BETALI(K)*BETALI(K)
      SIGLI=SQRT(SIG2LI(K))
      PSILI(K)=THETLI(K)*THETLI(K)+SIG2LI(K)
      WRITE(11,505)THETLI(K),SIGLI
      WRITE(12,505)THETLI(K),SIGLI
      WRITE(13,505)THETLI(K),SIGLI
      WRITE(16,505)THETLI(K),SIGLI
      WRITE(17,505)THETLI(K),SIGLI
505   FORMAT(20X,'MEAN MOL. WEIGHT ',F7.1,' STANDARD DEVIATION ',
      1F5.1)
122   CONTINUE
      RHOLI=0.
!
!     MASS DENSITY OF CHAR
!
      RHOCHAR=RHOLM(KPYRO)*FRACCHAR
      DO 141 K=1,KDIST
141   RHOLI=RHOLI+XFMI(K)/RHOLM(K)
      RHOLI=1./RHOLI
      WRITE(11,*)' FUEL COMPOSITION BY MASS:'
      DO 140 K=1,KDIST
      WRITE(11,507)FUEL(K),XFMI(K)*100.
      IF(IPYRO(K).EQ.1)THEN
      WRITE(11,508)ALIGNIN,ELIGNIN,FRACCHAR
140   ENDIF
       RHOLMASS=RHOLI
504   FORMAT(1X,'FUEL ',I2,': 'A23,'ALPHA = ',F6.2,
      1' BETA = ',F6.2,' GAMMA = ',F5.1)
511   FORMAT(2X,'AMBIENT CONDITIONS: TEMP. ',F5.0,'K, PRESSURE',F5.2,
      1'ATM',/)
512   FORMAT(10X,'XF = ',F5.3,';   AMBIENT: YF =',F6.4,' THETA =',F5.1,
      1' SIGMA =',F7.0)
507   FORMAT(5X,A23,1X,F6.3,'%')
508   FORMAT('LIGNIN KINETICS: A ',E9.2,'/S, E ',E9.2,'J/MOL, ULTIMATE
```

```
      1YIELD OF CHAR ',F5.3)
      RUGC=8.314
!
!     THERMAL EXPANSION COEFFICIENT
      THERMEXP=0.0008
!     THERMEXP=0.

! ********************************************************************
!  PROGRAMME CONTROL VARIABLES
!  CRITT IS CRITERION FOR CONVERGENCE OF DROPLET TEMPERATURE
!  CHICRIT IS CONV. CRIT. FOR NEWTON ROUTINE FOR CHI
!  XFCRIT IS CUTOFF MOL FRACTION FOR BYPASSING THE CALCULATION
!  OF VLE, LIQUID CHANGES, ETC. FOR A COMPONENT
! ********************************************************************
      CRITT = 1.E-5
      CHICRIT = 1.E-5
      XFCRIT = 1.E-10
      RELAX = 1.0
      NITER=0
      NITER1=0
      ICNT=0
      IFLAGT=0
      TIME=0.
      NPRINT=10
      TIMEPRT=NPRINT*DTIME0
      WRITE(12,100)
100   FORMAT(/,32X,'VAPOUR AT SURFACE')
      WRITE(12,137)
200   FORMAT(/,20X,'VAPOUR SOURCE DISTRIBUTION')
      WRITE(16,200)
237   FORMAT(16X,'DIST. MEAN', 12X,'STANDARD DEV.')
      WRITE(16,237)
137   FORMAT(16X,'MOL FRACT.',10X,'DIST. MEAN',10X,'STANDARD DEV.')
      WRITE(12,106)
106   FORMAT(3X,'TIME',6X,'1',6X,'2',6X,'3',6X,'1',5X,'2',5X,'3',
      18X,'1',6X,'2',6X,'3')
206   FORMAT(3X,'TIME',6X,'1',6X,'2',6X,'3',8X,'1', 6X, '2',6X,'3')
      WRITE(16,206)

!     WRITE(15,138)
138   FORMAT(/,10X,'PROPERTIES')
!     WRITE(15,139)
139    FORMAT(3X,'TIME',3X,'MREF',2X,'TREF',2X,'TC',6X,'PC',6X,'CPF',
      17X,'CPL',6X,'CONDK',1X,'FUEL K',3X,'DBAR1',4X,'DBAR2')

      WRITE(13,400)
! 400 FORMAT(3X,'TIME',4X,'T - K',1X,'CHI: 1',7X,'2',7X,'3',7X,'4',7X,
!     1'5',4X,'GAS',2X,'G - KMOL/M2S')
400   FORMAT(3X,'TIME',4X,'T - K',1X,'CHI: 1',7X,'2',7X,'3',7X,'4',4X,
      1'GAS',2X,'G - KMOL/M2S')
!
```

```
!       SET UP INITIAL VALUES
!
        DTLDT=0.
        DO 124 K = 1,KDIST
        DXFDT(K)=0.
        DTHLDT(K)=0.
        DPSLDT(K)=0.
        MA=28.97
124     CONTINUE
        CHIGAS=0.
        CHIVAP=1.-CHIGAS
        INITFLAG=0
        NCHIFLAG=0
        TR=TDROP
        TROLD=TR
         R=RDROP
        ROLD=R
!
!       MASS OF LIQUID FUEL:
!
        VOLUME=4./3.*PI*RDROP**3
        VOLINIT=VOLUME
        VOLOLD=VOLUME
        MASSINIT=VOLUME*RHOLI
        AREA=4.*PI*RDROP*RDROP
        MASSLIQ=MASSINIT
        MASSLIQO=MASSLIQ
        MASSCHAR=0.
        MASSCHAO=MASSCHAR
        MASSEV=0.0
        MASSP=MASSEV/MASSINIT*100.
        MASSLIG0=XFMI(KPYRO)*MASSINIT
        PCRESIDU=100.
        CCVOLC=0.
!
!       SETUP INITIAL LIQUID STATE

        YFRM=0.
        THETLM=0.
        THETLMM=0.
        DO 123 K = 1,KDIST
        AVLE(K)=(SFG(K)/RUGC)*(1.-AB(K)/TROLD)
        ABVLE(K)=SFG(K)/RUGC/TROLD*BB(K)
        XF(K)=XFI(K)
        XFO(K)=XF(K)
        THETL(K)=THETLI(K)
        THETLO(K)=THETL(K)
        SIG2L(K)=SIG2LI(K)
        PSIL(K)=PSILI(K)
        PSILO(K)=PSIL(K)
        SIG2LO(K)=SIG2L(K)
```

```
      CALL VLE(THETLO(K),SIG2LO(K),VLGAMA(K),YFR(K),THETR(K),SIG2R(K),
     1ALPHAL(K),BETAL(K),PATM,AVLE(K),ABVLE(K),XFO(K))

      YFRM=YFRM+YFR(K)
      THETLM=THETLM+XFI(K)*THETL(K)
      THETLMM=THETLMM+XFMI(K)*THETL(K)
      SIGL(K)=SQRT(SIG2L(K))
      SIGR(K)=SQRT(SIG2R(K))

123   CONTINUE
!     SELECT "PIVOT" COMP'T WITH LARGEST MOL FRACTION
      XFMAX=0.
      DO 160 K = 1,KDIST
      IF(K.EQ.KPYRO)GOTO 160
      IF(XF(K).GT.XFMAX)THEN
      XFMAX=XF(K)
        IPIVOT=K
      ENDIF
160   CONTINUE
      RHOD=RHOLI/THETLM
      YFR(KDIST+1)=0.
      THETLMO=THETLM
      THETLMI=THETLMO
      CLVOLL=MASSLIQ/THETLM
!
!     REFERENCE STATE FOR PROPERTIES CALCULATIONS
!
      TAVG=TFURN/3.+2.*TR/3.
      YFAVG=YFINFM/3.+2.*YFRM/3.
      SUMYFTHR=0.
      DO 133 K=1,KDIST
      YFTHTREF(K)=(2./3.*YFR(K)*THETR(K)+YFTHIN(K)/3.)
      THETREF(K)=YFTHTREF(K)/(2./3.*YFR(K)+YFINF(K)/3.)
      SUMYFTHR=SUMYFTHR+YFTHTREF(K)
133   CONTINUE
      THETREF(KDIST+1)=THETR(KDIST+1)
      YFRSUM=YFRM+YFR(KDIST+1)
      MF=SUMYFTHR/YFAVG
      MMIX=YFAVG*MF+(1.-YFAVG)*MA
      CALL PROPS
!*********************************************************************
      WRITE(18,600)
600   FORMAT(' VOLUME FLOW RATES OF GAS AND VAPOUR COMPONENTS')
      WRITE(18,601)
601   FORMAT('  EXPRESSED AS INITIAL DROPLET VOLUMES PER SECOND')
      WRITE(18,602)
602   FORMAT(/,'TIME',8X,'1',8X,'2',8X,'3',8X,'4',6X,'GAS',4X,
     1'VAP. TOTAL')
      WRITE(19,620)
620   FORMAT(' LIQUID COMPONENTS AS % OF INITIAL DROPLET MASS')
      WRITE(19,621)
```

```
!621    FORMAT(/,'TIME',8X,'1',8X,'2',8X,'3',8X,'4',8X,'5',6X,'LIQUID',
!       15X,'CHAR')
621     FORMAT(/,'TIME',8X,'1',8X,'2',8X,'3',8X,'4',6X,'LIQUID',
        15X,'CHAR')
        WRITE(11,510)RHOLI,THERMEXP,THETLM,THETLMM
        WRITE(17,510)RHOLI,THERMEXP,THETLM,THETLMM
 510    FORMAT(5X,'LIQUID DENSITY ',F6.1,'KG/M3, THERMAL EXPANSION COEFF.
        1',F9.6,' /K',/,6X,'NUMBER MEAN MOL MASS ',F6.1,
        2',  MASS MEAN MOL MASS',F6.1)
         WRITE(11,109)
         WRITE(11,101)
 109    FORMAT(/,32X,'CONVERSIONS  %   DIMLESS')
 101    FORMAT(3X,'TIME',2X,'T-K',4X,'CHIGAS',2X,'D-MM',3X,
        1' LIGNIN',2X,'LIQUID',2X,'GAS FLUX',2X,'%CHAR',1X,'%RESIDUE',1X,
        2'G',8X,'GGAS',2X,'TBUB')
        WRITE(17,201)
! 201    FORMAT(/,2X,'TIME',3X,'THETL1',1X,'THETL2',1X,'THETL3',
!        11X,'THETL4',1X,'THETL5',4X,'XF1',4X,'XF2',4X,'XF3',4X,'XF4',4X,'XF5')
 201    FORMAT(/,2X,'TIME',3X,'THETL1',1X,'THETL2',1X,'THETL3',
        11X,'THETL4',4X,'XF1',4X,'XF2',4X,'XF3',4X,'XF4',4X,
        2'XFR1',4X,'XFR2',4X,'XFR3',4X,'XFR4')
         WRITE(11,203)TIME,TR,CHIGAS,R*2000.,(1.-XLIGNIN)*100.,MASSP,
        1GASFLUX,PCCHAR,PCRESIDU,G,GGAS
203     FORMAT(F7.3,1X,F6.1,2(1X,F7.4),2(1X,F7.3),1X,F8.5,2(1X,F7.3),2(1X
        1,E8.2))
!       WRITE(17,202)TIME,THETL(1),THETL(2),THETL(3),THETL(4),THETL(5),
!       1XF(1),XF(2),XF(3),XF(4),XF(5)
        WRITE(17,202)TIME,THETL(1),THETL(2),THETL(3),THETL(4),
        1XF(1),XF(2),XF(3),XF(4),XFR(1),XFR(2),XFR(3),XFR(4)
         WRITE(12,105)TIME,YFR(1),YFR(2),YFR(3),YFR(4),THETR(1),THETR(2),
         1THETR(3),THETR(4),SIGR(1),SIGR(2),SIGR(3),SIGR(4)
        WRITE(16,205)TIME,THETR(1),THETR(2),THETR(3),THETR(4),SIGR(1),
        1SIGR(2),SIGR(3),SIGR(4)
205     FORMAT(F7.4,4X,4(2X,F5.1),4(1X,F6.2))

        WRITE(19,603)TIME,(XFMI(K)*100.,K=1,KDIST),100.,0.
603     FORMAT(F7.3,7(1X,F10.5))

105     FORMAT(F7.4,2X,3(1X,F6.4),1X,E7.1,4(1X,F5.1),4(1X,F6.2))
102     FORMAT(1X,F7.4,1X,F6.1,1X,F7.4,1X,F5.1,1X,F5.1,1X,F5.1,1X,F5.1,1X,
        1F6.4,1X,F6.4,1X,F6.2,1X,F6.1)

202     FORMAT(F7.4,1X,4(2X,F12.1),4(3X,F9.8),4(3X,F10.8))
        WRITE(30,354)
354     FORMAT(1X,'TIME', 5X,'THETL', 5X,'SIGL')
        WRITE(30,356)TIME,THETL(1),THETL(2),THETL(3),THETL(4),
        1SIGL(1),SIGL(2),SIGL(3),SIGL(4)

356     FORMAT(F5.2,1X,4(1X,F9.4),1X,4(1X,F9.4))

        NN=20
```

```
      DO 360 J=2, NN-1
360   ZETA(J+1)=((J-1)/(NN-2))**(0.333)
      ZETA(1)=0
      ZETA(2)=ZETA(3)/2

      SWITCHWM=0
      TIME=TIME+DTIME
!**********************************************************************
!
! BEGIN LOOP FOR TIME STEP
! ITERATION PROCEDURE FOR DROPLET SURFACE CONDITIONS IS FULLY IMPLICIT
! ESTIMATE TEMPERATURE, ETC. AT END OF TIME STEP USING HEATING RATE,
! FROM PREVIOUS TIME STEP
!
!**********************************************************************
300   EMISS=0.89*(1.-EXP(-5.4*R*1000.))
      IF(IRAD.EQ.0)EMISS=0.
      IF(IFLAGT.EQ.0)THEN
      write(14,*)'new time step',time
      DTIME=DTIME0
      ENDIF
      IF(CHIGAS.GT.0.4)THEN
      NCHIFLAG=1
      ENDIF
!
!     TIME STEP REDUCTION AFTER DROPLET BECOMES SMALL
!
      IF(MASSP.GT.80.0.AND.IFLAGT.LT.1)THEN
      DTIME=DTIME0/5.
      IFLAGT=1
      ENDIF

      IF(MASSP.GT.93.0.AND.IFLAGT.LT.2)THEN
      DTIME=DTIME0/20.
      IFLAGT=2
      ENDIF

      IF(MASSP.GT.97.0.AND.IFLAGT.LT.3)THEN
      DTIME=DTIME0/50.
      IFLAGT=3
      ENDIF
      CNTTEM=0
!
!     VLE AND MOL FLUX CALCULATION
!
      TR=TROLD+DTLDT*DTIME
      RELAXXF=1.0
      SUMXF=0.

      DO 125 K = 1,KDIST
      IF(XF(K).GT.XFCRIT)THEN
```

```
      AVLE(K)=(SFG(K)/RUGC)*(1.-AB(K)/TROLD)
      ABVLE(K)=SFG(K)/RUGC/TROLD*BB(K)
      XF(K)=XFO(K)+RELAXXF*DXFDT(K)*DTIME
      IF(XF(K).LT.0.)THEN
      XF(K)=0.
      ENDIF
      IF(XF(K).GT.1.)THEN
      XF(K)=1.
      ENDIF
      SUMXF=SUMXF+XF(K)
      THETL(K)=THETLO(K)+RELAXXF*DTHLDT(K)*DTIME
      PSIL(K)=PSILO(K)+RELAXXF*DPSLDT(K)*DTIME
      SIG2L(K)=PSIL(K)-THETL(K)*THETL(K)
      ELSE
      XF(K)=0.
      ENDIF
125   CONTINUE
      RHOL=RHOLMASS/THETLM
!     RE-SCALE XF IN THE EVENT OF AN XF BEING <0 OR >1
      DO 145 K=1,KDIST
145   XF(K)=XF(K)/SUMXF

!     SELECT "PIVOT" COMPONENT AS ONE WITH GREATEST LIQ. FRACTION
!
      YFRMAX=0.
       IF(XF(IPIVOT).GT.0.05) THEN
      GOTO 161
      ENDIF
      XFMAX=0.
      SUMTHETR=0.
      DO 136 K = 1,KDIST
      IF(K.EQ.KPYRO)GOTO 136
      IF(XF(K).GT.XFMAX)THEN
        XFMAX=XF(K)
      IPIVOT=K
      ENDIF

136   CONTINUE
161   CONTINUE
      IF(XFMAX.LT.XFCRIT)THEN
       IPIVOT=KPYRO
      ENDIF
      IF (SWITCHWM.EQ.0) THEN

!*********************************************************
!   DIFFUSION-LIMITED LIQUID PHASE SOLUTION
!*********************************************************
!     CALCULATE DGAMMA AND GAMMA FUNCTIONS

      DO 358 K=1, KDIST
      IF (VLGAMA(K).EQ.0.0) THEN
```

```
      G1(K)=ALOG(ALPHAL(K))
      G2(K)=1./(2*ALPHAL(K))
      G3(K)=1./(12*ALPHAL(K)**2)
      G4(K)=1./(120*(ALPHAL(K)**4))
      G5(K)=1./(252*(ALPHAL(K)**6))
      DGAMMA(K)=G1(K)-G2(K)-G3(K)+G4(K)-G5(K)
      ELSE
      F1(K)=(ALPHAL(K)-0.5)*ALOG(ALPHAL(K))
      F2=0.5*ALOG(2*3.14)
      F3(K)=1./(12*ALPHAL(K))
      F4(K)=1./(360*(ALPHAL(K)**3))
      F5(K)=1./(1260*(ALPHAL(K)**5))
      F6(K)=1./(1680*(ALPHAL(K)**7))
      GAMMA(K)=EXP(F1(K)-ALPHAL(K)+F2+F3(K)-F4(K)+F5(K)-F6(K))
      ENDIF
358   CONTINUE

      AV1(1)=-7.37
      AV2(1)=-0.015
      BV1(1)=818.714
      BV2(1)=7.07
      AV1(3)=-7.21
      AV2(3)=-0.015
      BV1(3)=511.85
      BV2(3)=7.07
!
!     VISCOSITY FOR ALDEHYDE GROUP
!
      K=3
      VISMIX(K)=ALOG(RHOLM(K))+AV1(K)+BV1(K)/TR+(AV2(K)+
      1BV2(K)/TR)*THETL(K)+DGAMMA(K)+ALOG(BETAL(K))
!
!     VISCOSITY FOR CARBOXYLIC ACIDS GROUP
!
      K=1
      SUM0=0.
      TVOLD=0
      H4OLD=0.
      NLOOP=400.
      DO 359 I=0, NLOOP
      L=I-VLGAMA(K)
      IF(L.GT.0.)THEN
      TV=L/BETAL(K)
      H1=TV**(ALPHAL(K)-1.)
      H2=EXP(-1.*TV)
      H3=ALOG(BETAL(K)*TV+VLGAMA(K))
      H4=H1*H2*H3
      H5=(H4+H4OLD)*(TV-TVOLD)*2.
      TVOLD=TV
      H4OLD=H4
      SUM0=SUM0+H5
```

```
      ENDIF
359   CONTINUE
      TINT0=SUM0
      VISMIX(K)=ALOG(RHOLM(K))+AV1(K)+BV1(K)/TR+(AV2(K)+
      1BV2(K)/TR)*THETL(K)+TINT0/GAMMA(K)

!     VISCOSITY FOR WATER
      IF(TR.NE.373)THEN
      VISMIX(2)=RHOLM(2)*18.*EXP(-16.25+1903.63/TR)
      ELSE
      VISMIX(2)=0.267
      ENDIF

!     VISCOSITY FOR PYROLYTIC LIGNIN
      VISMIX(4)=RHOLM(4)*750.*EXP(-18.18+6030/TR)
!
!     LIQUID MIXTURE VISCOSITY
!
      VISMIX1=XFI(1)*VISMIX(1)+XFI(2)*ALOG(VISMIX(2))+XFI(3)*VISMIX(3)+XFI(4)*1
      1ALOG(VISMIX(4))
      VISMIX1=EXP(VISMIX1)
      END IF
!
!     CALCULATE LIQUID DIFFUSIVITY
!
      NTEMP=0
301   IF (SWITCHWM.EQ.0) THEN
      DO 361 K=1, KDIST
      DBARL(K)=(7.4E-12)*(THETL(K)**0.5)*TR*((RHOLM(K)/THETL(K))
      1**0.6)/(VISMIX1)
361   CONTINUE

      MA=28.97
      YFRMASS=YFRM*SUMTHETR/(YFRM*SUMTHETR+(1-YFRM)*MA)
      BMASS=YFRMASS/(1-YFRMASS)

      DO 780 K=1,KDIST
      IF (TIME.EQ.0.0) THEN
      ETAO(K)=RHOAVG*DBAR(K)/RHOLMASS/DBARL(K)*ALOG(1+BMASS)*MMIX
      ELSE
      ETAO(K)=RHOAVG*DBAR(K)/RHOLMASS/DBARL(K)*ALOG(1+B(K))*MMIX
      END IF

      TERM(K)=1./ETAO(K)-2./ETAO(K)**2+2./ETAO(K)**3*(1.-EXP(-ETAO(K)))

      SUMTHETLR=1/(((1./3.*(1./THETLM-1./THETLMI))/TERM(K))+1./THETLMI)

      XFR(K)=(((1./3.*(XF(K)/THETLM-XFI(K)/THETLMI))/TERM(K))
      1+XFI(K)/THETLMI)*SUMTHETLR

      THETLR(K)=(((1./3.*(XF(K)*THETL(K)/THETLM-XFI(K)*THETLI(K)/
```

```
     1THETLMI))/TERM(K))+XFI(K)*THETLI(K)/THETLMI)*SUMTHETLR/XFR(K)

     PSILR(K)=(((1./3.*(XF(K)*PSIL(K)/THETLM-XFI(K)*PSILI(K)/THETLMI))/TERM(K))
     1+XFI(K)*PSILI(K)/THETLMI)*SUMTHETLR/XFR(K)

     SIG2LR(K)=PSILR(K)-THETLR(K)*THETLR(K)
     IF (SIG2LR(K).LT.0.) THEN
     END IF

     CALL VLEDL2(THETL(K),SIG2L(K),VLGAMA(K),YFR(K),THETR(K),SIG2R(K),
     1ALPHALR(K),BETALR(K),PATM,AVLE(K),ABVLE(K),XFR(K),THETLR(K),
     2SIG2LR(K))

     780  CONTINUE
     ENDIF
     DO 126 K=1,KDIST
     IF(XF(K).LT.XFCRIT)THEN
      YFR(K)=0.
     GOTO 126
     ENDIF

     IF (SWITCHWM.EQ.1) THEN
     CALL VLE(THETLO(K),SIG2LO(K),VLGAMA(K),YFR(K),THETR(K),SIG2R(K),
     1ALPHAL(K),BETAL(K),PATM,AVLE(K),ABVLE(K),XFO(K))
     ENDIF

     IF(SIG2R(K).GE.0.)THEN
      SIGR(K)=SQRT(SIG2R(K))
     ELSE
      SIG2R(K)=0.
     ENDIF
126  CONTINUE
     YFRM=0
     SUMTHETR=0
     THETLM=0
     THETLMM=0
     DO 811 K=1,KDIST
     YFRM=YFRM+YFR(K)
     SUMTHETR=SUMTHETR+YFR(K)*THETR(K)/YFRM
     THETLM=THETLM+XF(K)*THETL(K)
     SIGL(K)=SQRT(SIG2L(K))
     SIGR(K)=SQRT(SIG2R(K))
     PSILR(K)=SIG2LR(K)+THETLR(K)*THETLR(K)
     PSIR(K)=SIG2R(K)+THETR(K)*THETR(K)
811  CONTINUE
     NITER=NITER+1
     NITER1=NITER1+1
     AKLIG=ALIGNIN*EXP(-ELIGNIN/RUGC/TROLD)
     XLIGNIN=1./(1.+MCHAR*CCVOLC/(XF(KPYRO)*THETL(KPYRO)*FRACCHAR*
     1CLVOLL))
     GGAS=(1.-FRACCHAR)/AREA/THETR(KDIST+1)*(XF(KPYRO)*THETL(KPYRO)
```

```
      1*CLVOLL+MCHAR/FRACCHAR*CCVOLC)*AKLIG*XLIGNIN
!*********************************************************
!     ITERATE FOR DISTRIBUTION MOL FLUXES
!*********************************************************
      IF (INITFLAG.EQ.0) THEN
      CHI1TR=YFR(IPIVOT)/YFRM
      INITFLAG=1
      ELSE
       CHI1TR=CHI(IPIVOT)
      ENDIF
      NITERMOL=0
      IF(ICONV.EQ.0)THEN
      SHO=2.0
      ELSE
      GRASHOF=9.81*(TFURN-TR)*(2.*R)**3/TAVG/(VISCK**2)
      SCHMIDT=VISCK/DBAR(IPIVOT)
      SHO=2.+0.43*(GRASHOF*SCHMIDT)**0.25
      ENDIF
!
!     DIFFERENT SOLUTION METHODS USED FOR SMALL AND LARGE CHIGAS
!
      IF(NCHIFLAG.EQ.0)THEN

!*********SOLUTION METHOD FOR LOW CHIGAS*****************************

128   NITERMOL=NITERMOL+1
      IF(NITERMOL.GT.100)THEN
       WRITE(*,*)'ITERATIONS FOR CHI EXCEED 100 - ABORT'
      GOTO 6000
      ENDIF
      IF(IPIVOT.EQ.KPYRO)GOTO 96
      B(IPIVOT)=(YFR(IPIVOT)-YFINF(IPIVOT))/
      1(CHI1TR-YFR(IPIVOT))
      G=SHO*RHOAVG*DBAR(IPIVOT)/2./R*ALOG(1.+B(IPIVOT))
      CHIGAS=GGAS/G
      CHIVAP=1.-CHIGAS
      GROCSH=2.*G*R/RHOAVG/SHO
      CHISUM=CHI1TR
      ICHIFLAG=0
      DO 127 K=1,KDIST
      IF(XF(K).GT.XFCRIT)THEN
      IF(K.EQ.IPIVOT)GOTO 127
      CHI(K)=YFR(K)+(YFR(K)-YFINF(K))/(EXP(GROCSH/DBAR(K))-1.)
      CHISUM=CHISUM+CHI(K)
      ELSE
       CHI(K)=0.
       ICHIFLAG=ICHIFLAG+1
      ENDIF
127   CONTINUE
      CHI(IPIVOT)=CHI1TR
      PHI = 1.-CHIGAS-CHISUM
```

```
      DPHI = 0.
      DO 99 K=1,KDIST
      IF(XF(K).LT.XFCRIT)GOTO 99
      IF(K.EQ.IPIVOT)GOTO 99
      DPHIDCHI=(YFR(K)-YFINF(K))/(CHI1TR-YFR(IPIVOT))
      DPHIDCHI=DPHIDCHI*DBAR(IPIVOT)/DBAR(K)*B(IPIVOT)/(1.+B(IPIVOT))
      DPHIDCHI=DPHIDCHI*EXP(GROCSH/DBAR(K))/
      1(EXP(GROCSH/DBAR(K))-1.)**2
      DPHI=DPHI+DPHIDCHI
 99   CONTINUE
      DPHIDCHI=-1.0-DPHI-CHIGAS/GROCSH*DBAR(IPIVOT)*B(IPIVOT)/
      1(1.+B(IPIVOT))/(CHI1TR-YFR(IPIVOT))
!     CHI1TR=CHI1TR-PHI/DPHIDCHI
      CHINEW=CHI1TR-PHI/DPHIDCHI
      IF(CHINEW.GT.1.)THEN
      WRITE(*,*)'HELP! CHINEW IS CRAP!'
      CHINEW=0.99
      ENDIF
      CHI1TR=RELAX*CHINEW+(1.-RELAX)*CHI1TR
      IF(ABS(PHI).GT.CHICRIT)GOTO 128
      GOTO 95
!
! CHANGE IN SOLUTION WHEN PYROLYZING COMPONENT IS ONLY ONE LEFT
!
 96   CHI1TR=1.-CHIGAS
      DO 94 K=1,KDIST
       IF(K.EQ.IPIVOT)GOTO 94
      CHI(K)=0.
 94   CONTINUE
      CHI(IPIVOT)=CHI1TR
      B(IPIVOT)=(YFR(IPIVOT)-YFINF(IPIVOT))/(CHI1TR-YFR(IPIVOT))
      G=SHO*RHOAVG*DBAR(IPIVOT)/2./R*ALOG(1.+B(IPIVOT))
      CHIGAS=GGAS/G
      PHI=1.-CHI1TR-CHIGAS
      GROCSH=2.*G*R/RHOAVG/SHO
      IF(ABS(PHI).GT.CHICRIT)GOTO 128
95    CONTINUE
      ELSE
!
!*********SOLUTION METHOD FOR HIGH CHIGAS*****************************
!
152   G=GGAS/CHIGAS
      NITERMOL=NITERMOL+1
      IF(NITERMOL.GT.100)THEN
       WRITE(*,*)'ITERATIONS FOR CHIGAS EXCEED 100 - ABORT'
       GOTO 6000
      ENDIF
      GROCSH=2.*G*R/RHOAVG/SHO
      CHISUM=0.
      DO 97 K=1,KDIST
      IF(XF(K).GT.XFCRIT)THEN
```

```
        CHI(K)=YFR(K)+(YFR(K)-YFINF(K))/(EXP(GROCSH/DBAR(K))-1.)
        CHISUM=CHISUM+CHI(K)
       ELSE
        CHI(K)=0.
       ENDIF
 97    CONTINUE
       PHI=1.-CHISUM-CHIGAS
       DPHI=0.
       DO 98 K=1,KDIST
       IF(XF(K).LT.XFCRIT)GOTO 98
       DPHIDCHI=(YFR(K)-YFINF(K))*GGAS/CHIGAS**2
       DPHIDCHI=DPHIDCHI*2.*R/RHOAVG/SHO/DBAR(K)*EXP(GROCSH/DBAR(K))/
      1(EXP(GROCSH/DBAR(K))-1.)**2
       DPHI=DPHI+DPHIDCHI
 98    CONTINUE
       DPHIDCHI=-1.-DPHI
       CHIGASNEW=CHIGAS-PHI/DPHIDCHI
       IF(CHIGASNEW.GE.1.0)THEN
       CHIGASNEW=0.9
       ENDIF
       CHIGAS=RELAX*CHIGASNEW+(1.-RELAX)*CHIGAS
       IF(ABS(PHI).GT.CHICRIT)GOTO 152
       ENDIF
!      END OF SOLUTION FOR CHI'S AND CHIGAS
       CHIVAP=1.-CHIGAS
       BGAS=EXP(GROCSH/DBAR(KDIST+1))-1
       YFR(KDIST+1)=(CHIGAS*BGAS+YFINF(KDIST+1))/(1.+BGAS)
       YFRSUM=0.
       DO 154 K=1,KDIST+1
 154   YFRSUM=YFRSUM+YFR(K)
!
!      UPDATE LIQUID CONDITIONS
!
       THETLM=0.
       DTHLDTM=0.
       CPL=0.
       DO 129 K=1,KDIST
       IF(XF(K).GT.XFCRIT)THEN
       IF(IPYRO(K).EQ.1)THEN
        DXFDT(K)=G*AREA/CLVOLL*((CHIVAP*XF(K)-CHI(K))+
      1(XF(K)-1.)*CHIGAS/(1.-FRACCHAR)*THETR(KDIST+1)/THETL(KPYRO))
       ELSE
       DXFDT(K)=G*AREA/CLVOLL*((CHIVAP*XF(K)-CHI(K))+
      1XF(K)*CHIGAS/(1.-FRACCHAR)*THETR(KDIST+1)/THETL(KPYRO))
       ENDIF
       XF(K)=XFO(K)+DXFDT(K)*DTIME
       IF(XF(K).GT.1.0)THEN
            write(*,*)'   help - xf(',k,') = ',xf(k),time
            XF(K)=1.
       ENDIF
       SUMXF=SUMXF+XF(K)
```

```
      B(K)=EXP(GROCSH/DBAR(K))-1.
      IF(B(K).NE.0.0)THEN
      DTHLDT(K)=G*AREA/CLVOLL/XF(K)*((THETL(K)*CHI(K)-YFR(K)
      1*THETR(K))+(YFTHIN(K)-YFR(K)*THETR(K))/B(K))
      DPSLDT(K)=G*AREA/CLVOLL/XF(K)*((PSIL(K)*CHI(K)-YFR(K)
      1*PSIR(K))+(YFPSIN(K)-YFR(K)*PSIR(K))/B(K))
      ELSE
       DTHLDT(K)=0.
       DPSLDT(K)=0.
      ENDIF
      THETL(K)=THETLO(K)+DTHLDT(K)*DTIME
      PSIL(K)=PSILO(K) + DPSLDT(K)*DTIME
      SIG2L(K)=PSIL(K)-THETL(K)*THETL(K)
      THETLM=THETLM+XF(K)*THETL(K)
      DTHLDTM=DTHLDTM+XF(K)*DTHLDT(K)+THETL(K)*DXFDT(K)
      CPL=CPL+XF(K)*(AL(K)+ BL(K)*TR+CL(K)*TR**2)*THETL(K)*1000.
      ELSE
      XF(K)=0.
      B(K)=EXP(GROCSH/DBAR(K))-1.
      ENDIF
129   CONTINUE
!
!     CHAR SPECIFIC HEAT - EINSTEIN EQUATION
!
      CHARCP1=380./TR
      CHARCP1=EXP(CHARCP1)/((EXP(CHARCP1)-1.0)/CHARCP1)**2
      CHARCP2=1800./TR
      CHARCP2=EXP(CHARCP2)/((EXP(CHARCP2)-1.0)/CHARCP2)**2
      CPCHAR=1000.*RUGC*(CHARCP1+2.0*CHARCP2)
      CPD=(CLVOLL*CPL+CCVOLC*CPCHAR)/(CLVOLL+CCVOLC)
      RHOL=RHOLMASS/THETLM
!     RE-SCALE XF IN THE EVENT OF AN XF BEING <0 OR >1
      SUMXF=0.
      DO 146 K=1,KDIST
146   SUMXF=SUMXF+XF(K)
      DO 144 K=1,KDIST
144    XF(K)=XF(K)/SUMXF
      DO 130 K=1,KDIST
       IF(SIG2L(K).GE.0.)THEN
      SIGL(K)=SQRT(SIG2L(K))
      ELSE
      SIGL(K)=0.
      ENDIF
130   CONTINUE
!
!     DROPLET HEATING
!
      IF(ICONV.EQ.0)THEN
      NUO=2.
      ELSE
!      XLEWIS=RHOAVG*DBAR(IPIVOT)*CPFG/CONDK
```

```
      NUO=2.+0.43*(GRASHOF*PRANDTL)**0.25
      ENDIF
      BTHERM=EXP(2.*G*CPFG*R/CONDK/NUO)-1.
       IF(BTHERM.GE.0.01)THEN
        Q=NUO*CONDK/2./R*ALOG(1.+BTHERM)/BTHERM*(TFURN-TR)
      ELSE
        Q=NUO*CONDK/2./R*(TFURN-TR)
      ENDIF
      QRAD=SIGMA*EMISS*((TFURN)**4-TR**4)
      QTOT=Q+QRAD
!
!     CORRECTION FOR THERMOCOUPLE WIRE FOR COMPARISON WITH SUSPENDED
!     DROPLET EXPERIMENTS
      IF(IWIRE.EQ.1)THEN
      XLWIRE=XWIRE*RDROP
      TWIRE=(TR+TFURN)/2.
      CONDWIRE=ACONWIRE+BCONWIRE*TWIRE
      QWIRE=CONDWIRE*AWIRE*(TFURN-TR)/AREA/XLWIRE
      QTOT=QTOT+QWIRE
      ENDIF
      HFG=0.
      DO 131 K=1,KDIST
      IF(B(K).EQ.0.0.OR.XF(K).LT.XFCRIT)GOTO 131
      HFGR(K)=AH(K)*CHI(K)+BH(K)/B(K)*(YFR(K)*THETR(K)*
     1(1.+B(K))-YFTHIN(K))
      TC(K)=AT(K)+BT(K)*THETR(K)
      HFG=HFG+HFGR(K)*((TC(K)-TR)**0.38)/TCTB38(K)
131   CONTINUE
      QLIQ=QTOT-G*HFG
      DTLDT=3./(RHOL*CPD*R)*QLIQ
      TRP=TROLD + DTLDT*DTIME
!
!     CHECK IF CONVERGENCE HAS BEEN ACHIEVED:
!
      CNTTEM=CNTTEM+1
      IF(CNTTEM.GT.100)THEN
      WRITE(*,632)
632   FORMAT(' ITERATIONS FOR TEMP AND VELOCITY EXCEED 100 - ABORT ')
      WRITE(*,634)TIME,MASSEV,MASSP
634   FORMAT(/,' MASS EVOLVED AFTER ',F8.5,' SECONDS: ',E10.4,' KG',
     1    5X,F6.2,' %')
       GOTO 6001
      ENDIF
      TESTT=ABS(TRP-TR)/TR
      TR=TRP
       NTEMP=NTEMP+1
       IF(TESTT.GT.CRITT.OR.NTEMP.LT.7) GOTO 301
!
!     END OF TIME STEP - NEW DROPLET RADIUS, ETC.
!
150   FORMAT(F5.2,1X,E10.3,1X,F6.3,1X,2(1X,F9.5),2(1X,F9.3))
```

```
151     FORMAT(10X,' XF ',5F9.6)
!       WRITE(14,150)TIME,DBAR(KDIST+1),BGAS,YFR(KDIST+1),YFRSUM,CPF/1000.
!        1,CPFG/1000.
!       WRITE(14,*)TIME,TR,CPCHAR,CPL,CPD,THETLM,RHOD
        VOLDOT=G*AREA*(-CHIVAP/RHOL+CHIGAS*THETR(KDIST+1)/(1.-FRACCHAR)*
       1(FRACCHAR/RHOCHAR-1./RHOL/THETL(KPYRO)))
       VOLDOT=VOLDOT+CLVOLL/RHOLMASS*DTHLDTM
!       VOLDOT=VOLDOT+CLVOLL/RHOLI*DTHLDTM
       VOLDOT=VOLDOT+CLVOLL*THERMEXP/RHOL*DTLDT
       VOLUME=VOLOLD+VOLDOT*DTIME
       VOLOLD=VOLUME
       R=(0.75*VOLUME/PI)**(1./3.)

!       TAKE STOCK AT END OF TIME STEP
!       MASS OF FUEL THAT EVAPORATED OR PYROLYZED:
       DMASSLDT=-G*AREA*THETLM*(CHIVAP+CHIGAS/(1.-FRACCHAR)*
      1THETR(KDIST+1)/THETL(KPYRO))+CLVOLL*DTHLDTM
       MASSLIQ=MASSLIQO+DMASSLDT*DTIME
       MASSLIQO=MASSLIQ
       CLVOLL=MASSLIQ/THETLM
       PCLIQ=MASSLIQ/MASSINIT*100.
       DO 622 K=1,KDIST
622     PCMLIQ(K)=PCLIQ*XF(K)*THETL(K)/THETLM
       DMASSCDT=G*AREA*CHIGAS*FRACCHAR*THETR(KDIST+1)/(1.-FRACCHAR)
       MASSCHAR=MASSCHAO+DMASSCDT*DTIME
       MASSCHAO=MASSCHAR
       CCVOLC=MASSCHAR/MCHAR
       PCCHAR=MASSCHAR/MASSINIT*100.
       PCRESIDU=(MASSLIQ+MASSCHAR)/MASSINIT*100.
       RHOD=(CLVOLL+CCVOLC)/(4./3.*PI*R**3)
       AREA=4.*PI*R**2
       IF (SWITCHWM.EQ.1) THEN
       RHOLMASS=RHOLMASS*(1.-THERMEXP*DTLDT*DTIME)
       ENDIF
       MASS=MASSLIQ+MASSCHAR
       MASSEV=MASSINIT-MASSLIQ
!  PERCENTAGE OF LIQUID CONVERTED:
       MASSP=MASSEV/MASSINIT*100.
!  PYROLYSIS GAS FLUX RELATIVE TO INITIAL DROPLET MASS
       GASFLUX=GGAS*AREA*THETR(KDIST+1)/MASSINIT
!  GAS AND VAPOUR VOLUME FLOWS RELATIVE TO INITIAL DROPLET VOLUME
       GVOL=G*AREA*RUGC*TR/PRES/VOLINIT
       GASVOL=CHIGAS*GVOL
       VAPVOLUM=(1.-CHIGAS)*GVOL
       DO 610 K=1,KDIST
610    VAPVOL(K)=CHI(K)*VAPVOLUM
       ROLD=R
       TROLD = TR
        DCHIGASDT=(CHIGAS-CHIGASO)/DTIME
       DCHI1DT=(CHI(1)-CHI1OLD)/DTIME
       CHIGASO=CHIGAS
```

```
      CHI1OLD=CHI(1)
      DO 132 K=1,KDIST
      XFO(K)=XF(K)
      THETLO(K)=THETL(K)
      PSILO(K)=PSIL(K)
       SIG2LO(K)=SIG2L(K)
132   CONTINUE
      IF (SWITCHWM.EQ.1) THEN
      TBUB=TBOIL
      IF(CHIGAS.GT.0.95)GOTO 353
      CALL BOILIN(DXFDR,AT,BT,SFG,RUGC,TBUB,PATM,XF,SIG2L,
      1THETL,DTHTLDR,AB,BB,DSIG2LDR,VLGAMA,TBOIL,THETR,NTBFLAG,KDIST,
      2SWITCHWM)
      ENDIF

353   CONTINUE
      IF(NTBFLAG.EQ.1)GOTO 6000
      THETLMO=THETLM
!     COMPOSITION OF EVAPORATING VAPOUR
      DO 135 K=1,KDIST
      IF(CHI(K).EQ.0.)THEN
      THETVS(K)=THETR(K)
      PSIVS(K)=PSIR(K)
      ELSE
      THETVS(K )=THETL(K)-R*RHOL/3./G*XF(K)*DTHLDT(K)/(CHI(K)*CHIVAP)
      PSIVS(K)=PSIL(K)-R*RHOL/3./G*XF(K)*DPSLDT(K)/(CHI(K)*CHIVAP)
      ENDIF
      SIG2VS(K)=PSIVS(K)-THETVS(K)*THETVS(K)
      IF(SIG2VS(K).GE.0.)THEN
      SIGVS(K)=SQRT(SIG2VS(K))
      ELSE
      SIGVS(K)=0.
      ENDIF
135   CONTINUE
!
!   PRINT OUT RESULTS AT TIME INTERVALS NPRINT*DTIME0
!
      TIMETEST=TIMEPRT-DTIME0/20.
      IF(TIME.GE.TIMETEST)THEN
      TIMEPRT=TIMEPRT+NPRINT*DTIME0

!     WRITE(*,203)TIME,TR,CHIGAS,R*2000.,(1.-XLIGNIN)*100.,MASSP,
!     1GASFLUX,PCCHAR,PCRESIDU,G,GGAS,TBOIL
      WRITE(11,203)TIME,TR,CHIGAS,R*2000.,(1.-XLIGNIN)*100.,MASSP,
      1GASFLUX,PCCHAR,PCRESIDU,G,GGAS
!     WRITE(17,202)TIME,THETL(1),THETL(2),THETL(3),THETL(4),THETL(5),
!     1XF(1),XF(2),XF(3),XF(4),XF(5)
      WRITE(17,202)TIME,THETL(1),THETL(2),THETL(3),THETL(4),
      1XF(1),XF(2),XF(3),XF(4),XFR(1),XFR(2),XFR(3),XFR(4)
      WRITE(12,105)TIME,YFR(1),YFR(2),YFR(3),YFR(4),THETR(1),THETR(2),
     1THETR(3),THETR(4),SIGR(1),SIGR(2),SIGR(3),SIGR(4)
```

```
      WRITE(16,205)TIME,THETVS(1),THETVS(2),THETVS(3),THETVS(4),
     1SIGVS(1),SIGVS(2),SIGVS(3),SIGVS(4)
      WRITE(18,603)TIME,(VAPVOL(K),K=1,KDIST),GASVOL,VAPVOLUM
      WRITE(19,603)TIME,(PCMLIQ(K),K=1,KDIST),PCLIQ,PCCHAR
      WRITE(13,401)TIME,TR,(CHI(K),K=1,KDIST),CHIGAS,G
      WRITE(28,1112)TIME,TBOIL(NN)
1112  FORMAT (1X,F6.3,5X,F7.3)

! 401  FORMAT(F7.3,3X,F6.1,6(1X,F7.5),1X,E9.3)
 401  FORMAT(F7.3,3X,F6.1,5(1X,F7.5),1X,E9.3)
!      WRITE(11,624)G,Q,QRAD,QTOT,HFG
!      WRITE(11,625)CPF,CONDK,DBAR,TAVG,RHOAVG,CPL
!      WRITE(11,*)'   ALPHAL(K) ',ALPHAL(K),' BETAL(K) ',BETAL(K)
!      ICNT=0
      WRITE(29,356)TIME,THETL(1),THETL(2),THETL(3),THETL(4),
      1SIGL(1),SIGL(2),SIGL(3),SIGL(4)
      ENDIF
624   FORMAT(2X,'G',E10.4,' KMOL/M2S; Q ',E10.4,' W/M2;  QRAD ',E10.4,
      1' QTOT',E10.4,' HFG',E10.4,' J/KMOL')
625    FORMAT(2X,'CPF ',E10.4,' J/KMOLK; K ',E10.4,' W/MK; DIFF. ',
      1E10.4,' M2/S; TAVG ',F4.0,'K; RHOAVG ',E10.4,' KMOL/M3; CPL ',
      2E10.4)
      WRITE(21,405)TIME,SIG2LR(1),SIG2LR(2),SIG2LR(3),SIG2LR(4)
 405  FORMAT(F7.4,4X,F8.2,4X,F7.4,4X,F7.4,4X,F10.4)
      WRITE(22,406)TIME,THETLR(1),THETLR(2),THETLR(3),THETLR(4)
 406  FORMAT(F7.4,4X,F7.4,4X,F7.4,4X,F7.4,4X,F10.4)

      IF(MASSP.GE.99.9)THEN
      WRITE(11,203)TIME,TR,CHIGAS,R*2000.,(1.-XLIGNIN)*100.,MASSP,
     1GASFLUX,PCCHAR,PCRESIDU,G,GGAS
      WRITE(13,401)TIME,TR,(CHI(K),K=1,KDIST),CHIGAS,G
      WRITE(17,202)TIME,THETL(1),THETL(2),THETL(3),THETL(4),
     1XF(1),XF(2),XF(3),XF(4),XFR(1),XFR(2),XFR(3),XFR(4)
      WRITE(19,603)TIME,(PCMLIQ(K),K=1,KDIST),PCLIQ,PCCHAR
      WRITE(*,103)TIME
       WRITE(11,103)TIME
      WRITE(17,103)TIME
      WRITE(13,103)TIME
103   FORMAT(/,' LIQUID DISAPPEARS AT  ',F8.4,' SEC')
      WRITE(*,107)TFURN,PCRESIDU
      WRITE(11,107)TFURN,PCRESIDU
107   FORMAT(2X,'TEMPERATURE ',F5.0,' K, RESIDUAL MASS ',F5.1,'%')
      GOTO 6001
      ENDIF
      NITER=0
      TIME=TIME+DTIME
      TAVG=TFURN/3.+2.*TR/3.
      YFAVG=YFINFM/3.+2.*YFRSUM/3.
      SUMYFTHR=0.
      DO 134 K=1,KDIST+1
      YFTHTREF(K)=(2./3.*YFR(K)*THETR(K)+YFTHIN(K)/3.)
```

```
      IF(YFTHTREF(K).NE.0.)THEN
      THETREF(K)=YFTHTREF(K)/(2./3.*YFR(K)+YFINF(K)/3.)
      ELSE
      THETREF(K)=THETR(K)
      ENDIF
      SUMYFTHR=SUMYFTHR+YFTHTREF(K)
134   CONTINUE
      MF=SUMYFTHR/YFAVG
      CALL PROPS
      IF (SWITCHWM.EQ.0.0) THEN
      IF (TIME.EQ.(1*DTIME)) THEN
      TBUB=TR+100.
      ENDIF
      DO 782 J=1,NN
      DO 1022 K=1,KDIST
      TERM1(K)=EXP(-ETAO(K)*(1.-ZETA(J)))
      SUMTHETLDR(J)=1./(1./THETLMI+(1./SUMTHETLR-1./THETLMI)*
     1EXP(-ETAO(K)*(1.-ZETA(J))))
      DXFDR(K)=(XFI(K)/THETLMI+(XFR(K)/SUMTHETLR-XFI(K)/THETLMI)*
     1EXP(-ETAO(K)*(1.-ZETA(J))))*SUMTHETLDR(J)
      DTHTLDR(K)=(XFI(K)*THETLI(K)/THETLMI+(XFR(K)*THETLR(K)/
     1SUMTHETLR-XFI(K)*THETLI(K)/THETLMI)*EXP(-ETAO(K)*(1.-ZETA(J))))*
     2SUMTHETLDR(J)/DXFDR(K)
      DPSILDR(K)=(XFI(K)*PSILI(K)/THETLMI+(XFR(K)*PSILR(K)/
     1SUMTHETLR-XFI(K)*PSILI(K)/THETLMI)*EXP(-ETAO(K)*(1.-ZETA(J))))*
     2SUMTHETLDR(J)/DXFDR(K)
      DSIG2LDR(K)=DPSILDR(K)-DTHTLDR(K)*DTHTLDR(K)
1022  CONTINUE

      WRITE(25,708)TIME,ZETA(J),DXFDR(1),DXFDR(2),DXFDR(3),DXFDR(4)
708   FORMAT (1X,F6.3,5X,F6.3,4(3X,F9.8))
      WRITE(26,12)TIME,ZETA(J),DTHTLDR(1),DTHTLDR(2),DTHTLDR(3),
     1DTHTLDR(4)

12    FORMAT (1X,F6.3,5X,F6.3,4(10X,F10.5))
      WRITE(27,14)TIME,ZETA(J),DSIG2LDR(1),DSIG2LDR(2),DSIG2LDR(3),
     1DSIG2LDR(4)
14    FORMAT (1X,F6.3,5X,F6.3,4(8X,F10.3))

      CALL BOILIN(DXFDR,AT,BT,SFG,RUGC,TBUB(J),PATM,XF,SIG2L,
     1THETL,DTHTLDR,AB,BB,DSIG2LDR,VLGAMA,TBOIL(J),THETR,NTBFLAG,
     2KDIST,SWITCHWM)
      TBUB(J)=TBOIL(J)

!   CORRECTION FOR BUBBLING POINT
      TBOILC(J)=(TBOIL(J)-22)
      IF(TR.GT.TBOILC(J))THEN
      WRITE(17,9)ZETA(J),TIME
      9  FORMAT(5X,'BUBBLING AT: ',F6.3,'TIME',F6.3)
      SWITCHWM=1
      WRITE(17,241)
```

```
241     FORMAT("**********WELL-MIXED MODEL STARTS***********")
        GOTO 300
        ELSE
        WRITE (24,316)TIME,ZETA(J),TBOILC(J),TR
316     FORMAT(1X,"TIME:",F8.4,5X, "ZETA:",F6.3, 5X,"TBOIL:",F9.5,
        15X "TR:"F9.5)
        ENDIF
782     CONTINUE
        GOTO 300
        ENDIF

        IF(TIME.LT.TIMELIM)THEN
        GOTO 300
        ENDIF
        WRITE(*,107)TFURN,PCRESIDU
        WRITE(11,107)TFURN,PCRESIDU
6001    IF(TFURN.GT.TEND)THEN
        TFURN=TFURN-100.
        GOTO 6002
        ENDIF
6000     STOP
        END


!**********************************************************************
!
   SUBROUTINE VLE(THETL,SIG2L,VLGAMA,YFR,THETR,SIG2R,ALPHAL,
   1BETAL,PATM,AVLE,ABVLE,XF)
!
!**********************************************************************
!
        BETAL=SIG2L/(THETL-VLGAMA)
        ALPHAL=(THETL-VLGAMA)/BETAL
        YFR=(EXP(AVLE-VLGAMA*ABVLE))/((1.+ABVLE*BETAL)**ALPHAL)
        YFR=YFR*XF/PATM
        THETR=VLGAMA+(THETL-VLGAMA)/(1.+ABVLE*SIG2L/(THETL-VLGAMA))
        SIG2R=SIG2L*((THETR-VLGAMA)/(THETL-VLGAMA))**2
        RETURN
        END

!**********************************************************************
   SUBROUTINE VLEDL(THETL,SIG2L,VLGAMA,YFR,THETR,SIG2R,ALPHALR,
   1BETALR,PATM,AVLE,ABVLE,XFR,THETLR,SIG2LR)
!**********************************************************************
!
        BETALR=SIG2LR/(THETLR-VLGAMA)
        ALPHALR=(THETLR-VLGAMA)/BETALR
        YFR=(EXP(AVLE-VLGAMA*ABVLE))/((1.+ABVLE*BETALR)**ALPHALR)
        YFR=YFR*XFR/PATM
        THETR=VLGAMA+(THETL-VLGAMA)/(1.+ABVLE*SIG2L/(THETL-VLGAMA))
        SIG2R=SIG2L*((THETR-VLGAMA)/(THETL-VLGAMA))**2
```

```
      RETURN
      END
!**********************************************************************
   SUBROUTINE PROPS
!**********************************************************************
!
      REAL KTRAA,KTRAF,KTRFA,KTRFF,MF,MA,MMIX,CONDK,CPFG,VISCK,PRANDTL
      COMMON/PROPER/A0,A1,A2,A3,B0,B1,B2,B3,AT,BT,AP,BP,AD,BD,AKT,AKC,
     1BKT,BKC,AL,BL,CL,AH,BH,CONDK,DBAR,YFAVG,TAVG,RHOAVG,PRES,PATM,
     2RUGC,MF,CPF,CPL,TR,THETLM,VISCK,PRANDTL,SCHMIDT,KDIST,YFR,YFRM,
     3THETR,THETL,XF,TCF,THETREF,TIME,BPHI,CPFG,YFRSUM,CPMIX

      DIMENSION YFR(8),THETR(8),DBAR(8),AH(8),BH(8),AT(8),BT(8),AP(8),
     1BP(8),A0(8),A1(8),A2(8),A3(8),B0(8),B1(8),B2(8),B3(8),AKT(8),
     2AKC(8),BKT(8),BKC(8),AL(8),BL(8),CL(8),THETL(8),XF(8),AD(8),BD(8),
     3THETREF(8),BPHI(8)
      YOAMB=0.21
      YNAMB=0.79
      MA=28.97

! FUEL PSEUDO-CRITICAL TEMP. AND PRESSURE
! COMPONENTS COMBINED USING KAY'S RULE
      TCF=0.
      PCF=0.
      DO 10 K=1,KDIST+1
      TCF = TCF+YFR(K)*(AT(K)+BT(K)*THETREF(K))
      PCFX = (AP(K)+BP(K)*THETREF(K))
      IF(PCFX.LT.10.0) PCFX=10.0
      PCF = PCF+YFR(K)*PCFX
10    CONTINUE
      TCF=TCF/YFRSUM
      PCF=PCF/YFRSUM
!  CALCULATE SPECIFIC HEAT FOR FUEL AND AIR (J/KMOL.K):
!     CPF=0.
      CPFG=0.
      DO 11 K=1,KDIST+1
      ACP = A0(K)+A1(K)*TAVG+A2(K)*TAVG**2+A3(K)*TAVG**3
      BCP = B0(K)+B1(K)*TAVG+B2(K)*TAVG**2+B3(K)*TAVG**3
      CPFG = CPFG+YFR(K)*RUGC*1000.*(ACP+BCP*THETREF(K))
11    CONTINUE
      CPFG=CPFG/YFRSUM
      CPF=CPFG

      CPO=(6.713-0.879E-6*TAVG+4.170E-6*TAVG**2-2.544E-9*TAVG**3)
      1*4186.
      CPN=(7.440-0.324E-2*TAVG+6.400E-6*TAVG**2-2.790E-9*TAVG**3)
      1*4186.
      CPAIR=YOAMB*CPO+YNAMB*CPN
!
!   CALCULATION OF MOLAR DENSITY
!
```

```
      RHOAVG=PRES/RUGC/TAVG
!
!
!  DIFFUSION COEFFICIENT (M^2/S):

      DBARREF=1.397E-9*TAVG**(5./2.)/(PATM*(250.+TAVG))
      DO 14 K=1,KDIST+1
      DBAR(K)=(AD(K)+BD(K)*THETREF(K))*TAVG**(5./2.)/(PATM*
      1(BPHI(K)+TAVG))
      IF(DBAR(K).LT.DBARREF)DBAR(K)=DBARREF
14    CONTINUE
!
!  ESTIMATION OF THERMAL CONDUCTIVITY FOR MIXTURE ***
!  EUCKEN EQUATION USED FOR AIR CONDUCTIVITY
!  ESTIMATE AIR VISCOSITY USING THE LENNARD-JONES 12-6 POTENTIAL:
!  CONSTANTS REQUIRED FOR ESTIMATING THE VISCOSITY:
!  SIGMA, E/K FOR AIR:
      SA=3.711
      EKA=78.6
      AV=1.16145
      BV=0.14874
      CV=0.52487
      DV=0.77320
      EV=2.16178
      FV=2.43787
!  DIMENSIONLESS TEMPERATURE:
      TASTA=TAVG/EKA
      OMGVA=AV/TASTA**BV+CV/EXP(DV*TASTA)+EV/EXP(FV*TASTA)
!  VISCOSITY OF AIR (MICROPOISE):
      VISCA=26.69*(MA*TAVG)**(1./2.)/(SA**2.*OMGVA)
!
!  COMBINE AIR AND FUEL CONDUCTIVITIES WITH MASON-SAXENA RULE:
!  MONATOMIC VALUES OF THERMAL CONDUCTIVITY (KTR(I)/KTR(J)):
!
      TCA = 126.2
      PCA = 33.5
      TRA = TAVG/TCA
      TRF = TAVG/TCF
      GAMA = TCA**(1./6.)*MA**0.5/PCA**(2./3.)
      GAMF = TCF**(1./6.)*MF**0.5/PCF**(2./3.)
      KTRAF = (GAMF/GAMA)*((EXP(0.0464*TRA) - EXP(-0.2412*TRA))/
     1      (EXP(0.0464*TRF) - EXP(-0.2412*TRF)))
      KTRFA = GAMA*(EXP(0.0464*TRF) - EXP(-0.2412*TRF))/
     1      (GAMF*(EXP(0.0464*TRA) - EXP(-0.2412*TRA)))
      KTRAA =1.0
      KTRFF =1.0
!
!  FUNCTION (A(I,J)):
!
      AAA =1.0
      AFF =1.0
```

```
      AAF =(1.+KTRAF **(1./2.)*(MA/MF)**(1./4.))**2./(8.*(1.+MA/MF))
       1**(1./2.)
      AFA =(1.+KTRFA **(1./2.)*(MF/MA)**(1./4.))**2./(8.*(1.+MF/MA))
      1**(1./2.)
!
!     ESTIMATE INDIVIDUAL THERMAL CONDUCTIVITIES USING THE EUCKEN
!EQUATION
!
!  ESTIMATE CV AS CV=CP-R (CAL/GMOL.K):
      CVA=CPAIR*0.239/1000.-1.99
      CVF=CPF/4186.-1.99
      CV=YFAVG*CVF+(1.-YFAVG)*CVA
!   FUEL CONDUCTIVITY - COMBINE K'S FOR DISTRIBUTIONS BY MOL FRACTION
      CONDFK=0.
      DO 12 K=1,KDIST+1
      AK = AKT(K)*TAVG+AKC(K)
      BK = BKT(K)*TAVG+BKC(K)
      COMPTK = (AK + BK*THETREF(K))
      IF(COMPTK.LT.1.E-2)THEN
      COMPTK=1.E-2
      ENDIF
      CONDFK = CONDFK+YFR(K)*COMPTK
12    CONTINUE
      CONDFK=CONDFK/YFRSUM
      CONDAK=(CVA+4.47)*VISCA*1.E-6/MA*418.6
      YAMOLE= 1.-YFAVG
      YFMOLE= YFAVG
!
!  THERMAL CONDUCTIVITY OF AIR-FUEL MIXTURE:
      CONDK=(YAMOLE*CONDAK/(YAMOLE*AAA+YFMOLE*AAF)
      1+YFMOLE*CONDFK/(YAMOLE*AFA+YFMOLE*AFF))
!
!   VISCOSITY OF MIXTURE
      MMIX=YFAVG*MF+(1.-YFAVG)*MA
      CPMIX=(YFAVG*CPF+(1.-YFAVG)*CPAIR)/MMIX
!   CPMIX IN J/KG K
      VISCM=MMIX*CONDK/418.6/(CV+4.47)/10.
      PRANDTL=VISCM*CPMIX/CONDK
      SCHMIDT=VISCM/DBAR(1)/RHOAVG/MMIX
      VISCK=VISCM/RHOAVG/MMIX
      RETURN
      END

**********************************************************************
    SUBROUTINE BOILIN(DXFDR,AT,BT,SFG,RUGC,TBUB,PATM,XF,SIG2L,THETL,
1DTHTLDR,AB,BB,DSIG2LDR,VLGAMA,TBOIL,THETR,NTBFLAG,KDIST,SWITCHWM)

**********************************************************************

      IMPLICIT NONE
      REAL::TEPS,NNEWT,IFLAGBUB,TCF,AT(8),BT(8),THETR(8),TBUB,
```

```
     1T,YFRBOIL,BETAL,ALPHAL,SFGCRAP,SFG(8),RUGC,YBOIL,
     2AB(8),BB(8),DXFDR(8),PATM,F,TP,FP,DFDT,T2,TBOIL,XFAVG(8),
     3THETL(8),VLGAMA(8),AVLE,ABVLE(8),DSIG2LDR(8),DTHTLDR(8),
     4TC(8),BVLE,SWITCHWM,XF(8),SIG2L(8)

      INTEGER::K,KDIST,NTBFLAG
      TEPS=1.0
      NNEWT=0
      IFLAGBUB=0
      NTBFLAG=0
      TCF=0.
      DO 10 K=1,KDIST
      IF (SWITCHWM.EQ.1) THEN
      TCF = TCF+ XF(K)*(AT(K)+BT(K)*THETR(K))
      ELSE
      TCF = TCF+ DXFDR(K)*(AT(K)+BT(K)*THETR(K))
      ENDIF
10    CONTINUE
!   NEWTON'S METHOD TO SOLVE FOR BOILING TEMP.
!     T=TCF
      T = TBUB
30    YFRBOIL=0.
      DO 20 K=1,KDIST
      IF (SWITCHWM.EQ.1) THEN
!     AVLE=(SFG(K)/RUGC)*(1.-AB(K)/T)
!     BVLE=BB(K)/(T-AB(K))
      BETAL=SIG2L(K)/(THETL(K)-VLGAMA(K))
      ALPHAL=(THETL(K)-VLGAMA(K))/BETAL
!     YBOIL=(EXP(AVLE*(1.-VLGAMA(K)*BVLE)))/((1.+AVLE*
!    1  BVLE*BETAL)**ALPHAL)
      SFGCRAP=SFG(K)/RUGC/T
      YBOIL=(EXP(SFGCRAP*(T-AB(K)-VLGAMA(K)*BB(K)))/
     1  (1.+SFGCRAP*BB(K)*BETAL)**ALPHAL)
      YFRBOIL=YFRBOIL+YBOIL*XF(K)/PATM
      ELSE
!     AVLE=(SFG(K)/RUGC)*(1.-AB(K)/T)
!     BVLE=BB(K)/(T-AB(K))
      BETAL=DSIG2LDR(K)/(DTHTLDR(K)-VLGAMA(K))
      ALPHAL=(DTHTLDR(K)-VLGAMA(K))/BETAL
!     YBOIL=(EXP(AVLE*(1.-VLGAMA(K)*BVLE)))/((1.+AVLE*
!    1  BVLE*BETAL)**ALPHAL)
      SFGCRAP=SFG(K)/RUGC/T
      YBOIL=(EXP(SFGCRAP*(T-AB(K)-VLGAMA(K)*BB(K)))/
      1(1.+SFGCRAP*BB(K)*BETAL)**ALPHAL)
      YFRBOIL=YFRBOIL+YBOIL*DXFDR(K)/PATM
      ENDIF

20    CONTINUE
      F = 1. - YFRBOIL
      TP=T-TEPS
      YFRBOIL=0.
```

```
      DO 21 K=1,KDIST
      IF (SWITCHWM.EQ.1) THEN
!       AVLE=(SFG(K)/RUGC)*(1.-AB(K)/T)
!       BVLE=BB(K)/(T-AB(K))
        BETAL=SIG2L(K)/(THETL(K)-VLGAMA(K))
        ALPHAL=(THETL(K)-VLGAMA(K))/BETAL
!       YBOIL=(EXP(AVLE*(1.-VLGAMA(K)*BVLE)))/((1.+AVLE*
!     1  BVLE*BETAL)**ALPHAL)
      SFGCRAP=SFG(K)/RUGC/TP
      YBOIL=(EXP(SFGCRAP*(TP-AB(K)-VLGAMA(K)*BB(K)))/
     1  (1.+SFGCRAP*BB(K)*BETAL)**ALPHAL)
      YFRBOIL=YFRBOIL+YBOIL*XF(K)/PATM
      ELSE
!     AVLE=(SFG(K)/RUGC)*(1.-AB(K)/T)
!     BVLE=BB(K)/(T-AB(K))
      BETAL=DSIG2LDR(K)/(DTHTLDR(K)-VLGAMA(K))
      ALPHAL=(DTHTLDR(K)-VLGAMA(K))/BETAL
!     YBOIL=(EXP(AVLE*(1.-VLGAMA(K)*BVLE)))/((1.+AVLE*
!     1BVLE*BETAL)**ALPHAL)
      SFGCRAP=SFG(K)/RUGC/TP
      YBOIL=(EXP(SFGCRAP*(TP-AB(K)-VLGAMA(K)*BB(K)))/
     1(1.+SFGCRAP*BB(K)*BETAL)**ALPHAL)
      YFRBOIL=YFRBOIL+YBOIL*DXFDR(K)/PATM
      ENDIF
21    CONTINUE
      FP = 1. - YFRBOIL
      DFDT=(FP-F)/(TP-T)
      T2=T-F/DFDT
      IF(T2.LT.300.AND.IFLAGBUB.EQ.0)THEN
      T2=TBUB+300.
      IFLAGBUB=1
       WRITE(*,*)'BOILIN - T2<0, RESET'
       ENDIF
       IF(ABS(T2-T).LE.0.1)THEN
       GOTO 4
       ELSE
       T=T2
       IF(T2.GE.TCF)T2=(TCF-20.)
       NNEWT=NNEWT+1
       IF(NNEWT.GT.20)THEN
       WRITE(*,*)'BOILING TEMP. NEWTON DNCV'
       NTBFLAG=1
       GOTO 5
      ENDIF
      GOTO 30
      ENDIF
4     TBOIL=T2
5     RETURN
      END
```